Field Effect Transistor Based Biosensor for Detection of Glutathione

A
Thesis Submitted
in Partial Fulfillment of the Requirements
for the Degree of
DOCTORATE OF PHILOSOPHY

By

UJJWOL BARMAN

Centre for Nanotechnology
Indian Institute of Technology Guwahati
April, 2019

Declaration

This is to certify that the thesis entitled "**Field Effect Transistor Based Biosensor for Detection of Glutathione**", submitted by me to the *Indian Institute of Technology Guwahati*, for the award of the degree of Doctorate of Philosophy, is a bonafide work carried out by me under the supervision of Prof. Roy P. Paily and Prof. Siddhartha Sankar Ghosh. The content of this thesis, in full or in parts, have not been submitted to any other University or Institute for the award of any degree or diploma. I also wish to state that to the best of my knowledge and understanding nothing in this report amounts to plagiarism.

Signed: _____

Ujjwol Barman
Centre for Nanotechnology,
Indian Institute of Technology Guwahati,
Guwahati-781039, Assam, India.

Date: _____

Dedicated

To

My Parents

Certificate

This is to certify that the thesis entitled "**Field Effect Transistor Based Biosensor for Detection of Glutathione**", submitted by Ujjwol Barman (136153006), a Research Scholar in the *Centre for Nanotechnology*, *Indian Institute of Technology Guwahati*, for the award of the degree of Doctorate of Philosophy, is a record of an original research work carried out by him under our supervision and guidance. The thesis has fulfilled all requirements as per the regulations of the institute and in our opinion has reached the standard needed for submission. The results embodied in this thesis have not been submitted to any other University or Institute for the award of any degree or diploma.

Signed: _____

Supervisor: Prof. Roy P. Paily
Centre for Nanotechnology & Department of Electronics and Electrical Engineering,
Indian Institute of Technology Guwahati,
Guwahati-781039, Assam, India.

Date: _____

Signed: _____

Co-Supervisor: Prof. Siddhartha Sankar Ghosh
Centre for Nanotechnology & Department of Biosciences and Bioengineering,
Indian Institute of Technology Guwahati,
Guwahati-781039, Assam, India.

Date: _____

Acknowledgements

I would like to convey my sincere gratitude to my supervisors, Prof. Roy P. Paily and Prof. Siddhartha Sankar Ghosh for giving me this wonderful opportunity to carry out my research work under their guidance. I am highly obliged to them for their support, encouragement, and for providing the facilities required for accomplishment of the research objectives. Without their constant support, I would not have come this far.

I extend my thanks to my doctoral committee members, Prof. Harshal B. Nemade (Chairman), Prof. Arun Chattopadhyay and Dr. Biplab Bose for continuously evaluating my thesis work and for giving valuable ideas and suggestions for improvement. I would like to thank Center for Nanotechnology and Centre for Excellence in Nanoelectronics & Theranostic Devices (CENTD) for providing me with the much needed instrument facilities to carry out all my experiments. I would like to acknowledge the staff members of Centre of Nanotechnology: Paran Sir, Pranjoli Ma'am, Indrajit Sir, Naba Sir, Kaustubh Sir and Sandhan for their help.

I sincerely thank my lab seniors Jitendra Kumar, Brajesh Rawat, Sai Santosh, Shyam Trivedi, Asif, Archita; and my lab juniors Sid, Paromita and Monica for being a part of the wonderful memories made in the time spent in the lab.

I would like to specially mention Namami and Upashi ba, without whom my work and my life at IIT Guwahati would not have been memorable. I would also like to thank my collaborators and batchmates: Gargi, Anamika Kalita, Neha and Deepanjalee, who were not only good researchers, but also good friends. I would like to extend my deepest gratitude towards my friends Subhra da, Asif da and Sandip da for being such great companions during my tenure at IIT Guwahati. They always treated me like their younger brother and were with me whenever I needed them. Thank you Pralay, Satya, Nirmal, Prahlad da, Dhruba da and Dibya da for providing me with beautiful memories to cherish.

Last but not the least, I extend my heartfelt thanks to my parents for their selfless love, encouragement, and support in my journey of life. I thank them for giving me the best possible education which has helped me in achieving whatever I have today. They were the ones who inspired me to sow the seeds of hard work, sincerity and dedication in my life. I thank my sisters Krisnakshi and Kalyani for guiding me in all matters since childhood, and showing the right way with love and encouragement. I owe everything whatever I have earned in these years to my family. I thank the Almighty for gifting me with such wonderful people.

Sincerely
Ujjwol Barman

Abstract

The demand for reliable, low cost, compact and sensitive biosensors for the detection of disease causing pathogens is ever increasing in present time. Field Effect Transistor (FET) based biosensors have been serving that purpose for past few years quite effectively. This area has attracted much attention for development of reliable point of care sensors for detection of some acute diseases. However, glutathione (GSH), a central antioxidant found naturally in animals is a biomarker of cancer whose detection is yet to reach that level. Overexpression of glutathione has been observed due to oxidative stress in malignant tissues. But detection of glutathione is so far based on traditional methods. This work aims to develop an electrochemical biosensor device for detection of glutathione using a single platform technology, where nanomaterial - Glutathione-S-Transferase (GST) ensemble might be helpful for rapid and efficient detection of cancer in lab to clinical samples.

Design, fabrication and characterization of a novel device based electrochemical detection method of glutathione is the prime focus of this thesis. The device is a FET device, channel material of which consists of a conjugation of ZnO nanoparticles and purified recombinant GST protein. The novel concept of incorporating a protein in a channel material is reported here for the first time. The device successfully and selectively detects and quantifies glutathione as compound and as well as a human cell component. The device was also tested successfully with cultured HeLa and MCF-7 cancer cells and HEK (Human Embryonic Kidney) normal cells and it was found that the device could detect enhanced concentration of glutathione in cancerous cells, which indeed is the first step towards detecting certain types of acute cancer diseases. The device can be further improved upon by keeping primary working principle the same, in order to meet the requirements to make a deliverable product for marketization.

In summary, the main contribution of this thesis is the design, fabrication and characterization of a Glutathione-S-Transferase incorporated ZnO nanoparticles based Field Effect Transistor biosensor for detection of glutathione and its associated types of cancers. First contribution of this thesis is the development of a functionalized channel layer for the FET structure which consists of ZnO nanoparticles and GST conjugate.

The second major contribution of this thesis is design and fabrication of a FET structure for biosensing purpose. Simulation studies were carried out in order to find an optimized structure. Subsequently, the device was fabricated on a Si wafer using optical lithography technique. Then, the functionalized channel layer was deposited and the thesis involves characterization results of fabricated devices.

The third major contribution of this thesis is characterization of fabricated devices for detection of glutathione in cancer cells. The results show enhanced glutathione concentration in cancer cells compared to that of normal cells. The conclusion of the thesis gives an insight into the future prospects of this work and its possibility to be used as a point-of-care device.

Contents

List of Figures

List of Tables

List of Acronyms

CDNB	1-Chloro-2,4-dinitrobenzene
CDS	Circular Dichroism Spectrometer
DG-JLFET	Double Gate Junctionless Field Effect Transistor
DMSO	Dimethyl Sulfoxide
FESEM	Field Emission Scanning Electron Microscopy
FET	Field Effect Transistor
FWHM	Full Width Half Maximum
GSH	Glutathione
GSSG	Glutathione disulfide
GST	Glutathione-S-Transferase
HEK	Human Enbryonic Kidney
HMDS	Hexamethyldisilazane
MALDI	Matrix Assisted Laser Desorption/Ionization
MOS	Metal Oxide Semiconductor
PBS	Phosphate Buffered Saline
PDMS	Polydimethylsiloxane
SAED	Selected Area Electron Diffraction
SDS-PAGE	Sodium Dodecyl Sulfate Polyacrylamide Gel Electrophoresis
TEM	Transmission Electron Microscopy
XRD	X-ray Diffraction
ZnO	Zinc Oxide

Chapter 1
Introduction

1.1 Background

CANCER has different distinct types associated with it and can affect people across all age ranges. In order to survive such an acute disease, early diagnosis and treatment are indispensable; which requires development of efficient technologies for detection of cancer at an early stage [4] . Even though so much of research work is going on across the globe for detection of levels of cancer biomarkers; the progress gets halted in such cases where more than one biomarker is associated with a single type of cancer [5–7].

Some of the biosensing technologies developed to study and identify cell based biomarkers for diseases include live cell sensing, cellular diagnostics, cell counting. Presently, optical-based sensing technologies like immunofluorescence are used for cell-based diagnostics [8–10]. However, this method suffers from poor sensitivity, complexity and lack of receptor specificity. Flow cytometry, Surface plasmon resonance (SPR) and resonant waveguide grating (RWG) are some of the common optical technologies developed for live cell imaging, cellular manipulations, cell sensing and cell biology study related analysis [11–13]. However, requirement of bulky and extremely costly bench-top instruments

and necessity of well-trained laboratory staff to operate such delicate instruments are discouraging concerns associated with these techniques.

There arises the requirement of compact and simple diagnostic platforms with the scope of miniaturization, like microfluidics-based cellular diagnostics and specially semiconductor based electronic sensors, which are highly sensitive, simple, compact, have very low time and sample volume requirements, and are extremely cost-effective [14, 15]. For that matter, Field Effect Transistor (FET)-based biosensors have been reported to have high sensitivity, easy signal read-out capabilities and provide label-free cell detection [16]. FET based biosensors have been utilized successfully for diagnosis of several acute diseases in recent times. Scope of miniaturization is the main reason for such devices being admired and the demand for portable label-free diagnosis device continues to grow [17–19]. In the case of FET biosensors, the pronounced charge screening effect in high ionic strength solutions associated with the conventional FET structure, and the drift in electrical characteristics due to harsh test environments are some of the disadvantages which have impeded their clinical applications [20, 21]. But these two problems can be overcome by structural and material related modifications.

Tripeptide glutathione is an important aqueous antioxidant, mostly found in the cytosol of cell and blood plasma [20, 22]. Glutathione (GSH) is an important cellular molecule for its antioxidant abilities and has a role in multidrug resistance. Glutathione is the most abundant intracellular thiol in eukaryotic cells [23]. It was first discovered in 1888 in baker's yeast although it did not attain its current identity until 1921 when its molecular structure was established [24]. Glutathione is composed of three amino acids: glutamic acid, cysteine and glycine which are connected via a peptide bond and a γ-peptide linkage between glutamic acid and cysteine [25].

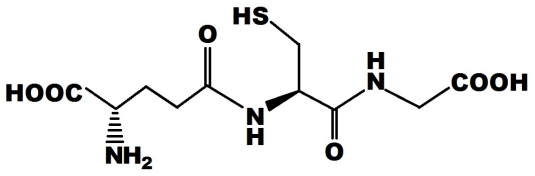

Figure 1.1: Structure of GSH [1]

Increased levels of glutathione in plasma and cytosol have been reported for a number of acute diseases including various types of malignant tumors like liver, breast and prostate cancer, which makes it an important biomarker diagnosis of cancer [26–29]. Glutathione concentration in the cytosol of cells remains in the range of 1-10 mM [30]. Most of the cells contain about 1-2 mM GSH, whereas in liver cells the concentration can reach about 10 mM [31]. Glutathione concentration increases about 100% in case of breast cancer, about 50% in case of cervical cancer and about 80% in case of lung cancer compared to disease-free cells [31].

HeLa and MCF-7 are two cancerous cells related to cervical and breast cancer respectively and concentration of glutathione in such tumorous cells have been found to be incremented compared to normal cells [32–36]. Hence, the detection and quantification of activity of glutathione becomes extremely critical for development of theranostic devices for the diseases associated with it. Optical techniques are the most commonly used methods for that purpose but electrochemical biosensors evolved to overcome some disadvantages of optical measurement techniques like optical interference and electrical integration, cost of analysis, lack of scope of miniaturization etc. [37–40]. Some of the other reported significant techniques for end point detection of glutathione are impedance spectroscopy [41], spectrophotometry [42], high-performance liquid chromatography (HPLC) [43], capillary electrophoresis [44], proton nuclear magnetic resonance (^{1}H NMR) [45]. Even though the application of electrochemical methods have been successful, still these methods reported for detection of GSH suffer from problems of poor selectivity, low electro-oxidation rate, and very weak voltammetric responses of the target analytes at the electrodes [46].

1.2 Scope of the thesis

This work presents a bottom gate nanoconjugate channel based FET biosensor that is free of such limitations. In a typical FET, a voltage is applied to the insulated metal top gate to regulate the current of the underlying semiconductor channel. For an n-type FET, a positive gate voltage results in an attraction of negative charge carriers in the drain-source-channel, thereby increasing the drain current. On the other hand, a negative gate

voltage results in a decrease in drain-source current due to repulsion of negative charge carriers within the channel [21]. In other words, the characteristics of the device can be modulated by changing the properties of the channel layer. The extension of this idea led to formulation of the functionalized channel layer specific to detection of glutathione. Keeping the gate voltage constant, presence of glutathione on the channel gets reflected on the output characteristics of the device; which indeed confirms the detection of GSH. This work covers the detection and quantification of glutathione in solution as well as in cancer cells.

1.3 Method

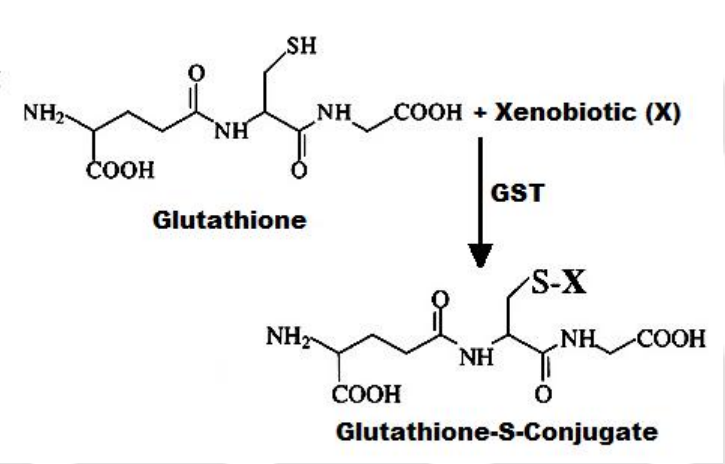

Figure 1.2: Conjugation of glutathione (GSH) [2]

GST enzyme catalyzes the conjugation reaction of glutathione with different hydrophobic and electrophilic compounds leading to detoxification of those compounds [47]. One such conjugation reaction involving 1-chloro-2,4-dinitrobenzene (CDNB) is: in presence of GST, glutathione (GSH) conjugates with CDNB forming GS-DNB and a byproduct HCl. CDNB is an ultraviolet chromogenic substrate, reported in literature as the most prevalent probe for the analysis of activity of glutathione and GST [48]. Detection of glutathione by means of this conjugation reaction is very effective and is mostly analyzed based on visual changes on occurrence of the reaction as reported [49]. Although it is a very simple, cost effective method for detection of glutathione, but this method lacks the ability to quantify the amount of glutathione present. Again the effectiveness of this method is not reliable in case of very low concentration of glutathione. This does not

help the fundamental cause of an early stage detection of cancer. There arises the need of a device based electrochemical detection method, which is cost effective, selective and reliable for detection and quantification of glutathione in human cell cytosol. This work reports for the first time, FET device fabricated and functionalized to detect the occurrence of a chemical reaction in real time from its output characteristics. Subsequently, it leads to the detection and quantification of glutathione.

1.4 Objectives

The main objectives of the thesis are:

- Development of a favourable functionalization mechanism for detection of glutathione using a chemiresistive device.
- Simulation, fabrication and characterization of FET device with functionalized channel layer for detection of glutathione in reaction as well as in cancer cells.

Chapter 2
Literature Review

GLUTATHIONE was detected as a thiol-containing compound in 1888 by J. de Ray-Pailhade and named "philothion," a term composed of the Greek words for love and sulfur [50] . The elucidation of its structure did not start but in the early 1920s and kept some scientists busy for more than a decade. It was Sir Frederick Gowland Hopkins who started with the isolation of philothion and renamed it glutathione, yet the chemical analysis of the isolated material led him to conclude that it was a dipeptide consisting of glutamic acid and cysteine. The addition of the missing third amino acid, glycin, goes back to Hunter and Eagles (1927), Pirie and Pinhey (1929), and Kendall et al. (1929). Its structure as γ-glutamyl-cysteinyl-glycin, however, had to wait for final proof by chemical synthesis in 1935 (Harrington and Mead) and 1936 (du Vigneaud and Miller) respectively [50].

2.1 Glutathione as cancer biomarker

L-Glutathione (GSH, L-γ-glutamyl-L-cysteinyl-glycine), an intracellular low molar mass thiol species, is an important antioxidant cofactor responsible for the metabolisms of living cells [51]. Reduced glutathione is composed of three amino acids namely L-cysteine,

L-glutamine and glycine. Reduced glutathione has L-glutathione on thecysteinyl portion, which acts as a strong electron donor. The usage of reduced and oxidized glutathione (often called as glutathione disulfide (GSSG)) in human's natural defence system is maintained by a dynamic balance between glutathione synthesis and it's recycling from GSSG [52, 53]. Reduced glutathione plays an important role in living being systems for enzyme activity maintenance, participation in bio reductive reactions, amino acid transport and detoxification of free radicals, hydrogen peroxide and toxins [52, 53]. glutathione is also responsible for programmed cell death, cell homeostasis and gene regulation [54, 55]. When the concentration of glutathione in biological fluids varies, the thiol-disulfide bond homeostasis gets disturbed and as a result, the living cells tend to increase their length to a greater extent to normalise the homeostasis [54, 55]. High concentrations of glutathione are found in mammalian and eukaryotic cells [54, 56–58]. Under oxidative stress, glutathione can be transformed into GSSG [52, 57–60]. Thus, the ratio of glutathione to GSSG determines whether a living cell is prone to oxidative stress or not. The normal glutathione level in both plant and mammalian tissue is between 1 and 10 mM [58]. However, elevated concentration of glutathione in mammalian tissues is known to induce several acute diseases including malignant disorders [51, 52, 61]. Studies also show that reduction in glutathione production in γ-glutamyl cycle may be due to the decrease in the amount of enzymes involved in the production of reduced glutathione [3, 62–65].

Table 2.1: Over-expression of glutathione [3]

Cancer type	% increase in concentration of glutathione
Breast	100
Cervical	50
Lung	80
Liver	50

In the human body the antioxidant properties of glutathione are well recognized [66] . Its ability to scavenge physiological free radicals is of particular importance considering the nitric oxide release associated with inflammatory disorders [67]. As a result, changes in physiological glutathione concentrations have been correlated with patients suffering from Alzheimer's disease, Parkinson's disease, diabetes mellitus, atherosclerosis, arthritis,

epilepsy, aging as well as numerous types of cancer. Normal concentration of glutathione in human whole blood is in the millimolar range and in plasma generally at micromolar levels [1].

2.2 Detection of glutathione

Due to its paramount importance, the concentration of glutathione has been directly linked as key biomarker for various diseases and cancers owing to the variation in the level of glutathione from its normal level in micromolar to millimolar range present in biological fluids and cells. Thus, the changes in physiological glutathione concentration cause diseases such as Parkinson, Alzheimer, diabetes mellitus, aging, arthritis, atherosclerosis, epilepsy, macular degeneration and HIV disease, as well as numerous types of cancer including breast cancer and colorectal cancer. Based on glutathione concentration level in correlation with above mentioned diverse medical conditions, the accurate and selective quantification of glutathione is highly essential in order to allow the relevant treatment to individual patients [68, 69]. In this regard, many important analysis methods like titrimetry [70], spectrophotometry [71, 72], spectrofluorimetry [73–75], high performance liquid chromatography (HPLC) [76, 77], capillary zone electrophoresis (CE) [78], proton nuclear magnetic resonance [79], enzymatic method [80], flow injection analysis [81], and electrochemical methods [82–85], have been developed successfully. It should be known that the analytical assay of any compound is dependent on few crucial parameters of limit of detection (LOD), sensitivity, selectivity, analysis time and cost effectiveness. Although, HPLC and CE have been the foremost techniques in terms of LOD of glutathione, but analysis time, selectivity, and cost effectiveness are few serious disadvantages for them. Among all techniques, electrochemical analysis methods offer significant merits considering all of the above analytical analysis criteria except LOD which is not a big issue in case of glutathione considering the range of concentration of glutathione in human blood. Some of the significant methods for detection of glutathione are discussed below:

2.2.1 Spectrophotometric methods

Tietze published his classical spectrophotometric method in 1969, often referred to as the GR-coupled enzymatic recycling assay or the glutathione-recycling assay [86]. In the presence of DTNB and GR, the addition of NADPH to the reaction mixture initiates the progressive reduction of GSSG to glutathione which, in turn, reacts with DTNB, the colored product 5-thionitrobenzoate being formed upon reduction. The rate of color change at 412 nm, typically followed over 3 or 4 min, is proportional to the total glutathione plus GSSG concentration. GSSG is determined via the blocking of glutathione with NEM in a separate sample. The GR-coupled recycling assay is still one of the most widely applied techniques to detect glutathione and GSSG, due to its simplicity, satisfactory sensitivity and low cost. Importantly, Rossi et al. reported similar levels of whole blood glutathione and GSSG with the method of Tietze (1161±151 and 3.51±2.09 μM, respectively) and with a validated, artifact free HPLC-UV absorbance assay, using FDNB derivatization and the thiol-masking agent NEM (1199±201 and 3.99±2.04 μM for glutathione and GSSG, respectively) [87]. The main drawbacks of the original assay were the unsatisfactory specificity and selectivity and, in the assay of GSSG, the need for the elimination of the excess of NEM due to its GR-inhibiting properties, which made the technique time-consuming. Slight modifications have previously been made to the original method, such as solid-phase extraction instead of solvent extraction to remove the excess of NEM and isolate GSSG [88, 89]. More recently, assays based on the same principles make use of 96-well microtiter plates [90, 91] or an automated sequential injection analysis system [92]. This switch was facilitated by the replacement of NEM by M4VP [91] or M2VP [92] as new thiol masking reagents for the determination of GSSG in human whole blood [91] and rat liver tissue and bile samples [92], as their excess does not need to be removed. The application of M2VP and M4VP makes the recycling method less time-consuming and less laborious, so that the technique is expected to become even more attractive. The GR-coupled recycling assay is also appropriate to be combined with CL techniques and biosensors.

Other spectrophotometric techniques frequently used are the GST 1-chloro-2,4- dinitrobenzene (CDNB) endpoint method, measuring solely glutathione, first reported by

Brigelius et al. (2006) in the assessment of hepatic glutathione [93], and a GSSG-endpoint determination, developed by Güntherberg and Rost in 1966 for the determination of erythrocyte GSSG [94]. The latter assay is based on the measurement of NADPH consumption by GR, a process that reduces GSSG present in the sample [94]. Even if quite specific, these methods offer much lower sensitivity than that of the glutathione-recycling assay.

2.2.2 Spectrofluorimetric methods

Several spectrofluorimetric methods have been developed for the analysis of glutathione, GSSG and related compounds in different matrices. Wang et al. measured glutathione in human blood serum with a fluorescent Zn(II)–8-hydroxyquinoline-5-sulfonic acid (HQS) system [95]. The use of OPA together with 1-pyrenemethylamine nanoparticles is associated with stronger fluorescence and an improved LOD than those with OPA alone [96]. Novel methods utilizing a dithiolic fluorophore [97], other rhodamine-based fluorescent probes [98–100], most of them reacting with all thiol functionalities in the cell, and newly synthetized members of the BODIPY family, DAMBO [101] and DABODIPY [102](both used for Snitrosothiol measurements in combination with Hg^{2+}), have also been published. A number of fluorophores [97–99] allow realtime assaying of thiols *in vivo*. Some of the most recent methods have not yet been applied to the determination of glutathione. An interesting novel approach for the detection and identification of multiple species is the use of multiparameter fluorescence detection (MFD) [103] or multiparameter fluorescence imaging (MFDi) [104]. In MFDi, the three spatial coordinates are stored in addition to the simultaneous monitoring of the fluorescence information. MFDi allows a real-time assessment of the dynamics of molecules in solution and in cells [104]. The quantitative value of the techniques and their potential application in peptide and glutathione analysis are yet to be determined.

2.2.3 Chemiluminescence methods

CL is an attractive means of detection for biological substance analysis in consequence of its low LOD values (nanomolar amounts) and wide linear working ranges, with relatively

simple instrumentation. The first method in which CL was used in the measurement of glutathione was developed by Hinze in 1984 [105], but its LOD was higher than that of the spectrophotometric methods in which Ellman's reagent was applied. In 1998, Romero and Mueller-Klieser detected total glutathione via coupling of the DTNB-GR recycling assay (with which to amplify the NADPH decrease) with the highly sensitive luminescent FMN oxidoreductase/bacterial luciferase reaction (to detect the consumption of NADPH) [106]. The first CL assay for GSSG, published in 2000 by Mourad et al., was based on the same principles, but used 4-chloro-7-trifluoromethyl-1-methylquinolinium to mask glutathione [107]. Since then, other bioluminescent systems for the determination of total glutathione and Cys have been developed, including luminol – $NaIO_4$ [108, 109], luminol – H_2O_2 [110], quinine–Ce(IV) [111, 112], $Ru(phen)_3^{2+}$ – Ce(IV) [113] and $Ru(phen)_3^{2+}$ – $KMnO_4$ [114]. Most assays are based on the oxidation reaction between a strong oxidant and glutathione or Cys, and the subsequent oxidation of the luminophore to produce CL. In the latter two assays, the weak basal CL of the $Ru(phen)_3^{2+}$ – Ce(IV) [113] or $Ru(phen)_3^{2+}$ – $KMnO_4$ [114] system is amplified by the addition of glutathione or Cys.

2.2.4 Nuclear magnetic resonance spectroscopic methods

NMR is a technique that allows the determination of glutathione and GSSG in the brain *in vivo* and in intact cells in cyto. Trabesinger et al. pioneered a method applicable to the human brain in 1999. They used ^1H NMR with double quantum coherence (DQC) filtering in combination with point-resolved spectroscopy (PRESS) volume selection with a relatively low strength field of 1.5 T, and estimated the glutathione concentration in the frontal lobe of 12 healthy volunteers as 2–5 mM [115]. The same research group improved the DQC filtering in a subsequent study, so as to minimize the contamination of the DQC-filtered glutathione signal with contributions from GABA [116]. Later, further improvements in the DQC filtering were achieved, which eliminated the need for calibration scans to optimize the signal yield and removed the influence of water saturation pulses on the glutathione yield. The authors suggested that the new filter was expected to be less sensitive to patient motion by virtue of its single shot nature [117].

In 2006, the contribution of both glutathione and GSSG to MEGA-PRESS (a frequency-selective refocusing technique) signals assessed by ^{1}H NMR were evaluated *in vitro* and *in vivo*. To mimic the *in vivo* conditions, PBS solutions containing glutathione and GSSG in concentrations similar to those existing *in vivo* were prepared. Solutions containing creatine, glutathione, aspartate and γ-aminobutyric acid were also prepared. In such solutions, GSH gave a single positive signal, whereas GSSG yielded a multiplet of reversed signals. The concentration of glutathione in the parietal lobe of healthy volunteers was 1.9±0.37 mM; no signal for GSSG was detected [118]. The simultaneous determination of glutathione, GSSG and ASC was achieved with ^{1}H NMR by using double editing with (DEW) MEGA-PRESS at 4.0 T. The glutathione and ASC levels in the occipital lobe of 4 healthy subjects were 1.0±0.1 and 0.8±0.1μ mol/g, respectively. GSSG was suggested to give detectable signals *in vivo* only at exceptionally high concentrations [119].

GSH concentration can also be assayed in blood through ^{19}F NMR by measuring the products of the exchange reactions of thiols with a newly synthetized fluorinated disulfide 2,3,5,6-tetrafluoro-4-mercaptobenzoic acid [120].

Another interesting field for NMR measurements is the investigation of intact cells. To resolve the issue of whether erythrocytes can utilize extracellular glutathione to enhance the intracellular free glutathione pool, the intracellular and extracellular glutathione redox status was measured by means of ^{1}H spin-echo NMR and ^{13}C[^{1}H-decoupled] NMR. It was concluded that the intracellular glutathione in glucose-starved erythrocytes cannot be increased from extracellular sources by the release of bound glutathione from mixed disulfides with membrane proteins [121], in contrast with what an earlier report suggested [122].

2.2.5 Electrochemical techniques

A biosensor is a device constituted by a biorecognition layer, the purpose of which is the biomolecular recognition of the analyte, and a transducer responsible for the conversion of the biorecognition event into a useful electrical signal. Enzymes, antigens, antibodies, nucleic acids, receptors and tissues have been used as biorecognition elements. Depending on the nature of this element, it is possible to divide biosensors into enzymatic (involving

a biocatalytic event) and affinity (involving an affinity event) biosensors [123]. The widespread use of biosensors and electronic tongue systems has been reviewed recently [124].

Timur et al. (2008) integrated a membrane modified with GR and sulfhydryl oxidase (SOX) onto the surface of spectrographic graphite rods. The working principle of the biosensor was based on the monitoring of O_2 consumption, which is correlated with the concentration of GSSG or glutathione during the enzymatic reaction. The combination of GR and SOX allows the detection of GSSG and glutathione in the same matrices. This biosensor has also been applied as an ECD after HPLC separation [125].

A biosensing approach including the indirect detection of current has also been reported. Horseradish peroxidase, immobilized on a rotating disk, catalyzes the oxidation of catechols in the presence of H_2O_2, back electrochemical reduction of which is detected on a GCE surface. GSH or Cys added to the solution participates in Michael addition reactions with catechols to form the corresponding thioquinone derivatives, which decreases the peak current obtained proportionally to the increase in their concentration. The detection of GSH and Cys in nanomolar concentrations is possible, in the processing of as many as 25 samples per hour [126].

Cha and Meyerhoff (2006) reported the development of an amperometric NO gas sensor modified with a thin hydrogel layer for the detection of S-nitrosothiols. Immobilized $3, 3^{/}$ – dipropionicdiselenide (an organoselenium catalyst) is covalently coupled to the primary amine groups in polyethylenimine, which is further cross-linked to form a hydrogel layer, reported to be capable of decomposing S-nitrosothiols to generate NO [127]. However, it should be noted that biosensors are rather of qualitative value in S-nitrosothiol analysis at present. Moreover, it is questionable whether low-molecularmass S-nitrosothiols are present in measurable amounts in the circulation [128].

A linear sweep cyclic voltammetry method at a hanging mercury drop electrode (HMDE) as a working electrode, polarized between potentials of -0.2 and -0.8 V, was developed by Kizek et al. (2004) for the measurement of glutathione and GSSG. The surface area of the working electrode was $0.4mm^2$; Ag/AgCl/3M KCl served as a reference electrode, and Pt wire as an auxiliary electrode [129].

A glassy carbon electrode (GCE) is a good material for modification, and the attachment of carbon nanotube (CNT) layers results in an electrode with widespread detection possibilities [123]. It should be noted that CNT-modified GCEs (and also carbon ceramic electrodes (CCEs)) do not primarily serve as stand-alone detectors (except with authentic compound mixtures), but rather as ECDs after chromatographic separations and transducers of the biorecognition event in biosensors for the analysis of biological samples [123, 130].

Salimi and Hallaj (2005) reported the preparation of a preheated GCE modified with multiwall CNTs and its use in the detection of glutathione, Cys and thiocytosine. Han and Tachikawa (2005) tested the electrocatalytic oxidation of 14 thiols, including glutathione, homocysteine (HCys), Cys and NAC, at a GCE coated with a single-wall CNT film. The enhanced catalytic properties of this electrode, as compared with bare GC and diamond electrodes, was further improved by its modification with pyrroloquinoline quinone (PQQ) [131].

A renewable three-dimensional sol–gel CCE chemically modified with $Ru[(tpy)(bpy)Cl]PF_6$ was constructed by Salimi and Pourbeyram (2003), and used for the amperometric detection of glutathione and Cys. This modified electrode had the advantages of high sensitivity, a short response time and long-term stability [132].

Table 2.2: Review of electrochemical detection of glutathione

Principle	Sample	pH	LoD	Ref
LSV	PBS	7.5	6.24 μM	[133]
LSV	PBS	4	0.14 μM	[134]
CV	PBS	7	0.93 μM	[135]
CV	PBS	6.6	100 nM/1 μM	[136]
CV	tissue media	7	1 μM	[137]
CV	-	7	0.867 μM	[138]
CV	-	4.7	50 μM	[139]
CV	KNO_3	3	49/15.2 mg/L	[140]
CV	-	7	0.5 μM	[141]

Continued on next page

Table 2.2 – continued from previous page

Principle	Sample	pH	LoD	Ref
CV	-	3	2 μM	[142]
CV	PBS	7.5	5.8 μM	[143]
CV	PBS	7	2.7 μM	[144]
CV	Phthalate buffer	3.5	36 nM	[145]
CV	PBS	7	0.07 μM	[146]
CV	PBS	7	1 mM	[147]
CV	Blood	7.4	2 μM	[148]
CV	Borax buffer	9.2	9 nM	[149]
CV	PBS	7.8	0.3 μM	[150]
CV	PBS	7.4	15 nM	[151]
CV	PBS	7	0.4 μM	[152]
CV	PBS	7	14 μM	[153]
CV	PBS	5.6	1 nM	[154]
Fast CV	AcOH buffer	4.7	0.05 μM	[155]
CSV	Estuary water	8.5	0.4 nM	[156]
CCSV	-	6.8	0.01 μM	[157]
CCSV	-	7.1	8 nM	[158]
CV-FIA	PBS	7	0.3 nM	[159]
CV-SWV	PBS	7	0.2 μM	[160]
CV-DPV	NaOH solution	-	25 mM	[161]
CV-HA	AcOH buffer	2	1 μM	[162]
DPV	-	9	160 μM	[163]
DPV	-	7.2	-	[164]
DPV	BR buffer	2	83 pM	[165]
DPV	PBS	6.7	10 μM	[166]
DPV	PBS	7	0.51 μM	[153]
DPV	PBS	7	98 nM	[167]
DPV	BR buffer	4	0.16 μM	[168]

Continued on next page

Table 2.2 – continued from previous page

Principle	Sample	pH	LoD	Ref
DPCSV	Plant cells	9.5	10 μM	[169]
DPASV	Sea water	8.5	1.2 nM	[170]
SWV	PBS	7	8.1 μM	[171]
SWV	PBS	7.4	0.5 μM	[172]
SWV	PBS	7	30 nM	[173]
AMP	PBS	6.5	5 μM	[174]
AMP	PBS	6.5	10 μM	[174]
AMP	Phathalte buffer	3.45	11.4 μM	[175]
AMP	Borate buffer	8.42	13.2 μM	[175]
AMP	-	2-8	5.6 μM	[176]
AMP	Serum	7.8	19 μM	[177]
AMP	PBS	6	3.3 μM	[178]
AMP	PBS	7.4	0.6 ppm	[179]
AMP	PBS	7	2.7 μM	[180]
AMP	PBS	7.2	0.09 μM	[181]
AMP	Lysis buffer	7.4	8.1 μM	[182]
AMP	BR buffer	7	0.4 μM	[183]
AMP	PBS	7.3	0.1 μM	[184]
CC	Tris-HCl buffer	7.4	0.4 pM	[185]
CZE-ED	PBS	7.5	2.3 μM	[186]
RDE	PBS	7.4	11.5 μM	[187]
FIA	PBS	7	0.47 μM	[188]
HPLC-ECD	PBS	2.5	2 fM	[189]
HPLC-FD	PBS	5.45	0.5 ng/10 μL	[190]
CE-LIF	Human erythrocytes in PSS	7.4	6.9 aM	[191]

Continued on next page

Table 2.2 – continued from previous page

Principle	Sample	pH	LoD	Ref
CZE-LIF	5-IAF	12.5	5 nM	[192]
FD	Tris-HCl buffer	7.5	4.2 nM	[193]
FD	Borate buffer	8	4.2 nM	[194]
FIA-CL	Na_2CO_3HCl	10.5	8 nM	[195]
CZE	Ammonium acetate buffer	7.5	23.4 μM	[196]

2.2.6 High performance liquid chromatographic methods

A number of HPLC and two ultra-performance liquid chromatography (UPLC) methods for the determination of glutathione, GSSG and related compounds have recently been developed or improved. Detection systems used in combination with them include UV absorbance, FD, ECD, MS, MS/MS and atomic fluorescence spectrometry (AFS). Most assays are reversed-phase (RP)-based, although anion-exchange HPLC has also found application. Common characteristics in almost all these methods are that eluents are buffered at acidic pH (to maintain glutathione and congeners in a non dissociated form, so as to improve interaction with the stationary phase, and to attenuate thiol autoxidation), and that TFA is added to the eluent (TFA is an ion-pairing reagent which helps the resolution of peak tailing associated with GSSG). To enhance the separation selectivity of HPLC, electrochemically modulated liquid chromatography (EMLC) was introduced by Saitoh et al. in 2006 [197]. EMLC works by altering retention through changes in the potential applied to the conductive stationary phase. Even if EMLC is potentially suitable for the determination of glutathione and GSSG, it has not yet been adopted. A summary of the HPLC methods reviewed in this article is given in table 2.3.

Only three recent HPLC methods have employed UV absorbance as a means of detection. Hansen et al. (2007) quantified protein thiols and dithiols in picomolar amounts by using 4-DPS as a derivatizing agent [198]. Vignaud et al. (2004) assayed disulfides produced

from the oxidation of glutathione and Cys using by using RP-HPLC coupled with either direct UV absorbance or ECD (coulometric) detection. In order to avoid derivatization, size exclusion was previously performed on a fast protein liquid chromatography (FPLC) system. ECD was found to provide a sensitivity 100 times higher for the disulfides than UV absorbance at 220 nm for underivatized samples. This method allowed the determination not only of glutathione, Cys and their symmetric disulfides, but also of their mixed disulfide, GSSC [199].

Table 2.3: Review of HPLC based detection of glutathione

Sample	**Label**	**LoD**	**Concentration in human blood**	**Ref**
Human blood	FDNB	0.5 μM	1401±113 μM	[200]
Human plasma	OPA	70 nM	-	[201]
Human blood	OPA	14 fM	4.69±0.93 μmol/g Hb	[202]
Rat liver	NPN	-	-	[203]
Human plasma	MBB	0.2 μM	-	[204]
Human urine	MIPBO	3.5 fM	-	[205]
Rat brain	ThioGlo	50 fM	-	[206]
Human plasma	MIAC	2 pM	2.11 μM	[207]
Human plasma	MBB	1.4 nM	-	[208]
Human plasma	SBD-F	-	-	[209]
Human serum	None	19 fM	-	[210]
Rabbit erythrocytes	NEM	-	-	[211]
Human blood	NEM	-	1.31±0.12 mM	[212]
Human blood	NEM	0.01 μM	74.4±21.2 nmol/mg protein	[213]
Rat brain	DTNB	0.16 μM	-	[214]
RAW 267.4 cell line	ABD-F13C	0.01 μM	13-16 nmol/mg protein	[215]
Mouse liver	IAA	-	-	[216]

Continued on next page

Table 2.3 – continued from previous page

Sample	Label	LoD	Concentration in human blood	Ref
Mouse liver	None	0.2 pM	-	[217]
Human urine	FEM	-	-	[210]
Human blood	PHMB	0.8 nM	539.4±70.9 μM	[218]

2.2.7 Gas chromatographic methods

Except for the assay reported in [219], utilizing a flame photometric detector, all GC methods introduced so far for the measurement of glutathione, Cys or their S-nitroso derivatives have utilized MS for detection. GC/C/IRMS was used to assay glutathione and Cys in erythrocytes from very-low-birth-weight infants, with ethyl chloroformate as a derivatizing agent. This method permitted the determination of low ^{13}C enrichments in glutathione following incubation with ^{13}C-Gly, thereby providing a good tool for study of the turnover of glutathione in infants, via determination of the fractional synthesis rate. The authors suggested that this facilitated research into the assessment of de novo glutathione synthesis. In another study by the same research group, GSH and Cys concentrations were determined in erythrocytes from microvolumes of neonate blood through the use of GC/MS. Additionally, ^{2}H-labeling was used to measure ^{2}H-enrichment in glutathione and Cys, which provided a means of kinetic assessment of the AT metabolism in neonates [220]. Cabral et al. (2008) reported the introduction of $^{2}H_2O$ for the estimation of glutathione synthesis. The use of the less invasive $^{2}H_2O$ as tracer offers advantages over radiolabeled AA infusions: the concentrations of precursors in the biosynthetic pathway are not increased, the cost is lower and there is a possibility to follow the synthesis over long time periods. The author swere able to maintain constant $^{2}H_2O$ enrichment for 2 weeks and to follow the synthesis until a plateau was reached, corresponding to the turnover of the entire glutathione pool [221].

2.2.8 Capillary electrophoresis methods

CE is a technique in which the analytes are separated in a narrow (internal diameter: 10–100 μm) capillary containing a background electrolyte. Because of the large resistance of the capillary, a high electric field must be applied. The heat produced is readily dissipated due to the large surface/volume ratio of the capillary.

The advantages of CE include a short duration of analysis, small sample amounts, efficient separation, easy automation and wide applicability. Because of the low amount of analytes arising from the relatively small volumes injected, the LOD is an important issue. Techniques with which the separation efficiency can be enhanced and consequently the sensitivity can be increased include sample stacking [222], microchip and microchannel CE [223], and the novel techniques gradient elution moving boundary electrophoresis (GEMBE) [224] and gradient elution isotachophoresis (GEITP) [225]. During sample stacking, analytes present at low concentrations in a long injected sample zone are concentrated into a short zone (stack). The stacked analytes are then separated and individual zones are detected [222].

For the separation and assay of glutathione and congeners, different CE approaches with different detectors (UV absorbance, FD, laser-induced fluorescence (LIF), ECD and MS) have been used. All methods employed bare fused silica capillaries, except for two studies involving the application of polyimide-coated [226] or polybrene-coated capillaries [227]. A summary of the most recent CE methods reviewed in this article is given in table 2.4.

Table 2.4: Review of CE based detection of glutathione

Sample	Label	LoD	Concentration in human blood	Ref
HaCat cell extracts	NEM	40 μM	-	[228]
Human erythrocytes	None	15 μM	6.77 μmol/g Hb	[229]
Human erythrocytes	None	75 fM	7.14 μmol/g Hb	[230]
Rat liver microdialysate	None	0.75 μM	-	[231]

Continued on next page

Table 2.4 – continued from previous page

Sample	**Label**	**LoD**	**Concentration in human blood**	**Ref**
Human erythrocytes	None	-	0.87 mM	[232]
Human plasma	None	2.35 μM	-	[233]
Human blood	None	5 μM	1078.1±17 μM	[234]
Human plasma	None	0.5 μM	-	[235]
Human plasma	6-IAF	-	7.01±0.51 μM	[236]
Unlysed MGC 803 cancer cell	NDA	-	-	[237]
Acute promyelocytic leukemia cell	NDA	0.5 μM	-	[238]
Human erythrocytes	NDA	6.9 aM	-	[239]
Human erythrocytes	5-IAF	-	6.78±0.92 μM	[240]
HepG2 hepatoma cell	5-IAF	-	-	[241]
HUVEC	5-IAF	0.1 aM	-	[241]
Human plasma	5-IAF	-	-	[242]
Human plasma	5-IAF	-	3.51±0.38 μM	[243]
HUVEC	5-IAF	-	9 nM	[244]
Human plasma	5-IAF	-	-	[245]
Human urine	None	0.134 μM	-	[246]
Human hepatocarcinoma cell	None	1.7 μM	-	[247]
Human blood	None	2.58 μM	-	[248]
Human urine	None	0.08 mg/ml	-	[249]
Cell and plant extracts	None	-	-	[250]
Human erythrocytes	Diazo-luminol	0.05 aM	64.9 aM/cell	[251]

Table 2.5 shows a qualitative comparison based on the problems associated some of the well known techniques for detection of glutathione.

Table 2.5: Comparison of methods for detection of glutathione

Method	Principle	Disadvantages
Colorimetric	Optical	Optical interference,
Chemiluminescence	Optical	lack of
Spectrophotometry	Optical	electrical integration
Liquid chromatography	Chromatography	Poor selectivity
Cyclic voltammetry	Electrochemical	Low electro
Square wave voltammetry	Electrochemical	oxidation rate,
Dual pulse voltammetry	Electrochemical	lack of scope of
Chronoamperometry	Electrochemical	miniaturization
Impedance spectroscopy	Electrochemical	
Proton nuclear magnetic resonance	NMR	Cost of analysis
Capillary electrophoresis	Electrophoresis	Poor selectivity

2.3 FET based biosensor

Field-effect transistor (FET)-based biosensors (BioFETs) have undergone great progress especially in the last decade, since they were first realized in 1980 by Caras and Janata in 1980. Recently, BioFETs have become one of the most important branches of biosensors.

Field-effect transistors (FETs) are suitable candidates for designated sensors, due to their ability to directly translate the interaction with analytes taking place on the FET surface into a readable signal. Consequently, the analytes need not to be labeled, and we classify this technique as the label-free technique for biosensors. From the electrochemical point of view, FET-based biosensors are a three-electrode system, including source, drain and gate electrodes. The work principle is that the electrical conductance of a sensing

component between the source and the drain is sensitive to its environment and varies significantly with surface adsorption of various chemicals and biomolecules.

Nowadays, a diversity of FET-based biosensors can be employed for specific interactions of biomolecules, such as enzymatic reaction, DNA hybridization and antibody–antigen reactions. We tried to classify these biosensors into enzymebased FETs (ENFETs) (Kharitonov et al., 2000), cell-based FETs (Duan et al., 2012) and immunodetection-based FETs (ImmunoFETs; Hideshima et al., 2011). ENFETs which combine ion-sensitive field-effect transistors (ISFETs) with enzymes, are based on biocatalytic reactions affecting the charge at the gate surface, and produce an electronic signal dependent on the enzyme substrate concentration. Various enzymes are studied in the ENFETs, such as glucose oxidase (Liu et al., 2008), urease (Sekiguchi et al., 2000), penicillinase (Gorohkov et al., 1996), horseradish peroxidase (Varma, 2002), tyrosinase (Anh et al., 2002), etc. Cell-based FETs are exploited in the detection of cells metabolism and the analysis interaction of drugs and cells. FETs can also record electric potentials inside cells. Duan et al. (2012) has reported a new approach in which a SiO_2 nanotube is synthetically integrated on top of a nanoscale FET. The nanotube can penetrate the cell membrane, bringing the cell cytosol in contact with the FET, which is then able to record the intracellular transmembrane potential.

ImmunoFETs are the most frequently used biosensors. It is expected to provide immediate and important information regarding initial therapy by detecting the charged antigens related to serious diseases using immobilized antibody modified FETs. However, ImmunoFET biosensing devices for use in the medical field have not been put into full-scale practice until now because there are two challenges. The first potential impediment is the fact that ImmunoFET sensors have difficulty detecting macromolecules in physiological solutions without pretreatment. The second is to overcome the inherent screening of the Debye length (Kulkarni & Zhong, 2012). Therefore, it is critical to increase the sensitivity of FET detection through controlling the Debye length based on the height of the adsorbed receptor. In fact, it has to structure the antibody-modified surface so that it can withstand the electric application throughout the FET measurements to improve reproducibility.

In recent years, many types of nano-materials have been intensely selected as the promising candidates of FET biosensors. One-dimensional semiconducting nanomaterials configured with FETs offer opportunities for real-time and label-free sensing applications, such as silicon nanowires and carbon nanotubes (referred to as carbon nanotube field-effect transistors (CNT-FETs; Iijima, 1991; Kim et al., 2007; Wang, 2005), and silicon nanowire field-effect transistor (SiNW-FETs; Gao et al., 2011; Zhang et al., 2010a). They are also amenable to large-scale and high-density integration. Two-dimensional semiconducting nanomaterials also have attracted great attention as they can be made an ideal biosensor with high selectivity and sensitivity, such as graphene field-effect transistor (GFET; Cheng et al., 2010; Novoselov et al., 2005, 2007).

Table 2.6: Comparison of types of FET biosensors for detection of glutathione

Principle	**Disadvantage**
Nanowire Nanotube	Difficult to functionalize
Liquid gate Floating gate	Charge screening
Graphene FET Organic FET	Reusability, stability
Dielectric modulated Junctionless	Difficult to fabricate

2.4 Channel material for FET

Zinc oxide has become an important material in variety of research areas by virtue of its electrical, sensory, and optical properties, along with being nontoxic and air-stable semiconductor. The increasing interest in fabrication and integration of ZnO based thin film devices is mainly because of its direct wide band gap (3.37 eV), which manifest the fact that it is semiconducting in nature and transparent to visible light. In order to design a low-cost device following a simple, high-throughput process of manufacture is often achieved by simple, solution-based techniques, such as spin coating, inkjet-printing,

or roll-to-roll processes. From that perspective, ZnO nanoparticles present a potential for solution-based manufacturing since it is possible to directly process the semiconductor from a liquid dispersion without the need of a costly or high-temperature process.

Chapter 3

Development of functionalized layer

THE most critical step towards designing a biosensor is development of an efficient functionalization mechanism. This chapter describes the process of developing such a mechanism that can serve the purpose of this work. The conjugation reaction between glutathione and CDNB in presence of GST is the most common method that comprises the core of most of the methods so far reported for detection of glutathione. The aim of this work is to implement this method into an FET based electrochemical device. However, in order to do so, a semiconducting channel layer was necessary where recombinant GST protein could be immobilized. Hence, experiments were carried out to test binding of GST with some semiconducting nanoparticles in order to find out the most suitable combination for this work. ZnO nanoparticles were the first priority to try out binding experiment based on their semiconducting properties and ease of synthesis.

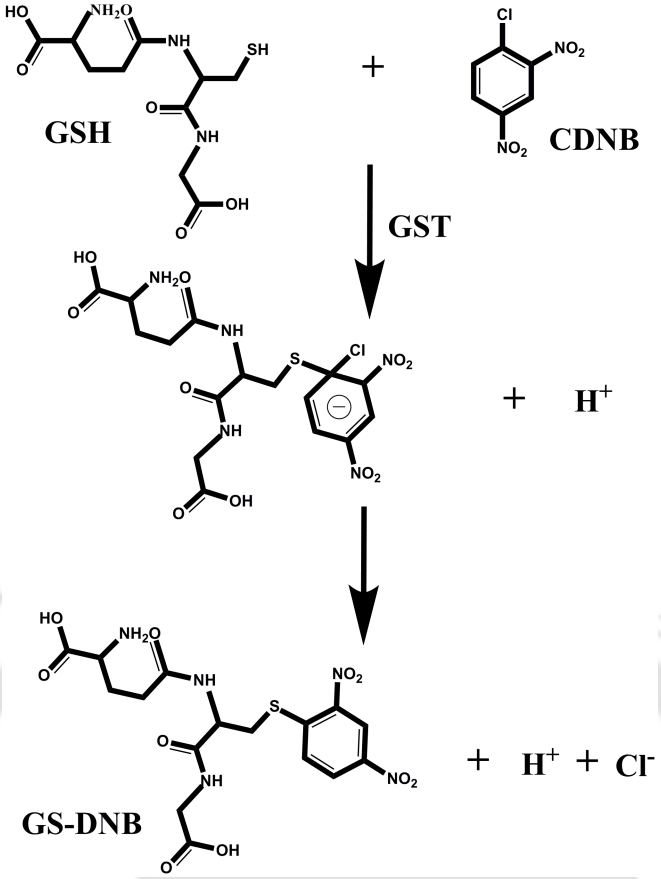

Figure 3.1: Conjugation reaction of GSH and CDNB in presence of GST

3.1 Synthesis of ZnO nanoparticles

3.1.1 Materials

All molecular grade chemicals and reagents were used in this experiment. Zinc acetate dihydrate ($Zn(CH_3COO)_2.2H_2O \geq 98\%$), dimethyl sulfoxide (DMSO $\geq 99\%$), ethanol (absolute) and potassium hydroxide (KOH $\geq 84\%$) were purchased from Merck, India. L-glutathione reduced ($\geq 99\%$) and Methanol ($\geq 99\%$) were obtained from Sigma.

3.1.2 Method

ZnO nanoparticles were synthesized using co-precipitation method reported in [252]. The synthesis process is described below: zinc oxide nanoparticles (ZnO-NPs) were synthesized by dissolving 0.2 M Zinc acetate dihydrate in 20 ml of dimethyl sulfoxide (DMSO)

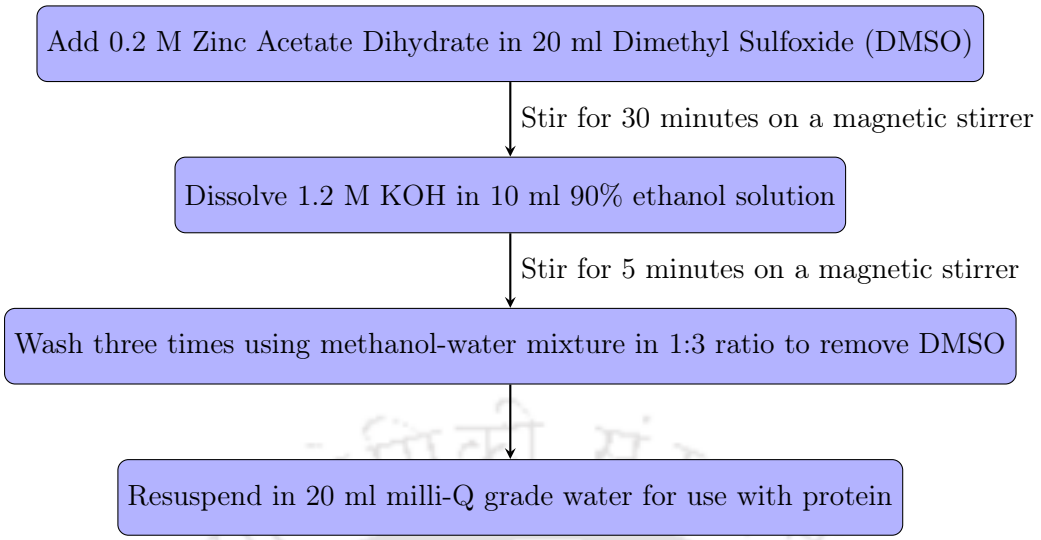

Figure 3.2: Flow chart for synthesis of ZnO nanoparticles

and stirring continuously for 30 minutes. 1.2 M potassium hydroxide (KOH) was dissolved in 10 ml of 90% ethanol and was added to the above solution. Milky white solution of zinc oxide nanoparticles were formed following 5 minutes of stirring as per the reported protocols of Juhi Soni et.al. [252]. The nanoparticles were washed five times (8000 rpm, 5 minutes each) using 1:3 mixture of methanol and water to eliminate DMSO. Finally the nanoparticles were washed with Milli-Q grade water and resuspensed in 10 mM PBS for further analysis and subsequent applications.

3.2 Characterization of ZnO nanoparticles

3.2.1 Transmission electron microscopy (TEM) studies

Synthesized nanoparticles were initially characterized using TEM. The aqueous dispersion of the nanoparticles was dropcast on a copper grid, and the grid was air dried at room temperature before loading for analysis. The average diameter of the nanoparticles was observed to be 18.3 nm $\pm$ 5.68 nm. Figure 3.3 shows the obtained TEM and Selected Area Electron Diffraction (SAED) pattern and the size distribution plot of the synthesized ZnO nanoparticles. The SAED pattern confirms the polycrystalline nature of the ZnO nanoparticles.

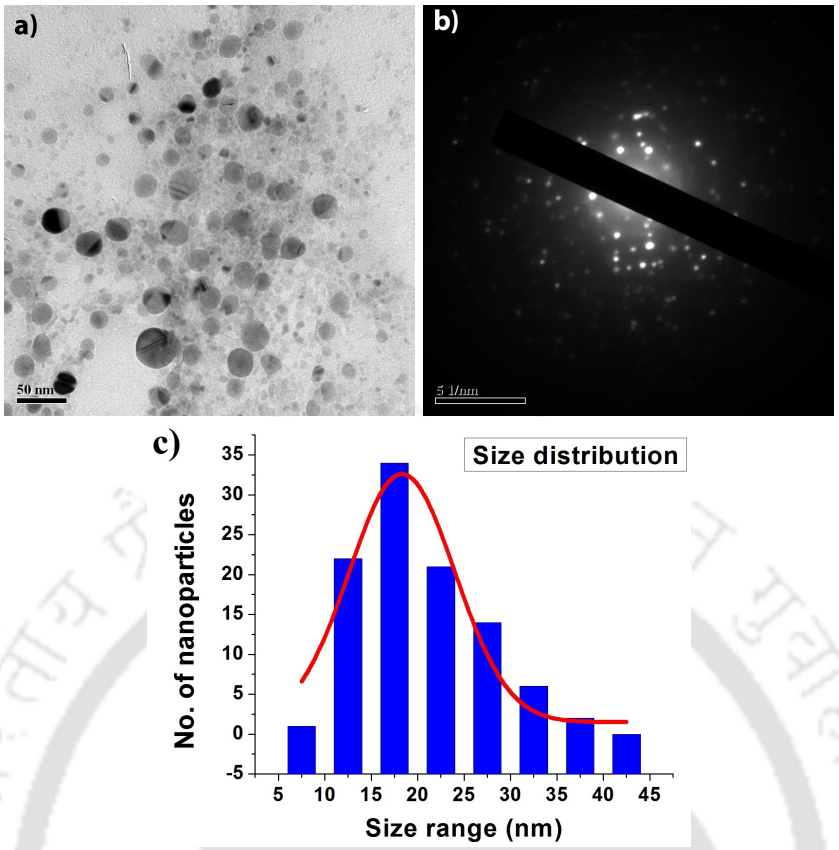

Figure 3.3: (a) TEM image (b) SAED image (c) Size distribution plot of synthesized ZnO nanoparticles

3.2.2 Field Emission Scanning Electron Microscope (FESEM) analysis

FESEM analysis of the synthesized nanoparticles was then carried out for the morphological characterization of the nanoparticles. The aqueous dispersion of the nanoparticles was dropcast on a piece of SiO_2 wafer, and the wafer was air dried at room temperature before loading for analysis. Figure 3.4 shows the obtained FESEM image along with the nanoparticle size distribution plot. Uniform spherical morphology of the ZnO nanoparticles can be prominently observed from the obtained FESEM image. The average nanoparticle diameter calculated from the analysis was 23.5 nm $\pm$ 4.23 nm.

3.2.3 X-Ray Diffraction (XRD) analysis

Synthesized nanoparticles were then centrifuged and the precipitate was air dried under room temperature for XRD analysis. The obtained XRD peaks of the ZnO nanoparticles

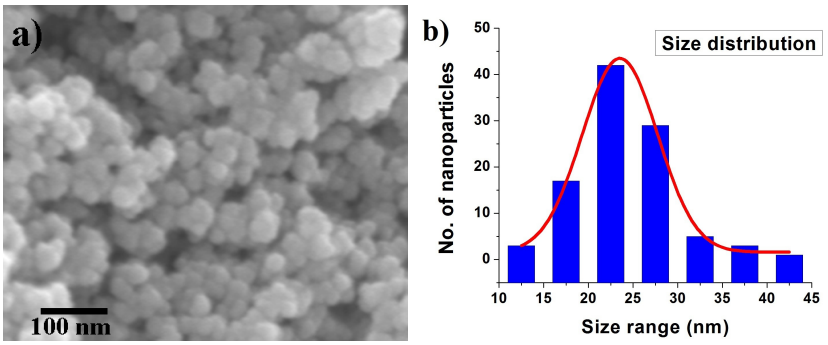

Figure 3.4: (a) FESEM image (with magnification 50000, acceleration voltage 5 kV and working distance 4.5 mm) (b) Size distribution plot of the synthesized ZnO nanoparticles

shown in figure 3.5 are similar to reported results [35]. The d-spacing (lattice spacing) value was calculated for the most prominent peak corresponding to (101) plane using Bragg's law, which is defined as,

$$n\lambda = 2d \sin\theta \tag{3.1}$$

where, n is an integer, λ is the wavelength of a beam of X-rays incident on a crystal with lattice planes separated by distance d, and θ is the Bragg angle. The d-spacing value calculated from this equation was found to be 2.46 Å. The lattice constants calculated from this d-value were found to be a = 3.23 Å and c = 5.19 Å. These values agree with previously reported results [36]. The average size of the nanoparticles can be calculated from the Debye-Scherer formula which is defined as,

$$D = [0.9\lambda]/\beta \cos\theta \tag{3.2}$$

where, λ is the radiation source wavelength, and β is the Full Width Half Maximum (FWHM in radians) of the most prominent diffraction peak located at $2\theta = 36.38°$ corresponding to the (101) plane. The average particle diameter was found to be 21.45 nm, which was similar to the FESEM data.

3.2.4 UV spectroscopic studies

UV spectroscopic studies of ZnO nanoparticles were performed using Perkin Elmer Lambda 25 UV/VIS Spectrometer. The UV spectroscopy revealed a characteristic peak

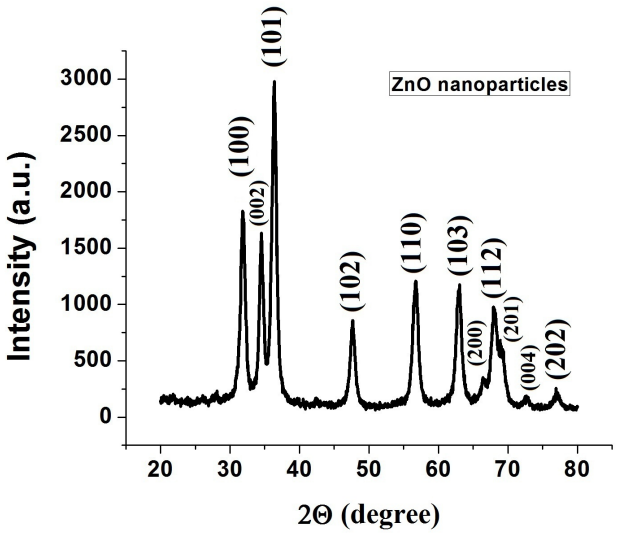

Figure 3.5: XRD analysis of ZnO nanoparticles

at 355 nm, which is a specific indicator for the presence of ZnO nanoparticles. (i.e., the nanoparticles synthesised are ZnO). Also the absence of any other peak indicates absence of impurities.

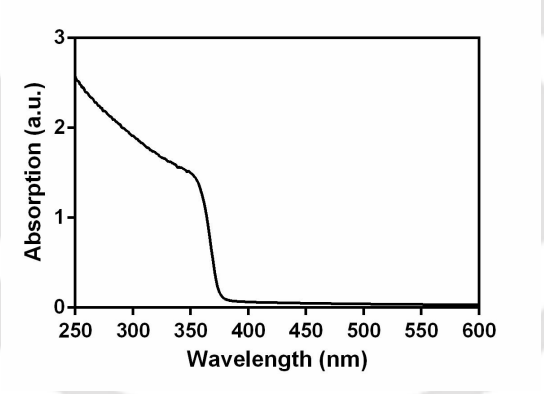

Figure 3.6: UV spectroscopic analysis of ZnO nanoparticles

3.3 Purification of protein

The solubilized protein (present in the supernatant) obtained by means of primary culture, secondary culture followed by cellular lysis of 30 μl of glycerol stock of bacteria E.coliBL21 harbouring the vector pGEX4t2 was passed through the glutathione agarose beads for purification by affinity chromatography. Elution buffer was prepared by adding

10 mM of reduced glutathione to 5 ml of 50 mM Tris, pH 9.5. The column bound recombinant GST was eluted with the elution buffer [33]. Flow through was collected in fractions and stored at -20°C. The protein fractions were analyzed using 12% sodium dodecyl sulfate polyacrylamide gel electrophoresis (SDS PAGE).

3.3.1 Estimation of protein by Bradford Assay

Bradford assay method was implemented in order to estimate the concentration of purified recombinant GST protein. The standard assay solution was prepared using bovine serum albumin of concentration 0.5 μg/mL to 10 μg/mL. 10 μL of the protein sample was incubated with 90 μL of Bradford reagent solution (Sigma) in a 96-well plate at room temperature for 10 minutes in dark condition, which resulted in development of a blue coloured solution. This solution was then put under TECAN Elisa plate reader at the wavelength of 595 nm for optical density measurement.

3.3.2 Enzyme activity

Activity of GST was determined with CDNB as substrate. The reaction medium contained 0.1 M PBS buffer (pH 7.5), 1.0 mM GSH and CDNB and protein in a total volume of 1.0 mL. Absorbance of the solution after addition of protein sample was measured at 340 nm for first 10 minutes at an interval of 1 minute and at an interval of 5 minutes for next 30 minutes. The change in absorbance was measured using TECAN Elisa plate reader at the wavelength of 340 nm in a 96-well plate against a reference containing CDNB and glutathione. One unit of activity is defined as the formation of 1 μM product per min at 25°C (extinction coefficient at 340 nm, in a 96-well plate is 5.3 for CDNB).

$$\text{Change in absorbance}(\Delta A_{340})/\text{min} = (A_{340\ \text{final}} - A_{340\ \text{initial}})/\text{reaction time} \quad (3.3)$$

$$\text{GST activity}(\mu\text{M/ml/min}) = (\Delta A_{340})/\text{min}*V(\text{ml})*D)/(V_{enz}(\text{ml})*E_{mM}) \quad (3.4)$$

Where, V = Total reaction volume, V_{enz} = Volume of enzyme used, D = Dilution factor, E_{mM} = Molar extinction co-efficient

Characterization results of purified protein (SDS PAGE, CD spectroscopy, MALDI plot, Bradford Assay standard curve and Enzyme activity plot) has been shown in figure 3.7.

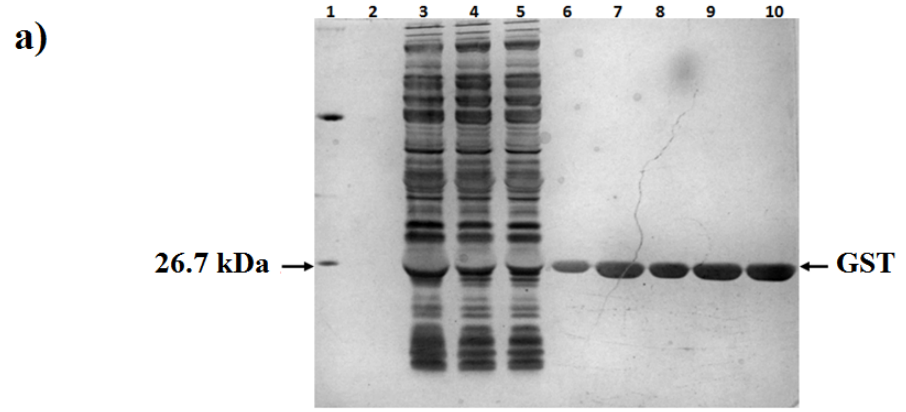

Protein purification analysis-SDS PAGE gel. Lane 1: Protein ladder (2-212 kDa), Lane 2: blank, Lane 3-5: Flowthrough, Lane 6-10: purified GST protein.

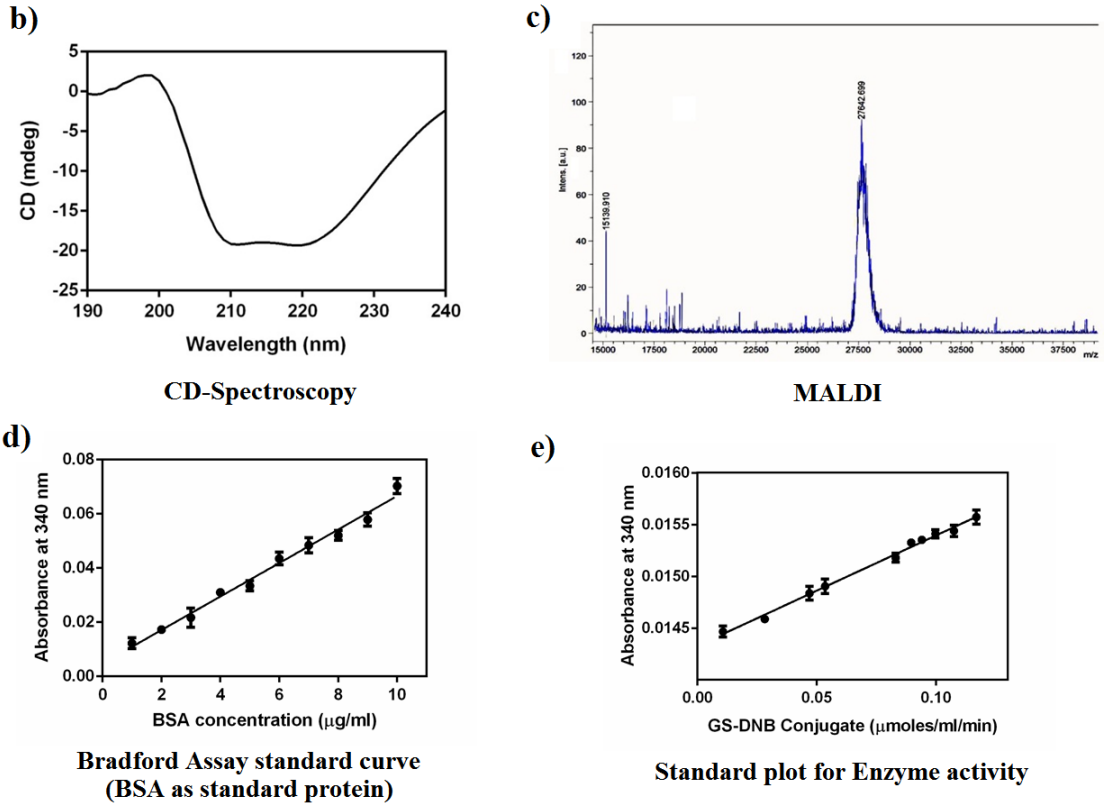

Figure 3.7: (a) SDS PAGE (b) CDS (c) MALDI (d) Bradfor Assay (e) Enzyme activity plot

3.4 Binding analysis

3.4.1 Binding of nanoparticles and protein

The binding of recombinant GST protein onto the surface of zinc oxide nanoparticles was analyzed using fluorescence spectroscopy. For the analysis, different concentrations of protein were incubated with a fixed amount of the nanoparticles synthesized for 3 hrs. at 37°C. After 3 hrs. the contents were centrifuged at 8000 rpm for 10 min, and the amount of unbound protein was quantified using spectrophotometer. The protein concentration was compared with the control protein. The percentage of binding was calculated as shown below:

$$\text{Binding}(\%) = [(\text{total protein} - \text{unbound protein})/\text{total protein}]*100 \qquad (3.5)$$

Before binding ZnO nanoparticles and the enzyme, zeta potential of each of them was measured using Laser Doppler Micro-Electrophoresis. Obtained values of zeta potential

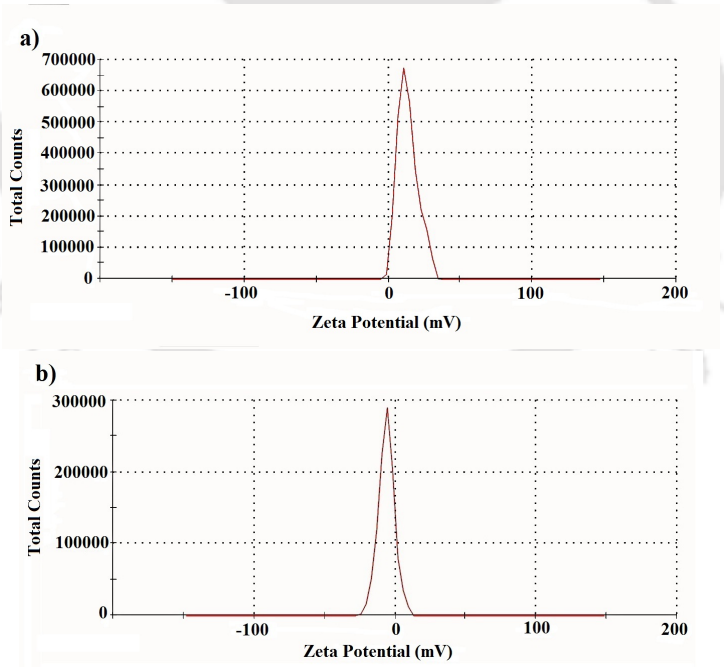

Figure 3.8: Zeta potential measurement of (a) ZnO nanoparticles and (b) purified GST at pH 7.5

for ZnO nanoparticles and purified recombinant GST at a pH level of 7.5 were 13.4 mV

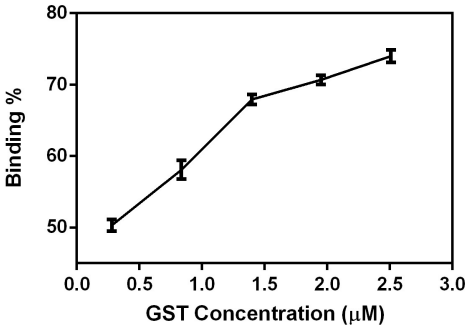

Figure 3.9: Binding analysis of GST-ZnO nanocomposite

and -6.21 mV respectively. Since both are of opposite polarity, the bonding between them is most probably electrostatic. Binding experiments resulted in 73.8% binding of recombinant GST with the ZnO nanoparticles as shown in figure 3.9.

3.4.2 Kinetic parameters

The kinetic parameters of both GST and GST bound ZnO nanoparticles were determined with respect to the substrates, GSH and CDNB, using Michaelis–Menten model. The enzyme concentration was held constant at 10 nM throughout the process. K_m and V_{max} were determined from the Michaelis-Menten plot of rate of reaction (μmol S-(2,4-dinitrophenyl)glutathione/min/ml protein) versus substrate concentration (mM). After that the catalytic efficiency was calculated using the following formula. The obtained values are described in table 3.1.

$$k_{cat} = V_{max}/[E_t] \tag{3.6}$$

Where, k_{cat} = turn over number, $[E_t]$ = concentration of total enzyme used, V_{max} = maximum rate of product formation per minute

In figure 3.10(a,b) concentration of one component is varied while the others are held constant. In figure 3.10(a), at 10 nM concentration of GST, when GSH is kept constant at 2.0 mM, increase of CDNB from 0.5 mM to 2.0 mM shows marked increase in the product (GS-DNB) formation, whereas increasing CDNB concentration beyond 2.0 mM does not show a large change in product formation. A similar trend is observed for figure

Table 3.1: Kinetic parameters

Parameters	GST	ZnO-GST	GST	ZnO-GST
	CDNB as substrate		GSH as substrate	
V_{max} (μmoles/ml/min)	48.67	188.2	61.32	135.3
K_m (mM)	1.431	1.713	0.427	0.3936
k_{cat} (s^{-1})	81.1	313	102.2	225
K_m/k_{cat} ($M^{-1}s^{-1}$)	$5.66x10^4$	$18.2x10^4$	$2.39x10^5$	$5.73x10^5$

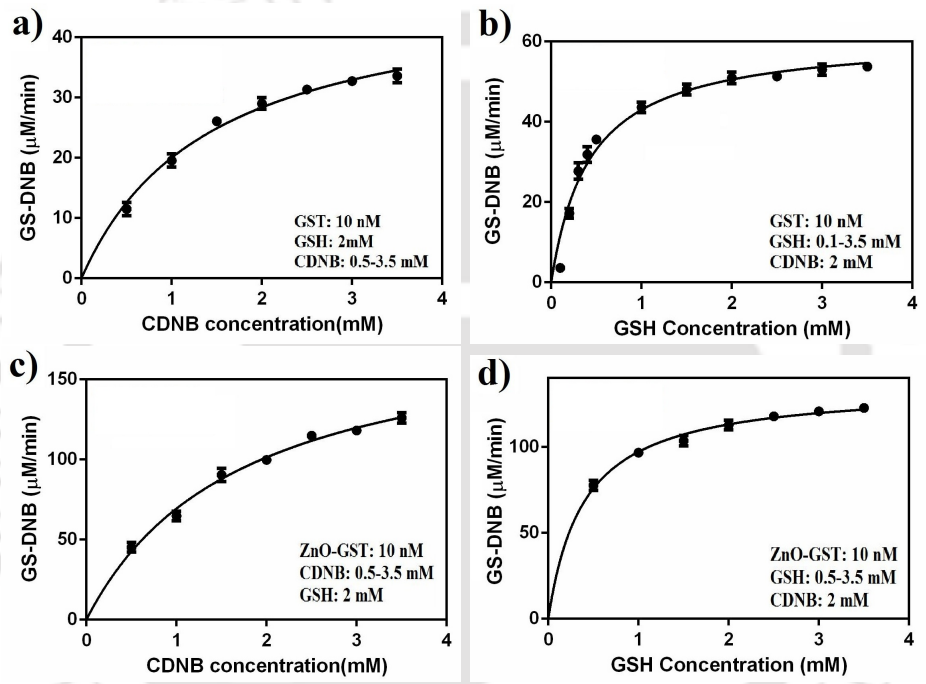

Figure 3.10: Michaelis Menten plot with (a) varying CDNB concentration (b) varying GSH concentration using GST alone and (c) varying CDNB concentration (d) varying GSH concentration using GST-ZnO composite nanoparticles

3.10(b). Therefore we can infer that the optimum reaction is obtained at a 1:1 ratio of GSH:CDNB. This study also forms the base for comparative analysis of enzyme efficiency when acting alone and in conjugation with ZnO nanoparticles. Figure 3.10(c,d) depicts the kinetic study of the enzyme when in conjugation with the ZnO nanoparticles. We can clearly observe that there is no change in the trend of the curves, and the optimum ratio of GSH:CDNB remains 1:1. This indicates that the conjugation does not interfere with the reaction. A large increase in the rate of GS-DNB formation is observed (maximum velocity (V_{max}) of the reaction has increased). This is most probably due to the increased

availability of GST enzyme to catalyze the reaction as it has now been immobilized. It is further confirmed by the fact that CDNB and GSH do not react in the presence of ZnO nanoparticle alone. From the data represented in table 3.1, it is clear that noticeable increase occurs in the catalytic efficiency (k_{cat}) of the enzyme when present in conjugation with ZnO nanoparticles (most probably due to enhanced availability following immobilization). The K_m remains nearly the same in case of GST and GST-ZnO conjugate for each of the substrates (GSH and CDNB) individually. This suggests that the affinity of the enzyme towards the substrates remain unchanged, further confirming the belief that ZnO nanoparticles do not harm the integrity or the functionality of GST when in conjugation. (Small K_m value indicates requirement of lower concentrations of substrate for the reaction to reach half of its maximum velocity.) The ratio of k_{cat}/K_m is considered as a measure of enzymatic efficiency. In this case, we observe that the efficiency remains in the same order of magnitude, but increases slightly on conjugation with ZnO nanoparticles.

3.5 Experiments on Au nanoparticles

Au nanoparticles were synthesized and similar binding experiment of Au nanopartilces and GST was carried out. Obtained results are shown below:

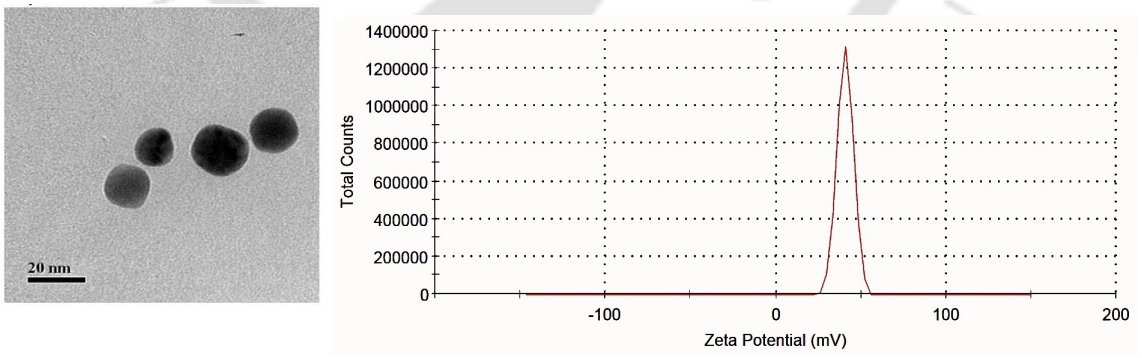

(a) TEM image (b) Zeta potential

Figure 3.11: Characterization of Au nanoparticles

Zeta potential of Au nanoparticles was found to 40.7 mV and after binding with purified recombinant GST, 70% binding was observed as shown in figure 3.12. But binding

percentage tends to saturate with further increase in concentration of GST as visible from the plot.

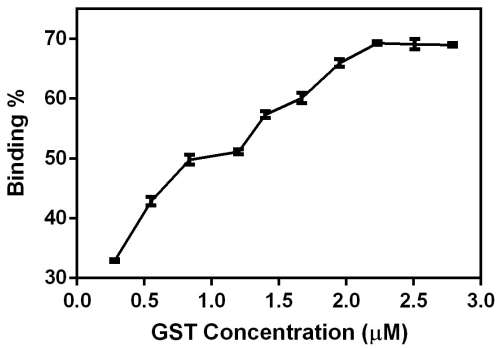

Figure 3.12: Binding analysis of Au nanoparticles and GST

3.6 Experiments on Cu nanoparticles

Cu nanoparticles were also synthesized and similar binding experiment of Cu nanoparticles and GST was carried out. Obtained results are shown below:

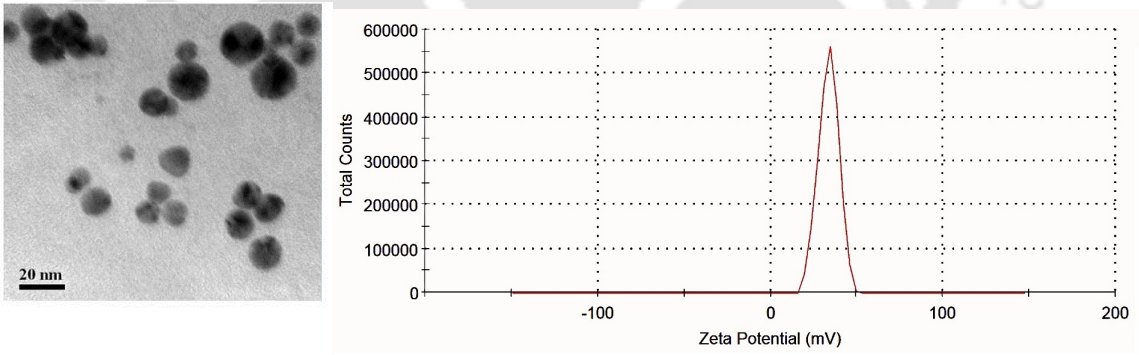

(a) TEM image (b) Zeta potential

Figure 3.13: Characterization of Au nanoparticles

Zeta potential of Cu nanoparticles was found to 34.4 mV and after binding with purified recombinant GST, 32% binding was observed as shown in fig.3.14.

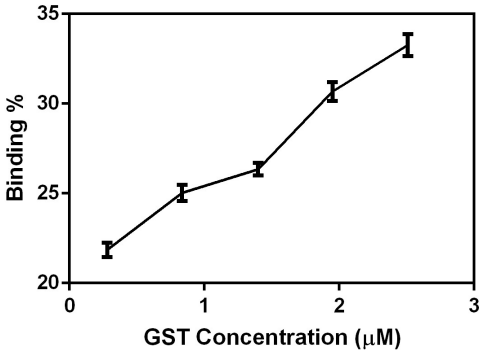

Figure 3.14: Binding analysis of Cu nanoparticles

3.7 Comparison of ZnO, Au and Cu nanoparticles

After completing similar binding experiments on ZnO, Au and Cu nanoparticles, finally binding of ZnO nanoparticles with purified recombinant GST was found to be the best one. A comparative table is shown below:

Table 3.2: Comparison of ZnO, Au and Cu nanoparticles

Nanoparticles	Zeta potential (mV)	Binding (%)
ZnO	13.4	73.8
Au	40.7	70
Cu	34.4	32

3.8 CV analysis

Synthesized ZnO nanoparticles were then characterized for their semiconducting properties and the first step was CV (Capacitance-Voltage) analysis. CV analysis confirms whether the nanoparticles behave as n-type or p-type material. This analysis was accomplished by characterizing a Metal-Oxide-Semiconductor (MOS) structure which was designed by depositing a layer of synthesized nanoparticles on a $Si-SiO_2$ wafer as shown in figure 3.15. The capacitance of a MOS structure depends upon the voltage applied on gate terminal and type of the semiconducting material.

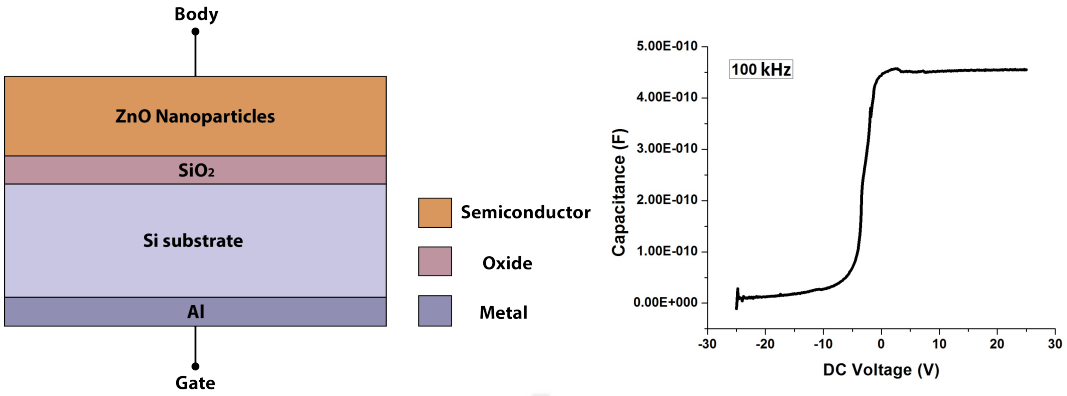

Figure 3.15: Schematic of MOS capacitor and CV analysis

It can be observed from figure 3.15 that negative gate voltage results in formation of depletion capacitance parallel to oxide capacitance resulting in decrease of overall capacitance across the terminals. Whereas for positive gate voltage the device capacitance remains at its maximum value of oxide capacitance due to accumulation of majority carriers near the oxide interface. This is a standard behaviour of n-type semiconducting material. Thus synthesized ZnO nanoparticles were confirmed to posses n-type semiconducting properties.

3.9 Synthesis of p-type ZnO nanoparticles

ZnO nanoparticles naturally exhibits n-type conductivity due to oxygen vacancies and Zn interstitials as well as the incorporation of hidden hydrogen atoms within the ZnO host lattice. The concentration of n-type carriers in ZnO can be further increased by doping with different donor dopants such as B, Al, Ga and In. On the other hand, the controlled doping of p-type ZnO nanoparticles remains a challenged goal for achieving the desired optical and electronic semiconductor properties. Different approaches have been proposed to obtain p-type ZnO nanoparticles among which nitrogen doping is proven to be the most effective. Nitrogen has been considered a good candidate for a shallow acceptor level in ZnO because of the similarity of the covalent radius of N (0.75 Å) and that of O (0.73 Å), and N-doped ZnO nanostructures are predicted to greatly improve the performance of ZnO-based optoelectronics and several other applications.

In this work, a method reported in [253] was followed in order to synthesize N-doped

p-type ZnO nanoparticles. This method is based on application of MWI (Microwave Irradiation) and has been reported to produce high-quality ZnO nanosturctures with controlled morphology and doping level. The aim of synthesizing p-type nanoparticles is to check if they offer better performance in terms of semiconducting properties compared to that of conventional n-type ZnO nanoparticles.

3.9.1 Synthesis process

100 mL of 0.1 M anhydrous zinc acetate was mixed with 100 mL of 0.1 M NaOH. After mixing, a white precipitate formed and was removed from solution by centrifugation (3000 rpm for 5 min) followed by three washing with water. The precipitate was dispersed in 50 mL of 1 M H_2O_2 and heated in a closed vessel at 70°C for 2 hrs. The gelatinous solution was then uncapped and dried at 70°C. The resulting ZnO_2 powder was used as the starting material. ZnO_2 and 1 mM urea were dissolved in Oleylamine (OAm), which acts as the solvent for the reactants and the capping agent for the resulting N-doped ZnO nanoparticles. The reaction mixture was heated in a hot oil bath with stirring to 110°C and the temperature was maintained for 1 hr. to assist in dissolving the reactants and removing water. After heating, the reaction mixture was transparent yellow in colour; MWI was applied for 3 min at ambient pressure in an open test tube, which resulted in the solution becoming pale pink and opaque, indicating the formation of ZnO.

3.9.2 Characterization

The UV spectrum analysis shows a blue shift as shown in figure 3.16(a) due to presence of urea or in other words due to N-doping. This shift due to N-doping is most likely a result of Burstein-Moss effect, where the shift of the fundamental absorption edge results from the high electron density in the conduction band (n-type) or in the valence band (p-type). The CV analysis also confirms that the nanoparticles are of p-type i.e. Nitrogen doping is apparent from figure 3.16(b).

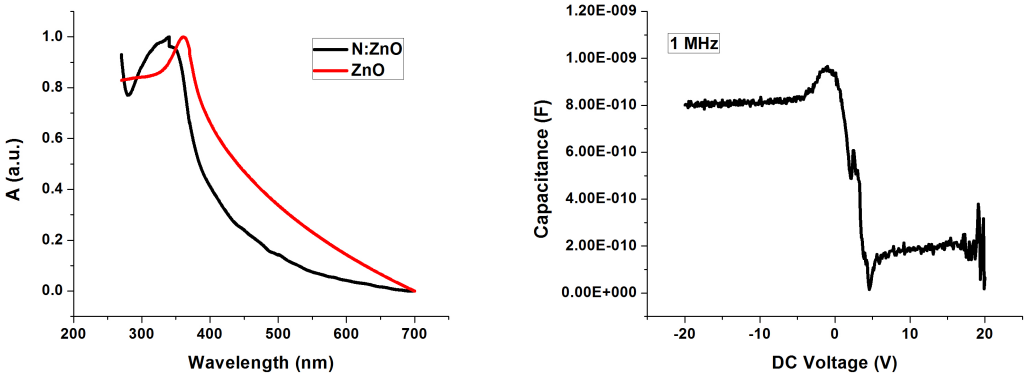

(a) UV analysis (b) CV analysis

Figure 3.16: Characterization of p-type ZnO nanoparticles

3.9.3 Binding analysis

Synthesized p-type ZnO nanoparticles were characterized for binding with GST protein. Zeta potential of p-type ZnO nanoparticles were found to be -2.4 mV, having the same polarity as that of GST protein; which dints the probability of electrostatic binding between them by principle. The binding analysis shown in figure 3.17 confirms that the binding between them is about 6%, which is negligible.

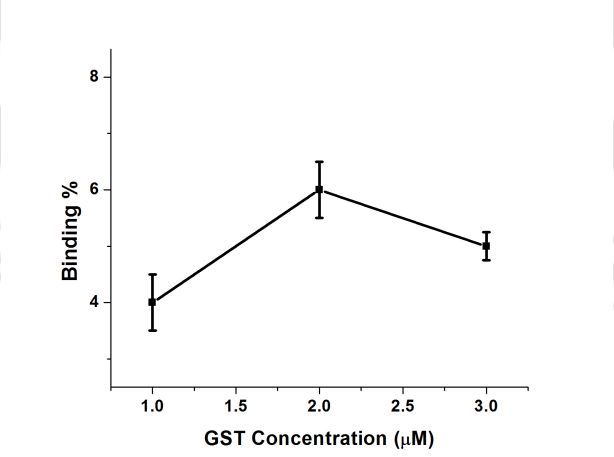

Figure 3.17: Binding analysis

3.10 Conclusion

This chapter dealt with development of an efficient functionalization mechanism which can be incorporated with an electrochemical device to be fabricated. Binding of recombinant GST were tried with different synthesized nanoparticles and ZnO nanoparticles were found to have formed highest binding with GST. This chapter also gives an insight on purification and kinetic studies of recombinant GST along with characterization of synthesized nanoparticles. Binding analysis was carried out based on measured zeta potential of analytes and binding efficiency was measured by means of UV analysis. Finally, p-type ZnO nanoparticles were synthesized as conventional ZnO nanoparticles were found to posses n-type semiconducting properties. In the context of FET characteristics, both type of semiconducting nature plays an important role because of which p-type ZnO nanoparticles were synthesized and tested; but they were less efficient in terms of binding with recombinant GST. Thus, from all the outcomes reported in this chapter, nanoconjugate of ZnO nanoparticles and GST stood out as the best material to be used as the channel material of FET device to be fabricated.

Chapter 4

Simulation studies of ZnO nanoparticle based FET

In this chapter a Field Effect Transistor (FET) having ZnO nanoparticles as the channel layer is simulated and proposed for possible biosensing applications. Based on simulations carried out using device simulation tool COGENDA TCAD, performance analysis in terms of threshold voltage, subthreshold slope, transconductance and on-off current ratio is measured. The structure under investigation is a bottom-gate FET device. The drain current flowing through the channel is controlled by the external potential applied at the gate terminal. The channel acts as a chemiresistive channel, whose conductivity changes on being electrostatically bound to certain biomolecule or protein. Based on its positive zeta potential, the electrostatic affinity of ZnO nanoparticles with certain proteins can be employed for specific detection of that protein. In addition, the simulated ZnO nanoparticles based FET device has dimensions favorable to be used as a biosensor along with scope of miniaturization. Hence, it can be stated that the proposed FET will be of great promise for future nanobiosensors, and if realized by proper fabrication, it may outperform the conventional sensors already in use for detection of biomolecules as well as for theranostic applications.

4.1 Simulation setup

2-D numerical simulation using COGENDA TCAD tool was carried out for a structure described in [254] . The purpose of simulating already reported structure was to validate our simulation setup by replicating the reported results. The Lombardi mobility model was employed; it accounts for the temperature, doping, and field-dependence effects. The Fermi–Dirac carrier statistics, along with standard recombination models, were used in the simulation. Throughout the simulations, the channel length and the device width were takes as 1 μm. In addition, the source and drain length (L_S and L_D) were assumed to be small (10 nm) compared to the channel length. This way, parasitic resistance effects were neglected. The results obtained after simulation were compared with the reported results in [254] and are shown below.

4.2 Simulation results

Using the simulation setup described above, different device characteristics of the structure reported in [254] were simulated and compared with the reported results in order to validate the simulation setup. Initially output and transfer characteristics of the device i.e. effect of drain and gate voltage on drain current were simulated. After that effect of oxide thickness, channel thickness and channel doping concentration on device characteristics were simulated and compared; followed by derivation of output and trans conductance curves from these analysis were performed. Figure 4.1 shows the structure that was simulated.

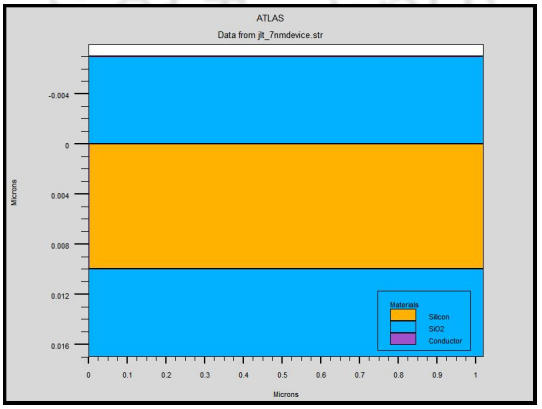

Figure 4.1: Simulated structure

4.2.1 Output characteristics

Figure 4.2 shows the simulated structure along with its output characteristics (simulated and reported). It shows the change in drain current with respect to drain voltage at different gate voltages.

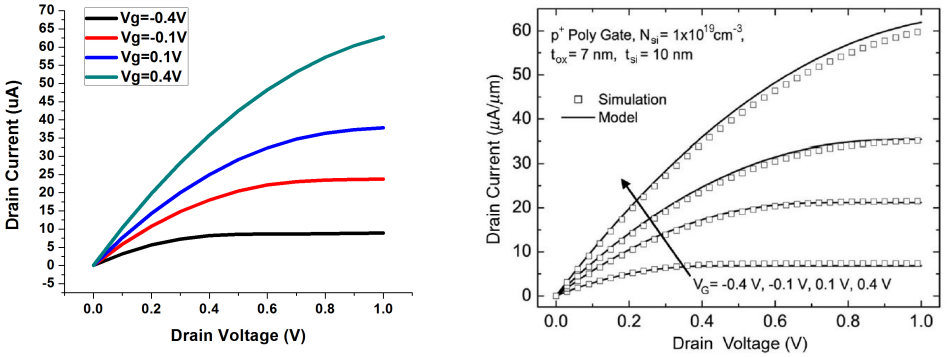

(a) reported (b) simulated structure

Figure 4.2: Output characteristics of a DG-JLFET for different gate voltages

4.2.2 Transfer characteristics

Figure 4.3 shows the transfer characteristics (simulated and reported) of the device. It shows the change in drain current with respect to gate voltage at different drain voltages.

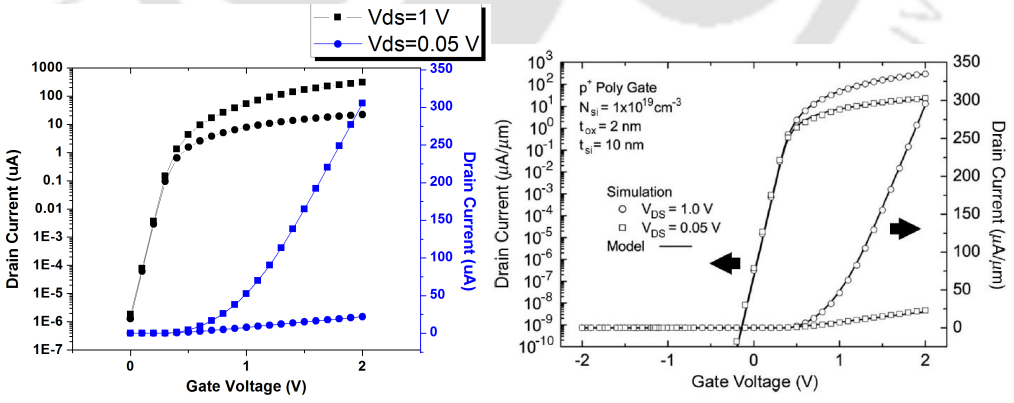

(a) simulated (b) reported

Figure 4.3: Transfer characteristics of a DG-JLFET for different drain voltages

4.2.3 Effect of oxide thickness

Figure 4.4 and figure 4.5 show the effect of change in oxide thickness on device characteristics; validated with reported results. With increase in oxide thickness oxide capacitance decreases, which results in lower threshold voltage and higher drain current.

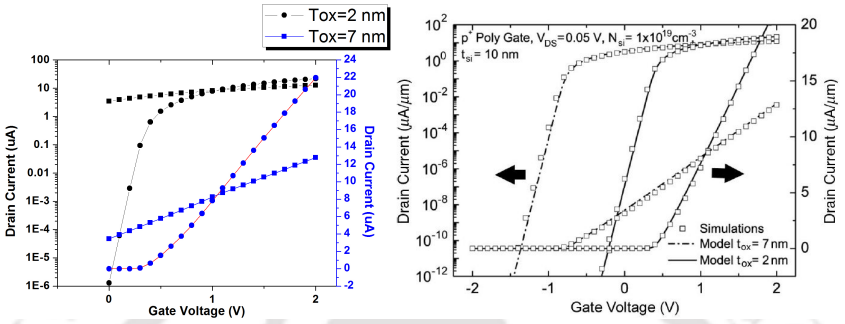

(a) simulated (b) reported

Figure 4.4: Transfer characteristics of a DG-JLFET for different oxide thickness

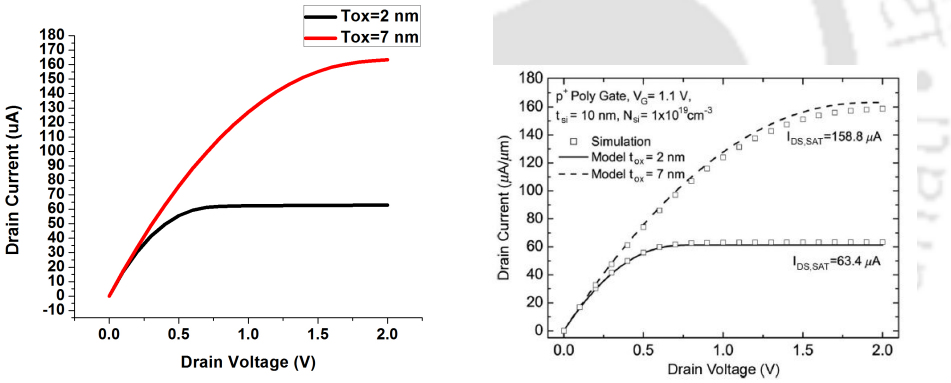

(a) simulated (b) reported

Figure 4.5: Output characteristics of a DG-JLFET for different oxide thickness. The transistors are biased at a gate voltage equal to 1.1 V (V_{FB})

4.2.4 Effect of channel thickness

Figure 4.6 shows effect of channel thickness on transfer characteristics of the device. Threshold voltage of a device decreases with increasing channel thickness due to variation in doping concentration. Figure 4.7 shows combined effect of oxide and channel thickness on it. It shows how oxide thickness and channel thickness can be tuned to keep threshold voltage constant.

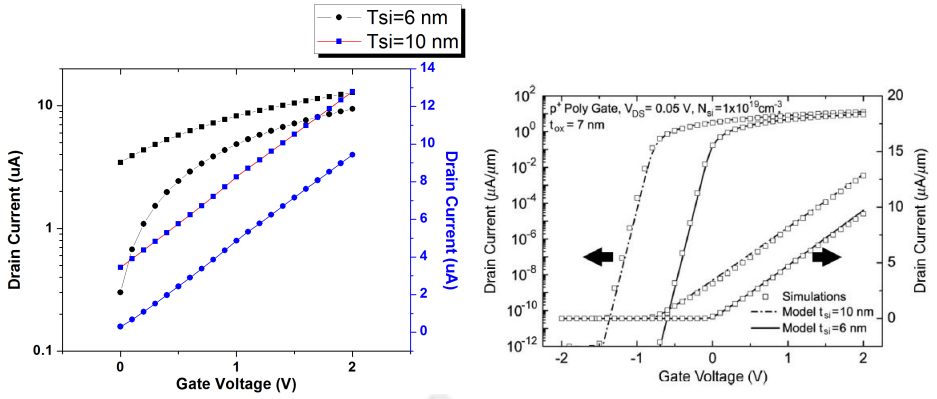

(a) simulated (b) reported

Figure 4.6: Transfer characteristics of a DG-JLFET for different channel thickness

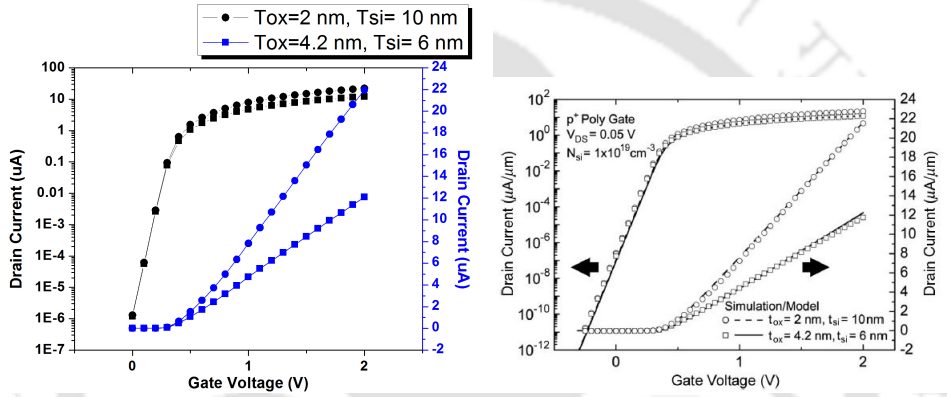

(a) simulated (b) reported

Figure 4.7: Transfer characteristics of two DG-JLFETs with equivalent threshold voltages and different channel and oxide thickness

4.2.5 Effect of channel doping concentration

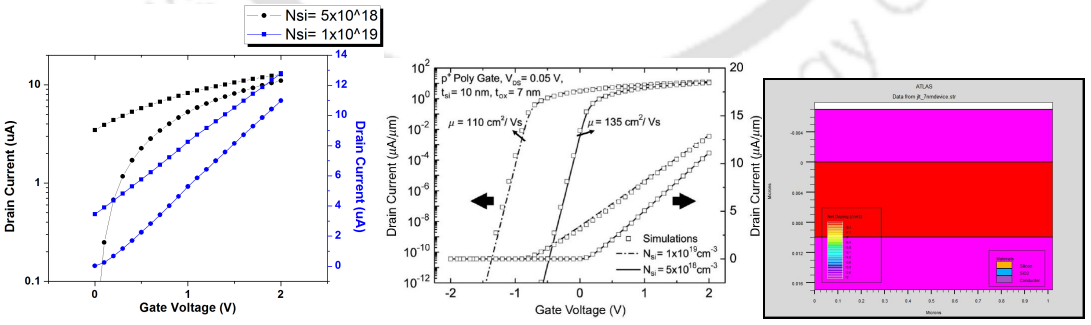

(a) simulated (b) reported (c) doping concentration

Figure 4.8: Transfer characteristics of a DG-JLFET for different channel doping concentrations

Figure 4.8 shows effect of change in channel concentration on transfer characteristics of

the simulated device. Higher doping concentration results in higher conductivity through the channel; which in turn results in higher drain current and lower threshold voltage.

4.2.6 Output and trans conductance

Figure 4.9 and figure 4.10 are output and trans conductance plots of the simulated device along with the corresponding reported results. These two plots were obtained from the derivative of output and transfer characteristics curves of the device.

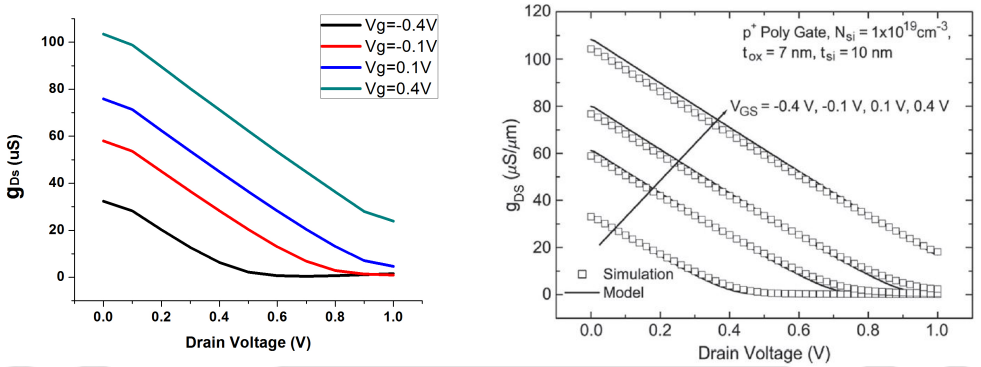

(a) simulated (b) reported

Figure 4.9: Output conductance versus drain voltage of a DG-JLFET for different gate biases

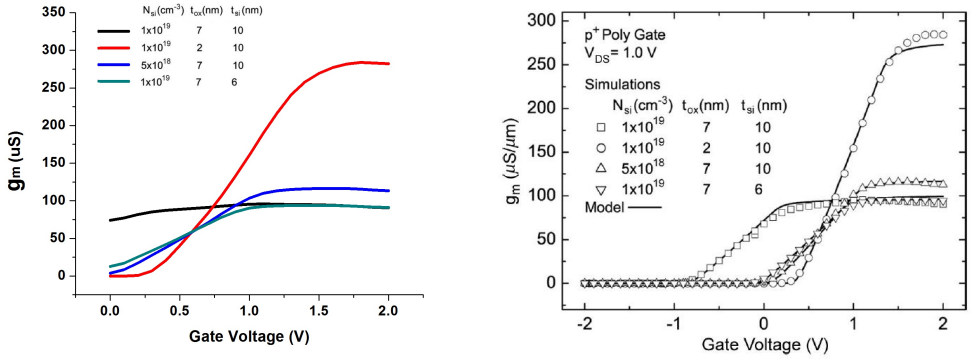

(a) simulated (b) reported

Figure 4.10: Transconductance versus gate voltage for different DG-JLFETs

The results reported in [254] were successfully obtained using the models mentioned in section 4.1. Hence the simulation setup used can be considered to be correct and can be implemented for simulating characteristics of the device proposed for this thesis and accordingly the structure can be optimized based on the simulation results.

4.3 Device structure

The structure of the proposed device is shown in figure 4.11 (not to scale). The channel consists of ZnO nanoparticles. The channel thickness and oxide thickness are 1 μm and 300 nm respectively. Below that lies a Si layer of thickness 500 μm and below that 1 μm thick Al contact, which acts as the bottom gate. The Si layer is doped with donor concentration of $1x10^{16}cm^{-3}$. The source/drain/gate contacts are formed with Al. Table 4.1 shows the complete dimensions of the simulated structure.

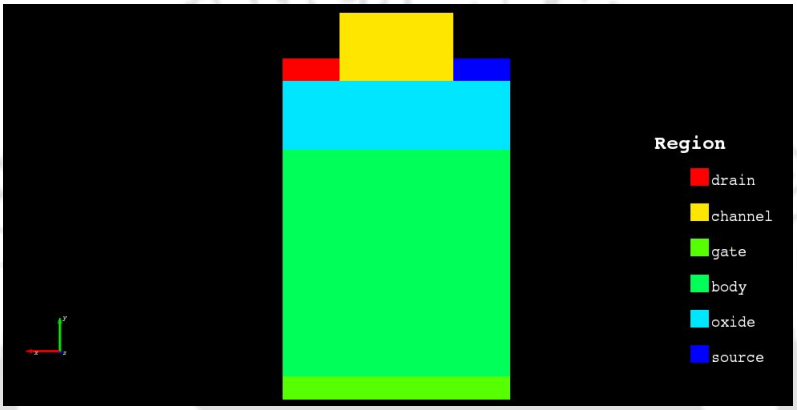

Figure 4.11: Simulated structure (not to scale)

Table 4.1: Dimensions of the simulated structure

	Dimensions (μm)	
	Length	Thickness
Si body	100	500
SiO_2	100	0.3
Channel	5	1

4.4 Simulation setup

The numerical analysis and 2-D simulation was carried out using device simulation tool COGENDA TCAD. Steady state analysis was implemented in order to evaluate the different characteristics of the device under varying potentials. Basic drift-diffusion

equations, Boltzmann carrier statistics, Lombardi mobility model and SRH recombination rates were applied in order to carry out the simulation. Doping concentration (donor and acceptor for n-type and p-type respectively) of $1.5x10^{13}cm^{-3}$ was applied to the channel material based on the experimentally calculated resistivity values of ZnO nanoparticles (discussed in next chapter). The electron mobility value of 75 $cm^2/V-s$ for ZnO nanostructures were considered for simulation [255].

4.5 Results and discussion

The structure shown in figure 4.11 was simulated using COGENDA TCAD device simulator tool. Figure 4.12(a) shows the output characteristics of the proposed device considering acceptor type doping, obtained by plotting the drain current versus drain voltage for different values of gate voltage. A drain current of 2 μA was exhibited at a gate voltage of -5 V and a drain voltage of 5 V. Figure 4.12(b) shows the transfer characteristics of the structure obtained after simulation. It shows the drain current versus gate voltage plotted by keeping the drain voltage fixed at different values for the different plots. A drain current of 1.1 μA and a threshold voltage of 0.9 V was obtained from this plot at a drain voltage of 5 V and a gate voltage of -2 V. For sensing applications, drain voltage can be kept fixed at 2 V and less than 0.9 V has to be applied through the gate region, so that the device operates in the linear region.

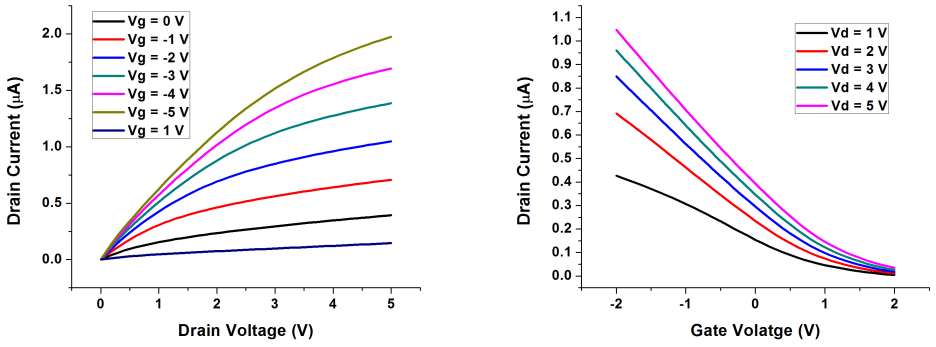

(a) Output characteristics (b) Transfer characteristics

Figure 4.12: Output and transfer characteristics of p-FET

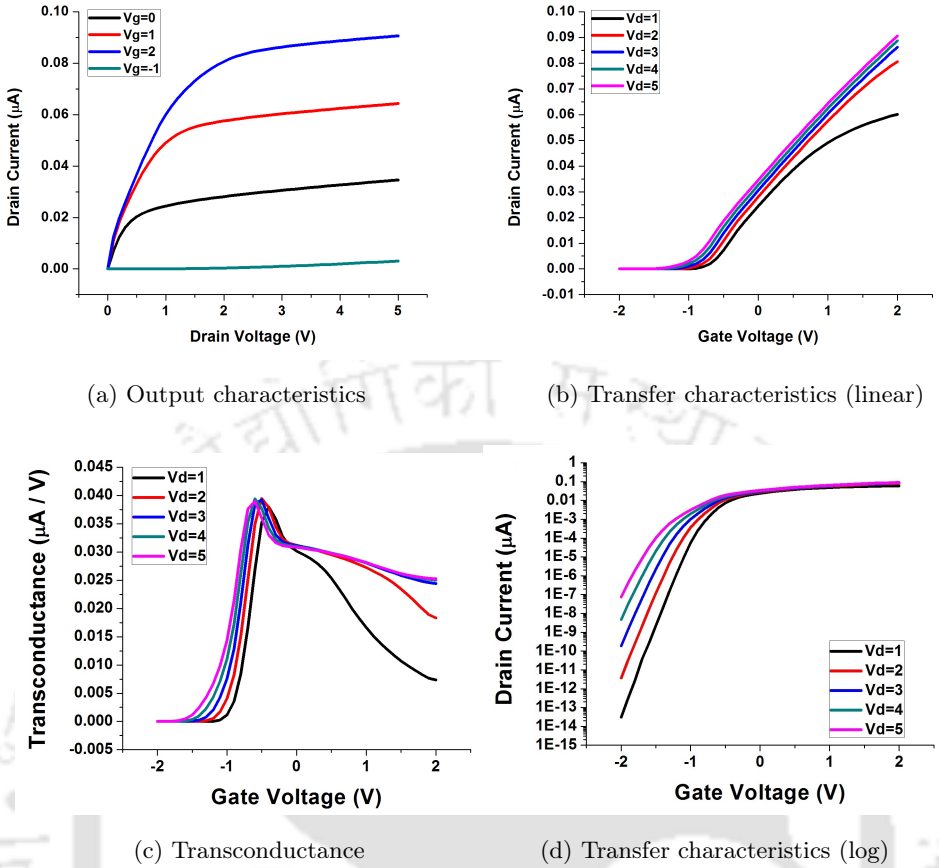

(a) Output characteristics

(b) Transfer characteristics (linear)

(c) Transconductance

(d) Transfer characteristics (log)

Figure 4.13: Output, transfer characteristics and transconductance of n-FET

Figure 4.13 shows the output, transfer characteristics (linear and log scale) and transconductance curve derived from the transfer characteristics for channel with donor type doping. From these characteristic curves the performance parameters of the device were calculated. The threshold voltage was found to be -0.9 V at drain voltage of 1 V. Again at same drain voltage subthreshold slope was calculated to be 119 mV/dec and on-off current ratio was found to be 10^{13}. Whereas transconductance of 379 nS was observed at the same drain voltage of 1 V.

Figure 4.14 shows the energy band diagram of the device across the channel-oxide-Si region under different Gate biasing voltages. The left side is the bottom gate side and the right side is the channel, separated by a dielectric and a doped si layer (substrate). The effect of gate voltage on channel is visible and results in bending of energy band at the interface of the channel with dielectric.

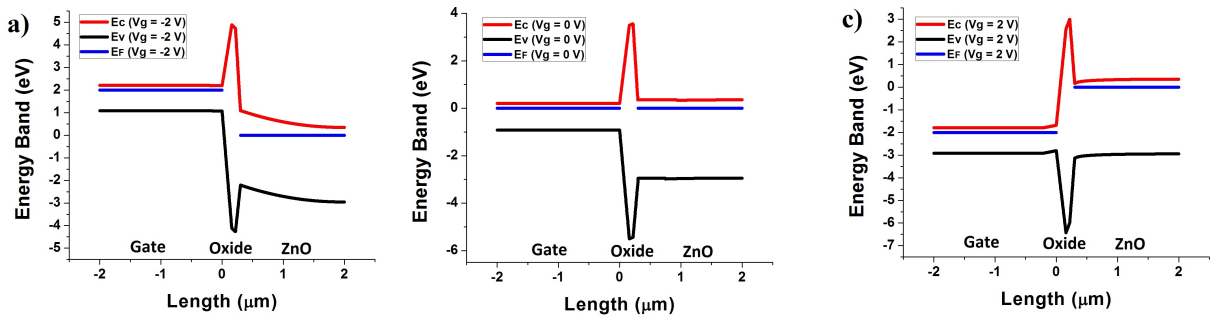

(a) Vg=-2 V (b) Vg=0 V (c) Vg= 2 V

Figure 4.14: Energy band diagram

The energy band diagrams correspond to the results shown in figure 4.13, which is n-channel depletion mode (normally on) device. Negative gate voltage results in depletion of majority carriers in the channel near the interface with dielectric. This results in series depletion capacitance with oxide capacitance, which decreases the overall capacitance, resulting in decrease in drain current. On the other hand, positive gate voltage results in accumulation of majority carriers near the dielectric interface, which basically enhances the flow of electrons through the channel.

The device being bottom-gate structured, the channel can be utilized for sensing purpose. ZnO nanoparticles have positive zeta potential as explained in first chapter of this thesis and this particular property can be used to detect any protein or biomolecule which can form electrostatic binding with the nanoparticles. ZnO nanoparticles thus act as a chemiresistive channel whose change in surface properties on being attached to biomolecules will get reflected in the device characteristic curves. ZnO nanoparticles behave as n-type material inherently; unless and until they are doped otherwise chemically or by high temperature processes. If p-type ZnO nanoparticles are synthesized, in that case the zeta potential will have opposite polarity than that of n-type ZnO nanoparticles. However p-type ZnO is not popular because of stability issues [256]. Let us consider a particular case. The net charge in a protein may be attributed to the presence of positive, negative or neutral amino acids constituting the protein. Every protein has an isoelectric point of pH at which it exhibits no net electrical charge. The negative log of the acid dissociation constant (pKa) for an amino acid side chain alters the charge in the protein. At a value of pH lower than the isoelectric point, the protein exhibits a net

positive charge while for higher values of pH it shows a net negative charge. Since ZnO nanoparticles have positive zeta potential, we can expect electrostatic binding between ZnO nanoparticles and proteins having negative surface charge i.e. zeta potential. Thus we can functionalize the channel region with a biomolecule in order to detect a target which is again specific to the attached protein/biomolecule.

4.6 Conclusion

The characteristic curves of a ZnO nanoparticle based FET has been evaluated using device simulation tool. Furthermore, our results include the calculation of important parameters of the FET that is crucial for its operation as a biosensing device. The simulation results reveal that the FET exhibits a threshold voltage of -0.9 V, a sub-threshold slope of 119 mV/dec, on-off current ratio of 10^{13} and transconductance value of 379 nS. From these analysis, it can be inferred that performance of ZnO nanoparticles as a channel material for FET is comparable with the commonly available semiconductor materials. In addition, the simulated device is of favourable dimensions, making it comparable in terms of miniaturization to many other commercially available sensors. In conclusion we can put that the proposed device will be of great promise for the field of nanobiosensor if realized by proper fabrication.

Chapter 5

Integration of nanoparticles, recombinant GST and device

THIS chapter presents an electrochemical method for detection of glutathione using Glutathione-S-Transferase (GST) - ZnO composite nanoparticles to investigate the prospects of the method for detection of cancer at an early stage. The purified recombinant GST enzyme was bound with ZnO nanoparticles by electrostatic interactions and the nanocomposite was dropcast on a silicon-silicon dioxide wafer. The GST functionalized deposited layer was then used as a chemiresistive channel to detect conjugation reaction between glutathione and 1-Chloro-2,4-Dinitrobenzene (CDNB). The zeta potential values of the ZnO nanoparticles and the GST were found to be 13.4 mV and -6.21 mV, respectively. Around 73.8% binding was observed between the enzyme and ZnO nanoparticles. I-V analysis of the chemiresistive channel showed an increase in conductivity of the channel due to conjugation reaction between glutathione and CDNB as compared to that of glutathione or CDNB alone. I-V characterization of the GST functionalized layer was performed at various concentrations of glutathione and a sensitivity and LOD (Limit of Detection) of 5.68 nA/μM and 41.9 nM were obtained, respectively. Thus from I-V analysis of the chemiresistive channel, the detection and quantification of glutathione could be obtained.

5.1 Experimental setup

5.1.1 Functionalization

In order to achieve highly specific detection, GST was bound electrostatically to the ZnO nanoparticles. In presence of both glutathione and CDNB, the conjugation reaction between them can take place only at the surface of ZnO nanoparticles since purified recombinant GST were attached to the nanoparticles only. Thus the possible impact of other oxidation-reduction reactions in the analyte on the output characteristic of the electrochemical device was completely avoided. As the device characteristics change according to the electrochemical reactions on the surface of the nanoparticles, so the detection of glutathione was very specific.

5.1.2 Deposition of electrolyte on wafer

The silicon wafer was cleaned with IPA (isopropyl alcohol) and ethanol using standard protocol. Then the GST bound ZnO nanoparticle composites were deposited on the oxide surface by three different techniques, namely, i) dropcast ii) doctor blade and iii) spin coating. The deposited layers were characterized for each case using Veeco Profilometer.

5.1.3 I-V measurement setup

Keithley 2420 source meter was used for I-V analysis of the device. The connections were made by external copper electrodes and conductive silver paste. The terminals on the device were properly isolated using a thin polydimethylsiloxane (PDMS) layer so that they were not shorted while making measurements with the electrolyte.

5.2 Steps of analysis

The GST bound ZnO nanoparticle composite was deposited on a Si/SiO_2 wafer as the first step towards further analysis. The I-V curve was then plotted for the blank surface in the absence of any analyte. In the next step, the I-V curve was plotted after application

of 5 μL 100 mM CDNB. The device was then washed twice using phosphate buffer saline (PBS). The next I-V analysis was done after application of 5 μL of 100 mM GSH. This was followed by washing with PBS. In the final step, 5 μL from a 1:1 mixture of GSH and CDNB (100 mM each) was applied on the surface and I-V plots were obtained at certain time intervals till the reaction was complete, marked by sharp decrease in output current. The detailed analysis of these I-V plots is carried out in upcoming sections of this chapter. After completion of experiment, the device was given a wash with PBS so that there remained no traces of products which could affect the subsequent measurements.

5.2.1 Device structure

As stated before, the ZnO nanoparticle-GST enzyme composite was deposited on oxide wafer using three different techniques out of which the layer deposited by means of drop-cast yielded the best results in terms of reusability. In other words, easily reproducible dropcast method provided us with a stable layer of deposition as compared to that of the others. The deposition was done on an area of 5 mm x 5 mm. Profilometer tests were carried out for all three techniques and the results have been shown in table 5.1.

Table 5.1: Structural schematic of the experimental setup

Method	Average thickness	Average Roughness	Reusability
Dropcast	10.28 μm	3.627 μm	Good
Doctor Blade	1.35 μm	934.6 nm	Bad
Spin Coat	1.21 μm	61.16 nm	Bad

After deposition of ZnO nanoparticle and GST composite layer, we arrived at the structure shown in figure 5.1. In this structure the Si and SiO_2 has been used as a substrate only as it did not contribute electrically towards current between the chemiresistor. The ZnO-GST layer, which was dropcast on top of it, was used as a resistive channel and based on the changes in conductivity of this layer all the measurements and detections were carried out.

In the structure shown in figure 5.1, ZnO nanoparticle not only acts as a base for binding and immobilization of GST onto its surface, but also as a semiconducting layer that allows

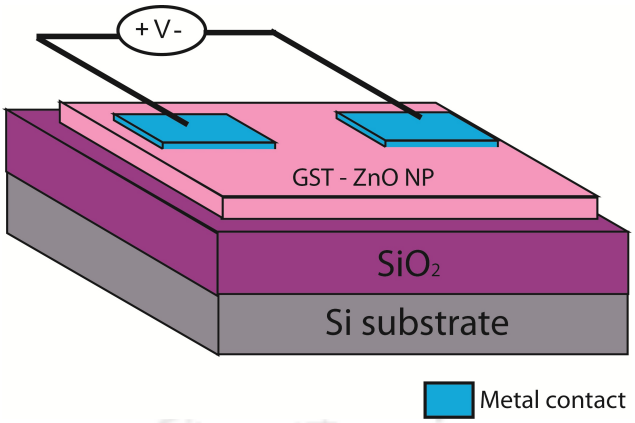

Figure 5.1: Structural schematic of the experimental setup

movement of current. Glutathione conjugates with CDNB forming GS-DNB and HCl on the surface of ZnO nanoparticles because of presence of GST bound to them. Any change in the conformation of GST due to its participation in the reaction between glutathione and CDNB, leads to a significant change in resistance of the GST-ZnO nanocomposite, therefore changing the current flow. This allows us to study fluctuations of glutathione concentration in the concerned samples. Following an approximate standardization, specific changes in current flow can be measured and related to quantitative measure of increase or decrease of glutathione concentration. The detection of glutathione with this structure was very specific due to fact that GST was functionalized on the surface; hence the conjugation reaction of GSH and CDNB could take place on the surface or the interface only. The other reactions which might be taking place in the analyte were not reflected in the I-V characteristics as they are not by linked to the conducting channel by any means.

5.2.2 Measurement of resistivity

Resistivity of synthesized ZnO nanoparticles and its conjugate with GST were measured and the values are shown in table 5.2. A PDMS channel of width 1 mm and length 3 cm was prepared using the following technique - PDMS and the cross linker was mixed in 10:1 ratio. The mixture was then stirred vigorously and then put in 20-50 mbar desiccator for 30 min in order to remove the air bubbles present. The final step was to heat the mixture at 60°C for 6 hrs. in hot air oven. The solutions were put in the channel and

the current through it was measured by applying a bias across different lengths. Copper wires of very low contact resistance were used as electrodes for connections. Since the cross sectional area of the channel is constant throughout, the resistance of the solution can be represented as a linear function of length. According to transmission line model (TLM) method [34], the slope of the resistance versus length plot is the resistivity per unit area value and the y-intercept of the plot is the value of the contact resistance. This is apparent from the following equation-

$$R = (\rho/A)*l + 2*R_c \tag{5.1}$$

Where, (ρ/A) is the resistivity per unit area, l is the length of the channel and R_c is the contact resistance at each terminal. Now, resistivity was calculated using the slope and the cross sectional area values.

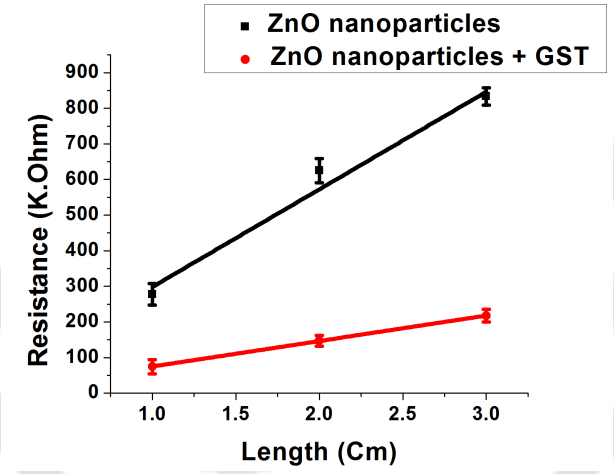

Figure 5.2: Measurement of resistance values at different channel lengths

Contact resistance was found to be 3.3 KΩ. It was observed that the resistivity value of the ZnO nanoparticles solution decreased when GST protein was bound to it, the reason being the GST protein molecules have negative surface charge at the buffer pH of 7.5. Due to this they act as charged ions that allow the flow of current. In case of Zinc oxide nanoparticles, only the nanoparticles allow the flow of current, where as in case of ZnO-GST, both the nanoparticles and the protein molecules contribute to the current flow. As discussed in previous section, the nanoconjugate was deposited on silicon dioxide wafer. Considering the deposition obtained by dropcast method, the average thickness of the

layer was 10.28 μm. Hence the sheet resistance value was calculated using the following equation-

$$R_s = \rho/t \tag{5.2}$$

Where, ρ is the resistivity and t is the average thickness of the layer.

Table 5.2: Measured resistivity values

Parameter	ZnO nanoparticles	ZnO nanoparticle bound GST
Resistivity (Ω.m)	21.8	5.61
Sheet Resistance (KΩ/sq)	-	545.72

5.2.3 Characterization and Detection of GSH

I-V analysis of the device was carried out for three different cases – i) in presence of glutathione only, ii) in presence of CDNB only, & iii) in presence of both glutathione and CDNB. It was observed that in presence of both glutathione and CDNB the current flowing through the channel increased significantly, which was concurrent with the expected outcome. This was because when the conjugation reaction of glutathione with CDNB took place, there was a flow of ions, which aided the flow of current through it. Since GST was present in the channel only, so the reaction and the event of transfer of ions took place at the interface only. This reaction was totally time dependent and the reaction stopped when the complete amount of glutathione formed conjugate with CDNB. As the conjugation process continued, there remained less and less amount of glutathione and CDNB. Hence the current value decreased with time as shown in figure 5.3(a). However the current value did not fall to its original value because the initial solution or analyte and the final product formed by the reaction were not electrically equivalent. For the reactions we have carried out, the assay time was in tens of seconds (in about 30-40 seconds reaction reached completion).

After each measurement, the device required washing with Phosphate Buffer Saline (PBS) in order to avoid nonspecific interactions and false results being generated in subsequent measurements. The device was successfully reused in its current model (without

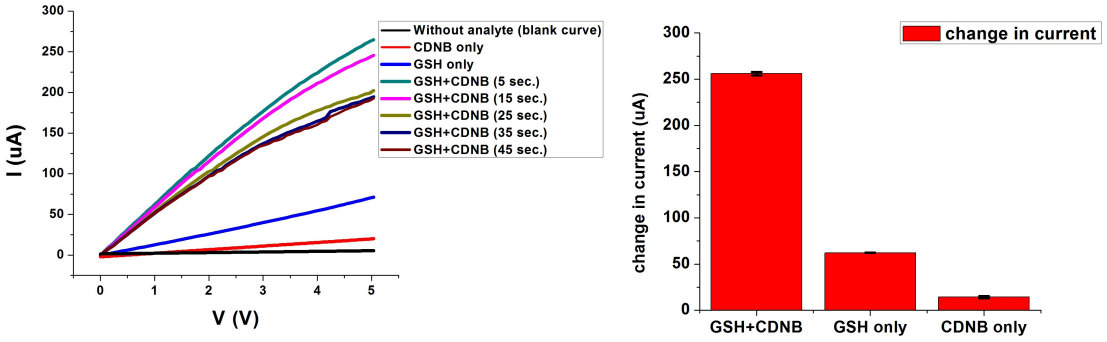

(a) I-V analysis (b) Change in current

Figure 5.3: (a) I-V analysis and detection of GSH at different instants of time (b) Change in output current due to various analytes at V = 5V

any further SiO_2 surface modification) for about 10 times. Following this, the nanoconjugate layer seemed to scrape off at places. But this issue can be fixed by carrying out certain modifications of the SiO_2 surface that would allow chemical bond formation between the surface and the ZnO of the GST-ZnO nanoconjugate, thereby increasing the reusability. The column bar graph shown in figure 5.3(b) summarizes the observed shift in current due to application of different analytes with respect to the blank curve.

5.2.4 Sensitivity analysis

In order to measure the sensitivity, the device was put under test with different concentrations of glutathione. Three different mixtures of glutathione and CDNB were prepared with concentrations of 50 μM, 100 μM and 200 μM respectively. I-V analysis was carried out separately for each of the analytes having different concentrations and the obtained results were calibrated as shown in figure 5.4. The calibration curve was obtained from the measured values of current flowing through the channel at different concentrations. Linear regression analysis was used to determine the slope, intercept and correlation coefficient (R^2). The results showed linear correlation between the obtained current value and glutathione concentration in the range of 100 nM – 10 mM with a regression equation of $I(\mu A) = (3.24255 \pm 0.01315) + [(0.00568 \pm 7.93362 \times 10^{-5}) \text{ X } C_{GSH}]$, ($R^2 = 0.99863$), where C_{GSH} is the concentration of glutathione (μM). Apparently, the slope of this calibration curve is the required sensitivity and it was calculated to be 5.68 nA/μM. The LOD (Limit of Detection) was calculated to be 41.9 nM from the

calibration curve using the following formula-

$$\text{LOD} = 3^*[\text{standard error/slope}] \tag{5.3}$$

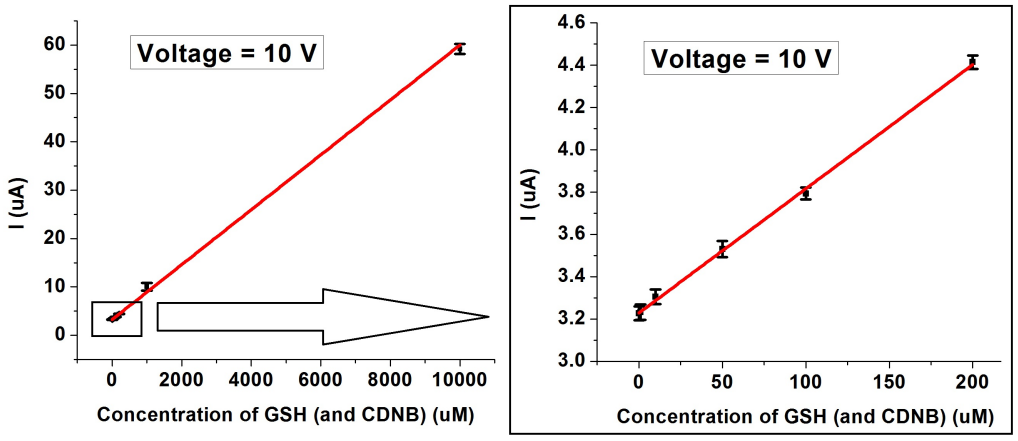

Figure 5.4: Calibration curve (No. of trials = 3)

5.2.5 Selectivity of the device

In order to achieve highly specific detection, GST was bound electrostatically to the ZnO nanoparticles. In presence of both glutathione and CDNB, the conjugation reaction between them can take place only at the surface of ZnO nanoparticles since purified recombinant GST were attached to the nanoparticles only. Thus the possibility of effect of other oxidation-reduction reactions in the analyte on the output characteristic of the electrochemical device was avoided. As the device characteristics change according to the electrochemical reactions on the surface of the nanoparticles, so the detection of glutathione was very selective. It would still be specific while using patient samples as we have immobilised the GST enzyme on the nanoparticles instead of the glutathione (substrate). The complex sample may have multiple enzymes that can react to glutathione, and immobilizing glutathione would take into consideration changes due to all such non-specific reactions. On the other hand immobilised GST would allow CDNB to react with glutathione only on the surface of the nanoparticles. Therefore all such reactions would specifically account for the CDNB-GSH interaction. As immobilised GST level will be

constant, any upregulation or downregulation of glutathione would be clearly visible as the current output.

5.2.6 Mathematical verification of experimental results

Mathematical verification of experimental outcomes is discussed in this section. The following equation incorporates all the parameters that control the amount of current flowing through the deposited thin film.

$$I = V/[R_s{*}(l/w) + 2R_c] \tag{5.4}$$

$$\text{Or}, I = V/[(\rho/t){*}(l/w) + 2R_c] \tag{5.5}$$

Where V is the applied voltage, l and w are the length and width of the deposited film, R_s and R_c are the sheet resistance of the thin film and contact resistance respectively, obtained by experimental measurements described in the section 5.2.2. The I-V plot obtained was compared with the experimentally obtained I-V plot. Figure 5.5 summarizes the comparison between experimental and modeled I-V characteristics of the GST-ZnO nanoparticle composite thin film.

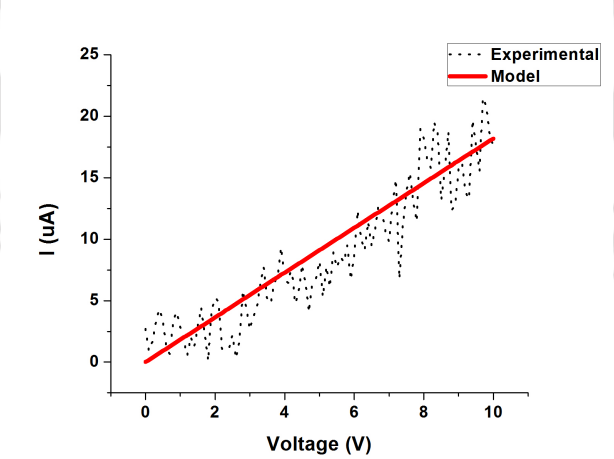

Figure 5.5: Comparison between analytical model and experimental I-V analysis of ZnO nanoparticles-GST conjugate thin film

It is apparent from figure 5.5 that experimental and simulated values are in close proximity with an average error of -11.75%. The deviation in the experimental I-V from a definite slope was possibly due to the non-uniformity of the thin film.

5.3 Conclusion

In this chapter, a novel method of electrochemical detection of glutathione has been demonstrated using composite nanoparticles of ZnO with GST. The kinetic parameters of purified recombinant GST along with its nanoconjugate solution with ZnO nanoparticles were calculated and binding analysis was performed. Then the nanoconjugate solution was deposited on oxide wafer to form a chemiresistive channel. This channel was used for successful detection of glutathione. This novel concept of forming a channel layer with a composite of ZnO nanoparticles and the protein itself is the first step towards device based specific detection of glutathione. However there is scope for improvement as this method can be further extended to a FET (Field Effect Transistor) structure for more accurate and sensitive in-vitro detection of glutathione which in turn will help in detecting certain types of cancer at an early stage.

Chapter 6

Fabrication and characterization of FET for detection of glutathione

THIS chapter outlines the fabrication and characterization of FET device for detection of glutathione in solution as well as in cancer cells. The process of device fabrication using optical lithography technique is discussed in detail. Followed by a brief discussion on characterization results of device without any analyte. Finally, outcomes of the device with respect to detection of glutathione are analysed.

6.1 Device fabrication

The steps followed for fabrication of the device are described below in sequential order:

Wafer cleaning: Standard 4-inch 500 μm thick Si wafer (Phosphorous doped, <100> oriented, 1-10 Ω.cm resistivity) was used as the starting material. Firstly, cleaning of the wafer was done using Piranha solution (3:1 mixture of concentrated sulfuric acid and hydrogen peroxide).

Growth of oxide: A layer of SiO_2 of thickness 300 nm was grown thermally on the polished side of the wafer using Oxidation-Diffusion furnace.

Dehydration bake: Dehydration bake was done for 10 minutes at 110°C to remove any residual liquid on the substrate surface.

Coating of primer: Hexamethyldisilazane (HMDS) was used as the primer in order to enhance the adhesivity of photoresist to be deposited next . It was spin coated at 3500 rpm for 1 minute.

Coating of photoresist: S1813 was used as the photoresist of choice. It is a positive photoresist. It was dispensed on the substrates and spin coated at 3500 rpm for 1 minute over the HMDS primer.

Soft bake: Soft bake was done for 3 minutes at 110°C to ensure proper adhesion of the photoresist to the substrate surface.

Lithography: Lithography is the process of transferring an image from a photographic mask to a substrate. Direct writing was done to define the device designs onto the photoresist on the wafer using Dilase 250 direct laser writer instrument. Figure 6.1 shows the mask designed in Clewin software which was used for photolithography. The channel length and width were designed to be 5 μm and 10 μm respectively.

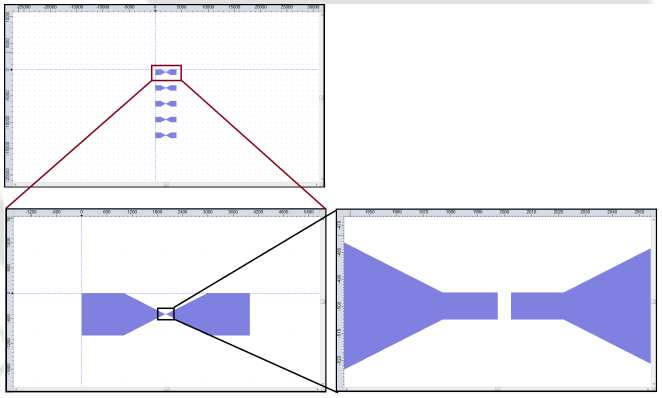

Figure 6.1: Mask layout designed for photolithography

Development: The development of the wafer post-lithography was done to remove the exposed resist using TMAH (Tetra Methyl Ammonium Hydroxide) developer solution for 1 minute.

Hard bake: The substrate was then heated at 110°C for 1 minute in order increase the stability of developed photoresist for subsequent processes. Figure 6.2 was a microscopic image of a pattern taken after completion of this step.

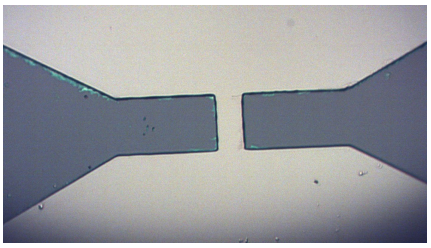

Figure 6.2: Image of the pattern after development

Metal deposition: Al was deposited using thermal evaporation technique. Deposition was done at room temperature.

Lift-off: REMOVER PG (N-Methyl-2-pyrollidone) solution was used at 60°C for 30 minutes to achieve proper lift-off of the deposited metal. Figure 6.3 shows a microscopic image of the device after lift-off.

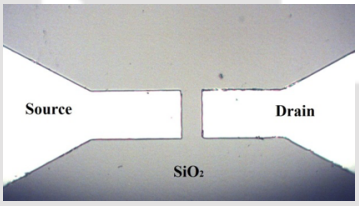

Figure 6.3: Microscopic image of the fabricated device (top view)

Back-gate deposition: The last step was deposition of back gate contact, which was again performed using thermal evaporation of Al on the back side of the wafer.

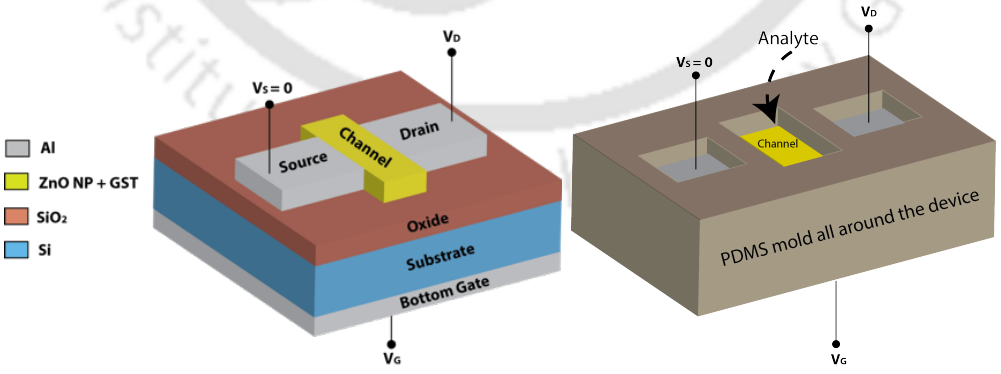

Figure 6.4: Schematic of the fabricated device

PDMS molding and channel deposition: A Polydimethylsiloxane (PDMS) molding was created across the channel in order to hold liquid samples without getting dispersed.

The channel material consisting conjugate of GST and ZnO nanoparticles was then deposited using dropcast method. Figure 6.4 show the schematic of the fabricated device.

Figure 6.5 describes the process flow of the complete fabrication process followed by two images of the fabricated device under test are shown in figure 6.6.

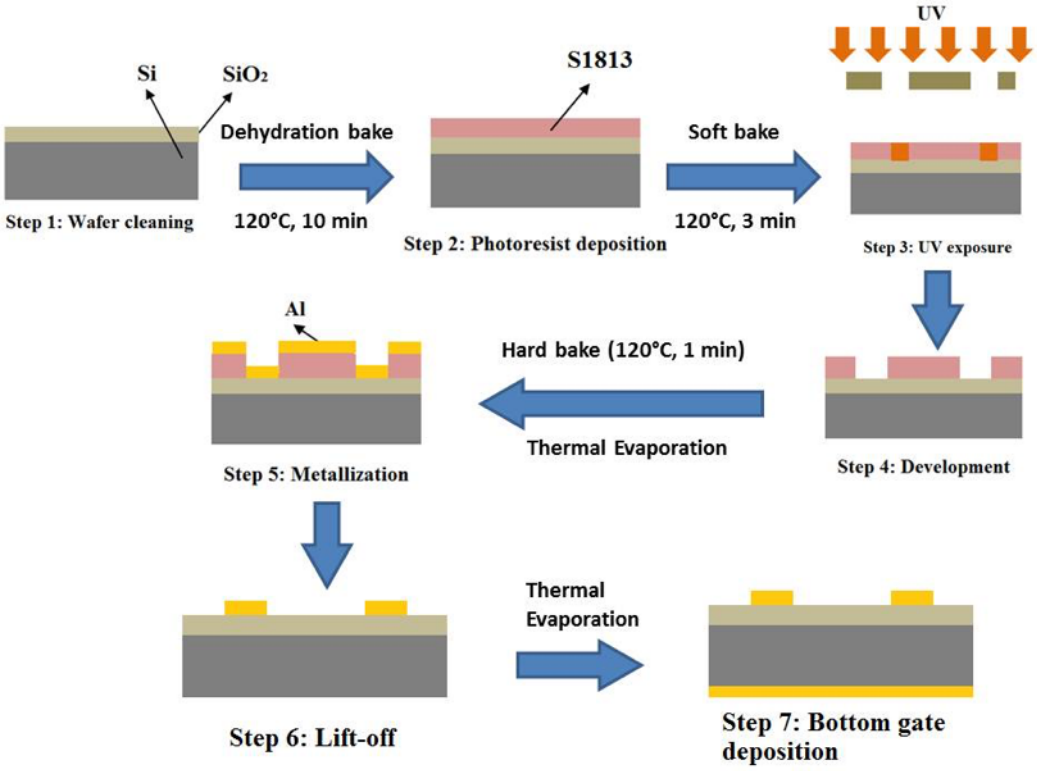

Figure 6.5: Process flow for fabrication of the device

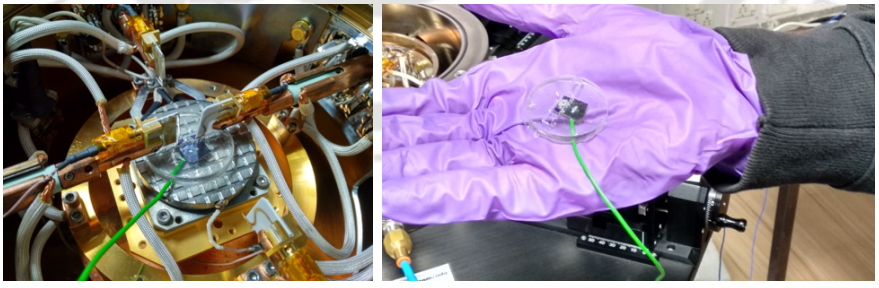

Figure 6.6: Images of fabricated device

6.2 Experimental setup

6.2.1 Functionalization

In order to achieve highly specific detection, GST was bound electrostatically to the ZnO nanoparticles. In presence of both glutathione and CDNB, the conjugation reaction between them can take place only at the surface of ZnO nanoparticles since purified recombinant GST were attached to the nanoparticles only. Thus, the possible impact of other oxidation-reduction reactions in the analyte on the output characteristic of the electrochemical device was completely avoided. As the device characteristics change according to the electrochemical reactions on the surface of the nanoparticles, so the detection of glutathione was very specific.

6.2.2 Measurement setup

All measurements were taken using Keithley 4200 parameter analyzer and probing was done using a Lakeshore DC probe station. Source, drain and gate terminals were probed by three terminals of the probe station connected to the SMU's of the parameter analyzer, which is capable biasing the device as well as measuring the response of the device.

6.3 Steps of analysis

The GST bound ZnO nanoparticle composite was dropcast at the region between source and drain, which indeed forms the channel layer of the FET device. The output characteristics of the device were then obtained for the blank surface in the absence of any analyte by applying varying gate as well as drain bias in order to confirm the effect of gate voltage on drain current. In the next step, output characteristics were again obtained after application of 1 μL of 100 mM CDNB. The device was then washed twice using phosphate buffer saline (PBS). The next analysis was done after application of 1 μL of 100 mM glutathione. This was followed by washing with PBS. In the final step, 1 μL from a 1:1 mixture of glutathione and CDNB (100 mM each) was applied on the channel and $I_d - V_d$ plot was obtained at certain time intervals till the reaction was complete.

The detailed analysis and comparison of these characteristic plots is carried out in the following section. After completion of experiment, the device was given a wash with PBS so that there remained no traces of products which could affect the subsequent measurements. After completion of these measurements, same analytes were applied again in same order and real time drain current was obtained for a fixed gate and drain bias. The sharp increase in drain current on application of mixture of glutathione and CDNB marks the detection of this reaction by the device. Finally, the device was again put under test for real life cancer cell environment. Sample having known concentration of MCF-7 and HeLa cells were used in order to confirm the detection. These results were compared with that of Human Embryonic Kidney (HEK) cells having no cancer cells at all. The results obtained are described in the following sections.

6.4 Results and discussion

6.4.1 Fabricated device

The fabricated device had dimensions as described in the following table.

Table 6.1: Parameters of fabricated device

Parameter	Value
Channel length	5 μm
Channel width	10 μm
Oxide thickness	300 nm
Substrate thickness	500 μm

6.4.2 Characterization and detection of glutathione

The fabricated device was initially characterized with functionalized ZnO nanoparticles with GST as the channel material. Figure 6.7 shows the output and transfer characteristics of the device measured under varying drain and gate voltages. The gate dependence of the device is prominent from the transfer characteristics. From this analysis gate

voltage of -2 V from the subthreshol region was fixed as the gate bias for subsequent experiments. In practice, FET devices biased in subthreshold region gives maximum sensitivity. That is why gate biasing of -2 V was selected for this application.

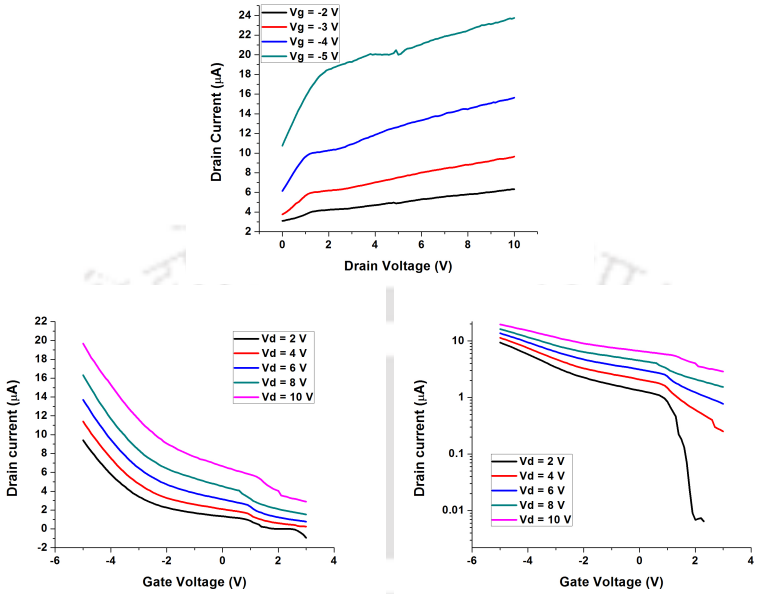

Figure 6.7: Output and Transfer characteristics (linear and log scale) of the device

Subsequently, output characteristic of the device was measured under different analytes being applied. Initially only CDNB was applied, followed by glutathione only and finally GSH and CDNB combined.

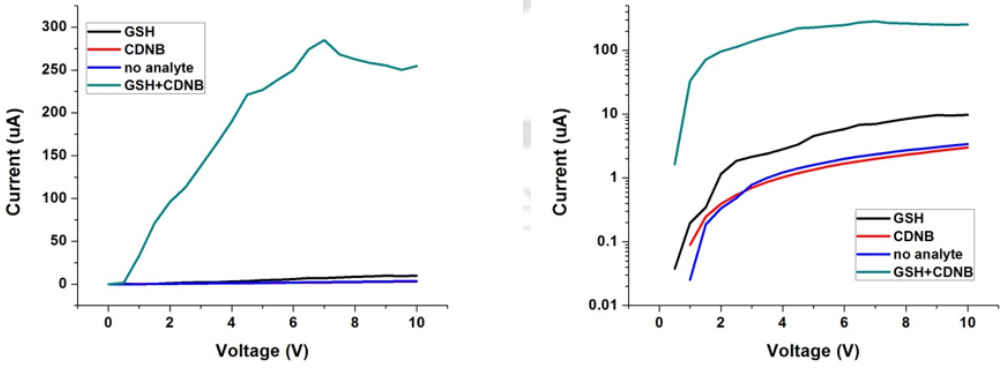

Figure 6.8: Output characteristics of the device ($I_d - V_d$ at V_g = -2 V) in linear and log scale

Obtained $I_d - V_d$ plots are shown in the figure 6.8. It can be observed from the plot that the response due to glutathione and CDNB is much higher than that of glutathione

or CDNB individually. This is because in presence of both glutathione and CDNB conjugation reaction between them takes place on the channel where GST is present. Since this reaction takes place on the surface of the channel, the occurrence of this reaction gets reflected on the device characteristics.

As visible from the output characteristics of the device, current flowing through the channel clearly increases by significant amount in presence of both glutathione and CDNB. Figure 6.9 shows a column graph quantifying the change in drain current due to presence of different type of analytes.

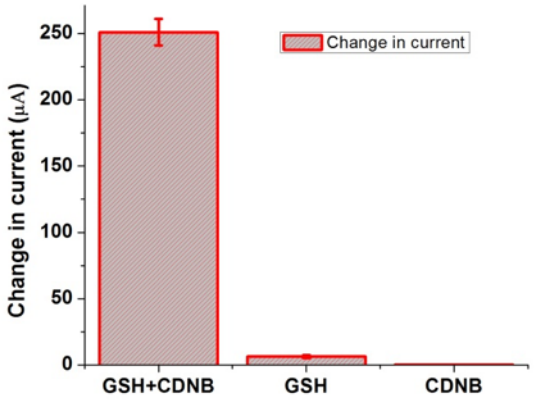

Figure 6.9: Change in drain current (V_d = 10 V, V_g = –2 V)

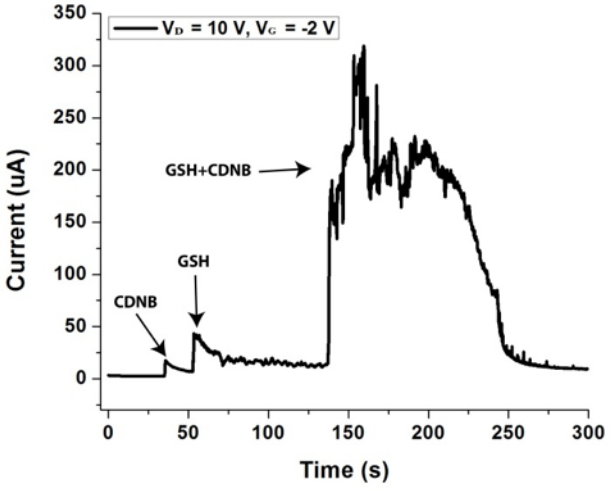

Figure 6.10: Real time analysis

Figure 6.10 shows real time measurement of drain current at a fixed gate voltage of -2 V and drain voltage of 10 V. The sudden peaks depict sudden increase of output current due to presence of an anlayte on the channel. As can be seen, current increases significantly when GSH and CDNB both are present on the channel. The current reaches a peak, then slowly reduces to somewhere nearby its original value. So, from this plot, we can know the time for which the channel undergoes the conjugation reaction. For 1 μl sample volume of 1:1 GSH and CDNB assay time was found to be 30 s.

After each measurement the device was washed with Phosphate Buffer Saline (PBS) and deionized water in order remove the analyte from the channel so that the subsequent measurement is free from any kind residue from the previous test.

6.4.3 Sensitivity analysis

Sensitivity analysis of the device was carried by measuring drain current at fixed gate voltage for different concentration of glutathione. Obtained calibration curve is shown in figure 6.11. Both sensitivity and Limit of Detection were calculated from this calibration curve. The values of sensitivity and LOD were found to be 60.22 μA/dec change in concentration and 13.1 nM, respectively. The linear range of operation is 0.1 μM to 0.1 M and regression equation is I = (444.70 $\pm$8.82) + (60.22 $\pm$1.59) log(c), [R^2 = 0.989], where I is drain current in μA and c is molar concentration of glutathione.

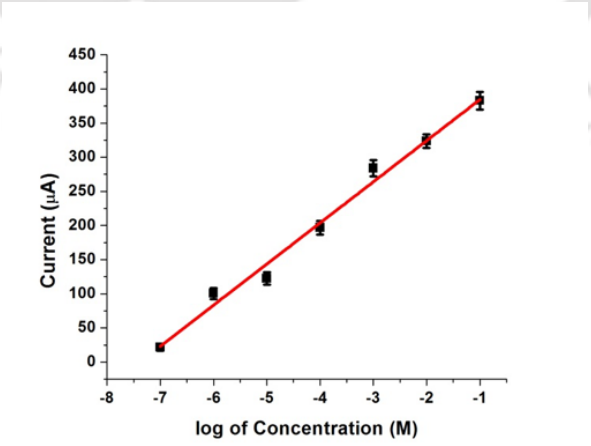

Figure 6.11: Calibration curve (Number of trials=5)

6.4.4 Characterization in presence of cancer cells

After successful detection of glutathione, the device was tested for actual cancer cells to see if the device can detect increased glutathione levels in HeLa and MCF-7 cancer cells. Cancer cells were grown by cell culture in laboratory. HeLa and MCF-7 are human cervical and breast cancer cells, respectively and these cells contain higher concentration of GSH compared to normal cells as reported [34]. Cancer cells and CDNB were applied on the channel followed by measurement of output characteristic of the device at fixed gate bias. Drain current obtained corresponding to cancer cells had higher current levels compared to that of HEK cells. Moreover, a comparison between HeLa and MCF-7 were also carried out for same number of cell lines. HeLa cells recorded higher current implying that HeLa cells contain higher concentration of glutathione compared to MCF-7. Following figure shows the result of comparison between HeLa, MCF-7 and HEK cells.

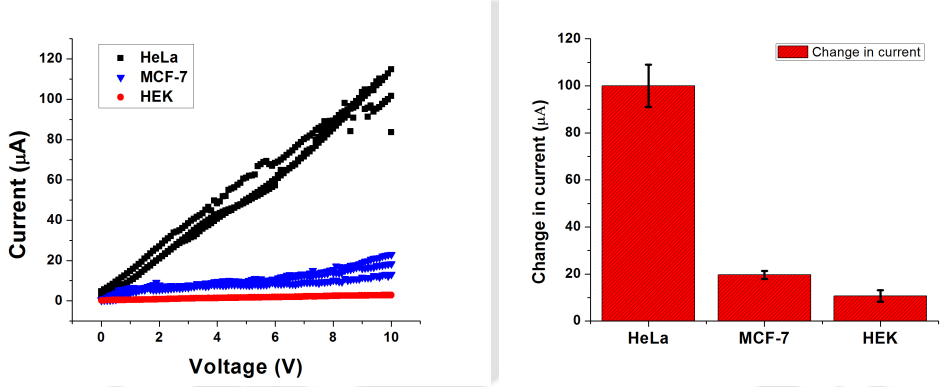

Figure 6.12: (a) Output characteristic ($I_d - V_d$) for HeLa and MCF-7 cells at V_g = -2 V, (b) Comparison of change in current for HeLa, MCF-7 and HEK cells (V_d = 10 V, V_g = -2 V)

Once detection of cancerous cell was confirmed, next step was to calculate the sensitivity in terms of number of cells and formulation of calibration curve. Various analytes having different number of HeLa cells were prepared and tested. The drain current was observed to be varied in relation with the number of cells present. Calibration curve was plot from these results as shown in figure 6.13. The calibration curve showed a linear response till 50 numbers of cells and below that it was not possible to separate them from the response corresponding to HEK cells. So the linear range of operation was from 50 to 1000 number

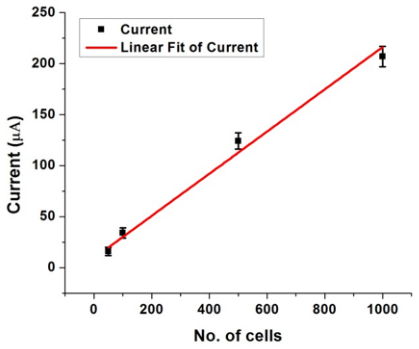

Figure 6.13: Calibration curve (Number of trials=5)

of cells. The values of sensitivity and LOD were found to be 206.7 nA/cell and 38 cells respectively. The regression equation is I = (9.5 ±3.43) + (0.2067 ±0.0102)N, [R^2 = 0.984], where I is drain current in μA and N is number of cells.

6.5 Conclusion

A novel device based electrochemical detection method of glutathione has been described in this chapter. The device is a FET device, channel material of which consists of a conjugation of ZnO nanoparticles and purified recombinant GST protein. The novel concept of incorporating a protein as a channel material is reported here for the first time. The device successfully and selectively detects and quantifies glutathione as compound and as well as a human cell component. The device was also tested successfully with real laboratory grown HeLa and MCF-7 cancer cells and it was found that the device could detect enhanced concentration of glutathione in cancerous cells, which indeed is the first step towards detecting certain types of acute cancer disease. The device can be further improved upon keeping the primary working principle same, in order to meet the requirements to make a deliverable product for marketization.

Chapter 7
Conclusion and Future Scope

7.1 Conclusion

THIS chapter presents the summary and future aspects of the work described in this thesis. The overall target of this work was the design and fabrication of FET based device for detection of glutahtione. It started with development of a favourable functionalization mechanism to be incorporated with FET. The mechanism was tested on a two terminal platform for successful detection of glutathione. Subsequently FET device was fabricated with functionalized channel layer for detection of glutathione. The device was also tested for detection of enhanced concentration of glutathione in cancerous cells. The conclusion related to different aspects of this work drawn from chapters is summarized below:

The first two chapters provide a general overview, introduces the main objectives and scope of this thesis and present a detailed literature review of the topic.

Development of a favourable and efficient functionalization mechanism is the most critical point towards designing a biosensor. The third chapter dealt with several issues related to development of funtionalization scheme for this work. In order to detect glutathione by dint of its conjugation reaction with CDNB, recombinant GST has to be functionalized

on the device and as GST itself not being semiconducting, it was bound with ZnO nanoparticles based on their opposite polarities of zeta potential. This nanoparticle-protein ensemble is the final outcome of this chapter which could be incorporated as the channel material of FET device to be fabricated.

In order optimize a structure to be fabricated, simulation studies beforehand is essential as many modifications after fabrication can not be afforded. The fourth chapter is all about design and optimization of the device structure based on simulation results. Device simulation setup was finalized by reproducing reported results, which was then utilized for simulation of the proposed structure. The results showed FET characteristics for the structure that encouraged us to go ahead with the proposed structure. As a subsequent step, device dimensions were also finalized based on the simulation results in accordance with constraints of fabrication processes and the suitability of liquid chamber volume requirements.

The fifth chapter elaborates a vital part of this thesis which is the combining three individual parts of the final biosensing device to be designed. Channel material was finalized in this chapter and then the efficiency of this layer with respect to detection of GSH was described. The channel material is combination of nanoparticles and protein and this combination was applied to fabricate a two terminal resistive device. Detection of GSH was successfully accomplished with sensitivity and LOD of 5.68 nA/μM and 41.9 nM respectively. The device showed linear response for a range 100 nm - 10 mM of GSH concentration. This is a crucial step towards fabrication of FET for the same purpose.

The sixth chapter outlined the final outcome of this whole thesis work, which is the fabrication of FET and utilization of it for detection of glutathione. The channel material discussed in previous chapter was incorporated to FET device and characterized for detection of glutathione in solution and as cell component. Sensitivity and LOD were calculated to be 60.22 μA/dec change in concentration and 13.1 nM respectively with a linear response for 0.1 μM - 0.1 M concentration of glutathione when the device was tested for glutathione as solution. On the other hand, when characterized with cancer cells, 206.7 nA/cell of sensitivity and LOD of 38 cells were obtained.

Table 7.1: Comparison with existing techniques

Detection Principle	**Type**	**Assay Time (s)**	**Sensitivity**	**Linear range of operation (μM)**	**Limit of Detection (nM)**	**Sample Type**	**Sample Volume (μL)**	**Ref.**
Colorimetric	-	600	0.06 U/mL	100-400	10.5	GST	200	[257]
Liquid Chromatography	-	900	0.39 μA/μM	0.01-50	0.6	Human blood	20	[258]
Chemi luminescence	-	8	0.8 au/μM	0.01-10	8	Human blood	600	[259]
Electro- chemical	CVV	-	4.8x10^5 cm^3	0.3-3350	80	GSH	-	[260]
	SWV	-	0.64 nA/μM	10-60	300	Human saliva	50	[261]
	SWV	1200	0.76 μA/μM	5x10^{-4}-5	0.14	GSH	-	[262]
	DPV	1200	96 nA/μM	10^{-3}-1.0	0.6	GSH	50	[263]
	CA	-	84.2 nA/μM	0.1-5.0	95	GSH	-	[264]
Device	Chemi resistive	30	5.68 nA/μM	$0.1 - 10^4$	41.9	GSH and CDNB	5	This work
Device	FET	30	60.22 μA/dec	$0.1 - 10^5$	13.1	GSH and CDNB	1	This work

Finally, table 7.1 provides a comparative analysis of the performance of the devices presented in this thesis with some of the existing techniques reported in literature. From this quantitative comparison, it can be concluded that the devices presented in this thesis definitely offers advantages in terms of assay time, linear range of operation and sample volume. Sensitivity is comparable to most of the existing techniques. Limit of detection can be improved further but it is decent enough considering the concentration of glutathione in human blood (mostly mM) which is way higher than the LOD of the devices.

7.2 Scope for future work

As mentioned before, device based detection of glutathione has been reported for the first time through this work. Although the results are encouraging and better than most of the conventional techniques for detection of glutathione, still there is scope for improvement in device dimension aspect. There is scope of testing the device characteristics with channel length in nanometer regime. Next comes the most important feature of a typical biosensing device, the feasibility of being converted into a point-of-care device for commercial use. The device fabricated in this work is capable of achieving that target if manufactured with proper realization. This aspect of future prospect of this work is probably the most significant point to be taken good care of so that a point-of-care device can realized in near future.

Bibliography

[1] J. C. Harfield, C. Batchelor-McAuley, and R. G. Compton, "Electrochemical determination of glutathione: a review," *Analyst*, vol. 137, no. 10, pp. 2285–2296, 2012.

[2] D. M. Townsend and K. D. Tew, "The role of glutathione-s-transferase in anti-cancer drug resistance," *Oncogene*, vol. 22, no. 47, p. 7369, 2003.

[3] N. Nesakumar, S. Berchmans, and S. Alwarappan, "Chemically modified carbon based electrodes for the detection of reduced glutathione," *Sensors and Actuators B: Chemical*, 2018.

[4] K. Si, S. Cheng, S. Hideshima, S. Kuroiwa, T. Nakanishi, and T. Osaka, "Multi-analyte detection of cancer biomarkers in human serum using label-free field effect transistor biosensor," *Sensors and Materials*, vol. 30, no. 5, pp. 991–999, 2018.

[5] J. D. Wulfkuhle, L. A. Liotta, and E. F. Petricoin, "Early detection: proteomic applications for the early detection of cancer," *Nature reviews cancer*, vol. 3, no. 4, p. 267, 2003.

[6] J. Lin, Z. Wei, and C. Mao, "A label-free immunosensor based on modified mesoporous silica for simultaneous determination of tumor markers," *Biosensors and Bioelectronics*, vol. 29, no. 1, pp. 40–45, 2011.

[7] A. Poghossian and M. J. Schöning, "Label-free sensing of biomolecules with field-effect devices for clinical applications," *Electroanalysis*, vol. 26, no. 6, pp. 1197–1213, 2014.

[8] S. Varma, A. Fendyur, A. Box, and J. Voldman, "Multiplexed cell-based sensors for assessing the impact of engineered systems and methods on cell health," *Analytical chemistry*, vol. 89, no. 8, pp. 4663–4670, 2017.

[9] D. W. Domaille, E. L. Que, and C. J. Chang, "Synthetic fluorescent sensors for studying the cell biology of metals," *Nature Chemical Biology*, vol. 4, no. 3, p. 168, 2008.

[10] B. Hong and Y. Zu, "Detecting circulating tumor cells: current challenges and new trends," *Theranostics*, vol. 3, no. 6, p. 377, 2013.

[11] N. S. Barteneva, E. Fasler-Kan, and I. A. Vorobjev, "Imaging flow cytometry: coping with heterogeneity in biological systems," *Journal of Histochemistry & Cytochemistry*, vol. 60, no. 10, pp. 723–733, 2012.

[12] P. N. Abadian, C. P. Kelley, and E. D. Goluch, "Cellular analysis and detection using surface plasmon resonance techniques," *Analytical chemistry*, vol. 86, no. 6, pp. 2799–2812, 2014.

[13] Y. Fang, A. M. Ferrie, N. H. Fontaine, J. Mauro, and J. Balakrishnan, "Resonant waveguide grating biosensor for living cell sensing," *Biophysical journal*, vol. 91, no. 5, pp. 1925–1940, 2006.

[14] M. H. Jakob, B. Dong, S. Gutsch, C. Chatelle, A. Krishnaraja, W. Weber, and M. Zacharias, "Label-free sno2 nanowire fet biosensor for protein detection," *Nanotechnology*, vol. 28, no. 24, p. 245503, 2017.

[15] J.-H. Ahn, J.-Y. Kim, K. Choi, D.-I. Moon, C.-H. Kim, M.-L. Seol, T. J. Park, S. Y. Lee, and Y.-K. Choi, "Nanowire fet biosensors on a bulk silicon substrate," *IEEE Transactions on Electron Devices*, vol. 59, no. 8, pp. 2243–2249, 2012.

[16] T. Sakata and Y. Matsuse, "In situ electrical monitoring of cancer cells invading vascular endothelial cells with semiconductor-based biosensor," *Genes to Cells*, vol. 22, no. 2, pp. 203–209, 2017.

[17] M. Kaisti, "Detection principles of biological and chemical fet sensors," *Biosensors and Bioelectronics*, vol. 98, pp. 437–448, 2017.

[18] S. MacKay, D. Wishart, J. Z. Xing, and J. Chen, "Developing trends in aptamer-based biosensor devices and their applications," *IEEE transactions on biomedical circuits and systems*, vol. 8, no. 1, pp. 4–14, 2014.

[19] M. Sasmal, T. K. Maiti, and T. K. Bhattacharyya, "Synthesis of zno nanosphere for picomolar level detection of bovine serum albumin," *IEEE transactions on nanobioscience*, vol. 14, no. 1, pp. 129–137, 2015.

[20] M. Taei, H. Hadadzadeh, F. Hasanpour, G. Zahedi, and Z. Dehbanipour, "A voltammetric sensor based on multiwalled carbon nanotubes and a new azoferrocene derivative for determination of glutathione," *IEEE Sensors Journal*, vol. 15, no. 8, pp. 4472–4479, 2015.

[21] A. K. Pulikkathodi, I. Sarangadharan, Y.-H. Chen, G.-Y. Lee, J.-I. Chyi, G.-B. Lee, and Y.-L. Wang, "Dynamic monitoring of transmembrane potential changes: a study of ion channels using an electrical double layer-gated fet biosensor," *Lab on a Chip*, vol. 18, no. 7, pp. 1047–1056, 2018.

[22] B. M. Lomaestro and M. Malone, "Glutathione in health and disease: pharmacotherapeutic issues," *Annals of Pharmacotherapy*, vol. 29, no. 12, pp. 1263–1273, 1995.

[23] R. Ozols, P. O'Dwyer, T. Hamilton, and R. Young, "The role of glutathione in drug resistance," *Cancer treatment reviews*, vol. 17, pp. 45–50, 1990.

[24] Y. Li, G. Wei, and J. Chen, "Glutathione: a review on biotechnological production," *Applied microbiology and biotechnology*, vol. 66, no. 3, pp. 233–242, 2004.

[25] H. SIES and K.-H. SUMMER, "Hydroperoxide-metabolizing systems in rat liver," *European journal of biochemistry*, vol. 57, no. 2, pp. 503–512, 1975.

[26] W. A. Kleinman and J. P. Richie Jr, "Status of glutathione and other thiols and disulfides in human plasma," *Biochemical pharmacology*, vol. 60, no. 1, pp. 19–29, 2000.

[27] J. M. Estrela, A. Ortega, and E. Obrador, "Glutathione in cancer biology and therapy," *Critical reviews in clinical laboratory sciences*, vol. 43, no. 2, pp. 143–181, 2006.

[28] N. Traverso, R. Ricciarelli, M. Nitti, B. Marengo, A. L. Furfaro, M. A. Pronzato, U. M. Marinari, and C. Domenicotti, "Role of glutathione in cancer progression and chemoresistance," *Oxidative medicine and cellular longevity*, vol. 2013, 2013.

[29] H. J. Forman, H. Zhang, and A. Rinna, "Glutathione: overview of its protective roles, measurement, and biosynthesis," *Molecular aspects of medicine*, vol. 30, no. 1-2, pp. 1–12, 2009.

[30] A. Meister, "Glutathione metabolism and its selective modification." *Journal of biological chemistry*, vol. 263, no. 33, pp. 17 205–17 208, 1988.

[31] M. P. Gamcsik, M. S. Kasibhatla, S. D. Teeter, and O. M. Colvin, "Glutathione levels in human tumors," *Biomarkers*, vol. 17, no. 8, pp. 671–691, 2012.

[32] J. A. Cook, H. I. Pass, S. N. Iype, N. Friedman, W. DeGraff, A. Russo, and J. B. Mitchell, "Cellular glutathione and thiol measurements from surgically resected human lung tumor and normal lung tissue," *Cancer research*, vol. 51, no. 16, pp. 4287–4294, 1991.

[33] M. McCully, Y. Hernandez, J. Conde, P. V. Baptista, M. Jesus, A. Hursthouse, D. Stirling, and C. C. Berry, "Significance of the balance between intracellular glutathione and polyethylene glycol for successful release of small interfering rna from gold nanoparticles," *Nano Research*, vol. 8, no. 10, pp. 3281–3292, 2015.

[34] E. Drozd, B. Gruber, J. Marczewska, J. Drozd, and E. Anuszewska, "Intracellular glutathione level and efflux in human melanoma and cervical cancer cells differing in doxorubicin resistance." *Advances in Hygiene & Experimental Medicine/Postepy Higieny i Medycyny Doswiadczalnej*, vol. 70, 2016.

[35] F. Benyettou, H. Fahs, R. Elkharrag, R. Bilbeisi, B. Asma, R. Rezgui, L. Motte, M. Magzoub, J. Brandel, J.-C. Olsen *et al.*, "Selective growth inhibition of cancer cells with doxorubicin-loaded cb [7]-modified iron-oxide nanoparticles," *RSC Advances*, vol. 7, no. 38, pp. 23 827–23 834, 2017.

[36] A. Rosi, S. Grande, A. M. Luciani, A. Palma, C. Giovannini, L. Guidoni, O. Sapora, and V. Viti, "Role of glutathione in apoptosis induced by radiation as determined by 1h mr spectra of cultured tumor cells," *Radiation research*, vol. 167, no. 3, pp. 268–282, 2007.

[37] N. Khedimallah, A. Zazoua, A. Sbartai, and N. Jaffrezic-Renault, "A high sensitivity impedimetric biosensor using the tannin from quercusmacrolepis as biorecognition element for heavy metals detection," *IEEE transactions on nanobioscience*, vol. 14, no. 7, pp. 694–699, 2015.

[38] S. Mukherjee, X. Meshik, M. Choi, S. Farid, D. Datta, Y. Lan, S. Poduri, K. Sarkar, U. Baterdene, C.-E. Huang *et al.*, "A graphene and aptamer based liquid gated fet-like electrochemical biosensor to detect adenosine triphosphate," *IEEE transactions on nanobioscience*, vol. 14, no. 8, pp. 967–972, 2015.

[39] C. Yang, Y. Huang, B. L. Hassler, R. M. Worden, and A. J. Mason, "Amperometric electrochemical microsystem for a miniaturized protein biosensor array," *IEEE transactions on biomedical circuits and systems*, vol. 3, no. 3, pp. 160–168, 2009.

[40] Y. Huang, Y. Liu, B. L. Hassler, R. M. Worden, and A. J. Mason, "A protein-based electrochemical biosensor array platform for integrated microsystems," *IEEE transactions on biomedical circuits and systems*, vol. 7, no. 1, pp. 43–51, 2013.

[41] A. Manickam, A. Chevalier, M. McDermott, A. D. Ellington, and A. Hassibi, "A cmos electrochemical impedance spectroscopy (eis) biosensor array," *IEEE Transactions on Biomedical Circuits and Systems*, vol. 4, no. 6, pp. 379–390, 2010.

[42] M. Raggi, L. Nobile, and A. Giovannini, "Spectrophotometric determination of glutathione and of its oxidation product in pharmaceutical dosage forms," *Journal of pharmaceutical and biomedical analysis*, vol. 9, no. 10-12, pp. 1037–1040, 1991.

[43] M. Kominkova, P. Horky, N. Cernei, K. Tmejova, B. Ruttkay-Nedecky, R. Guran, M. Pohanka, O. Zitka, V. Adam, and R. Kizek, "Optimization of the glutathione detection by high performance liquid chromatography with electrochemical detection in the brain and liver of rats fed with taurine," *International Journal of Electrochemical Science*, vol. 10, pp. 1716–1727, 2015.

[44] J. Zhang, Z. Hu, and X. Chen, "Quantification of glutathione and glutathione disulfide in human plasma and tobacco leaves by capillary electrophoresis with laser-induced fluorescence detection," *Talanta*, vol. 65, no. 4, pp. 986–990, 2005.

[45] D. L. Rabenstein, D. W. Brown, and C. J. McNeil, "Determination of glutathione in intact and hemolyzed erythrocytes by titration with tert-butyl hydroperoxide with end point detection by proton nuclear magnetic resonance spectrometry," *Analytical chemistry*, vol. 57, no. 12, pp. 2294–2299, 1985.

[46] M. Taei, H. Hadadzadeh, F. Hasanpour, G. Zahedi, and Z. Dehbanipour, "A voltammetric sensor based on multiwalled carbon nanotubes and a new azoferrocene derivative for determination of glutathione," *IEEE Sensors Journal*, vol. 15, no. 8, pp. 4472–4479, 2015.

[47] T. J. Mozer, D. C. Tiemeier, and E. G. Jaworski, "Purification and characterization of corn glutathione s-transferase," *Biochemistry*, vol. 22, no. 5, pp. 1068–1072, 1983.

[48] W. H. Habig, M. J. Pabst, and W. B. Jakoby, "Glutathione s-transferases the first enzymatic step in mercapturic acid formation," *Journal of biological Chemistry*, vol. 249, no. 22, pp. 7130–7139, 1974.

[49] S. Ren, F. Zhou, C. Xu, and B. Li, "Simple method for visual detection of glutathione s-transferase activity and inhibition using cysteamine-capped gold nanoparticles as colorimetric probes," *Gold Bulletin*, vol. 48, no. 3-4, pp. 147–152, 2015.

[50] L. Flohe, "Glutathione," *ACS nano*, 2018.

[51] P. Pasakon, C. Karuwan, C. Sriprachuabwong, A. Wisitsoraat, D. Phokharatkul, T. Lomas, and A. Tuantranont, "Electrochemical detection of glutathione based on inkjet-printed graphene modified screen printed carbon paste electrode," *Sensor Letters*, vol. 11, no. 12, pp. 2218–2226, 2013.

[52] T. H. Tsai, S. Thiagarajan, and S.-M. Chen, "www. spm. com. cn," *Int. J. Electrochem. Sci*, vol. 6, pp. 3878–3889, 2011.

[53] G. Chen, J. Wang, C. Wu, C.-z. Li, H. Jiang, and X. Wang, "Photoelectrocatalytic oxidation of glutathione based on porous tio2–pt nanowhiskers," *Langmuir*, vol. 28, no. 33, pp. 12 393–12 399, 2012.

[54] Y. Oztekin, A. Ramanaviciene, and A. Ramanavicius, "Electrochemical glutathione sensor based on electrochemically deposited poly-m-aminophenol," *Electroanalysis*, vol. 23, no. 3, pp. 701–709, 2011.

[55] L. Zhao, L. Zhao, Y. Miao, and C. Zhang, "Selective electrochemical determination of glutathione from the leakage of intracellular gsh contents in hela cells following doxorubicin-induced cell apoptosis," *Electrochimica Acta*, vol. 206, pp. 86–98, 2016.

[56] X. Wang, J. Wang, H. Fu, D. Liu, and Z. Chen, "Determination of glutathione in single hepg2 cells by capillary electrophoresis with reduced graphene oxide modified microelectrode," *Electrophoresis*, vol. 35, no. 23, pp. 3371–3378, 2014.

[57] A. A. Ensafi, M. Monsef, B. Rezaei, and H. Karimi-Maleh, "Nanostructure-based electrochemical sensor for determination of glutathione in hemolysed erythrocytes and urine," *Journal of analytical chemistry*, vol. 69, no. 9, pp. 892–898, 2014.

[58] B. Yuan, C. Xu, R. Zhang, D. Lv, S. Li, D. Zhang, L. Liu, and C. Fernandez, "Glassy carbon electrode modified with 7, 7, 8, 8-tetracyanoquinodimethane and graphene oxide triggered a synergistic effect: Low-potential amperometric detection of reduced glutathione," *Biosensors and bioelectronics*, vol. 96, pp. 1–7, 2017.

[59] H. Xu, J. Xiao, B. Liu, S. Griveau, and F. Bedioui, "Enhanced electrochemical sensing of thiols based on cobalt phthalocyanine immobilized on nitrogen-doped graphene," *Biosensors and Bioelectronics*, vol. 66, pp. 438–444, 2015.

[60] J. Zhou, T. J. O'Shea, and S. M. Lunte, "Simultaneous detection of thiols and disulfides by capillary electrophoresis-electrochemical detection using a mixed-valence ruthenium cyanide-modified microelectrode," *Journal of Chromatography A*, vol. 680, no. 1, pp. 271–277, 1994.

[61] P. Muthirulan and R. Velmurugan, "Direct electrochemistry and electrocatalysis of reduced glutathione on cnfs–pdda/pb nanocomposite film modified ito electrode for biosensors," *Colloids and Surfaces B: Biointerfaces*, vol. 83, no. 2, pp. 347–354, 2011.

[62] J. B. Raoof, R. Ojani, H. Karimi-Maleh, M. R. Hajmohamadi, and P. Biparva, "Multi-wall carbon nanotubes as a sensor and ferrocene dicarboxylic acid as a mediator for voltammetric determination of glutathione in hemolysed erythrocyte," *Analytical Methods*, vol. 3, no. 11, pp. 2637–2643, 2011.

[63] H. Karimi-Maleh, F. Tahernejad-Javazmi, A. A. Ensafi, R. Moradi, S. Mallakpour, and H. Beitollahi, "A high sensitive biosensor based on fept/cnts nanocomposite/n-(4-hydroxyphenyl)-3, 5-dinitrobenzamide modified carbon paste electrode for simultaneous determination of glutathione and piroxicam," *Biosensors and Bioelectronics*, vol. 60, pp. 1–7, 2014.

[64] A. Ensafi, H. Karimi-Maleh, and S. Mallakpour, "A new strategy for the selective determination of glutathione in the presence of nicotinamide adenine dinucleotide (nadh) using a novel modified carbon nanotube paste electrode," *Colloids and Surfaces B: Biointerfaces*, vol. 104, pp. 186–193, 2013.

[65] J. Raoof, R. Ojani, and H. Karimi-Maleh, "Electrocatalytic oxidation of glutathione at carbon paste electrode modified with 2, 7-bis (ferrocenyl ethyl) fluoren-9-one: application as a voltammetric sensor," *Journal of applied electrochemistry*, vol. 39, no. 8, pp. 1169–1175, 2009.

[66] N. H. Cnubben, I. M. Rietjens, H. Wortelboer, J. van Zanden, and P. J. van Bladeren, "The interplay of glutathione-related processes in antioxidant defense," *Environmental Toxicology and Pharmacology*, vol. 10, no. 4, pp. 141–152, 2001.

[67] J. W. Coleman, "Nitric oxide in immunity and inflammation," *International immunopharmacology*, vol. 1, no. 8, pp. 1397–1406, 2001.

[68] S. A. Zaidi and J. H. Shin, "A review on the latest developments in nanostructure-based electrochemical sensors for glutathione," *Analytical Methods*, vol. 8, no. 8, pp. 1745–1754, 2016.

[69] H. Sies, "Glutathione and its role in cellular functions," *Free Radical Biology and Medicine*, vol. 27, no. 9-10, pp. 916–921, 1999.

[70] P. Nagendra, H. Yathirajan, K. Rangappa, K. Mohana, and P. Nagaraja, "Silver salt of n-bromo-4-methylbenzenesulfonamide as a new oxidimetric reagent," *Journal of the Indian Chemical Society*, vol. 79, no. 7, pp. 602–604, 2002.

[71] M. Raggi, L. Nobile, and A. Giovannini, "Spectrophotometric determination of glutathione and of its oxidation product in pharmaceutical dosage forms," *Journal of pharmaceutical and biomedical analysis*, vol. 9, no. 10-12, pp. 1037–1040, 1991.

[72] K. Kamata, M. Takahashi, K. Terajima, and M. Nishijima, "Spectrophotometric determination of sodium chondroitin sulfate in eye drops after derivatization with 4-amino-3-hydrazino-5-mercapto-1, 2, 4-triazole," *Analyst*, vol. 120, no. 11, pp. 2755–2758, 1995.

[73] Z. Ma, Y. Qiu, H. Yang, Y. Huang, J. Liu, Y. Lu, C. Zhang, and P. Hu, "Effective synergistic effect of dipeptide-polyoxometalate-graphene oxide ternary hybrid materials on peroxidase-like mimics with enhanced performance," *ACS applied materials & interfaces*, vol. 7, no. 39, pp. 22 036–22 045, 2015.

[74] J. Zhang, Z. Hu, and X. Chen, "Quantification of glutathione and glutathione disulfide in human plasma and tobacco leaves by capillary electrophoresis with laser-induced fluorescence detection," *Talanta*, vol. 65, no. 4, pp. 986–990, 2005.

[75] R. Kand'ár, P. Žáková, H. Lotková, O. Kučera, and Z. Červinková, "Determination of reduced and oxidized glutathione in biological samples using liquid chromatography with fluorimetric detection," *Journal of pharmaceutical and biomedical analysis*, vol. 43, no. 4, pp. 1382–1387, 2007.

[76] A. E. Katrusiak, P. G. Paterson, H. Kamencic, A. Shoker, and A. W. Lyon, "Pre-column derivatization high-performance liquid chromatographic method for determination of cysteine, cysteinyl–glycine, homocysteine and glutathione in plasma and cell extracts," *Journal of Chromatography B: Biomedical Sciences and Applications*, vol. 758, no. 2, pp. 207–212, 2001.

[77] F. Xu, L. Wang, M. Gao, L. Jin, and J. Jin, "Amperometric determination of glutathione and cysteine on a pd-iro2 modified electrode with high performance liquid chromatography in rat brain microdialysate," *Analytical and bioanalytical chemistry*, vol. 372, no. 7-8, pp. 791–794, 2002.

[78] E. Caussé, P. Malatray, R. Calaf, P. Charpiot, M. Candito, C. Bayle, P. Valdiguié, R. Salvayre, and F. Couderc, "Plasma total homocysteine and other thiols analyzed by capillary electrophoresis/laser-induced fluorescence detection: Comparison with two other methods," *ELECTROPHORESIS: An International Journal*, vol. 21, no. 10, pp. 2074–2079, 2000.

[79] D. L. Rabenstein, D. W. Brown, and C. J. McNeil, "Determination of glutathione in intact and hemolyzed erythrocytes by titration with tert-butyl hydroperoxide with end point detection by proton nuclear magnetic resonance spectrometry," *Analytical chemistry*, vol. 57, no. 12, pp. 2294–2299, 1985.

[80] I. Satoh, S. Arakawa, and A. Okamoto, "Flow-injection determination of glutathione with amperometric monitoring of the enzymatic reaction," *Analytica Chimica Acta*, vol. 214, pp. 415–419, 1988.

[81] A. Ensafi, T. Khayamian, and F. Hasanpour, "Determination of glutathione in hemolysed erythrocyte by flow injection analysis with chemiluminescence detection," *Journal of pharmaceutical and biomedical analysis*, vol. 48, no. 1, pp. 140–144, 2008.

[82] J. Raoof, R. Ojani, and H. Karimi-Maleh, "Electrocatalytic oxidation of glutathione at carbon paste electrode modified with 2, 7-bis (ferrocenyl ethyl) fluoren-9-one: application as a voltammetric sensor," *Journal of applied electrochemistry*, vol. 39, no. 8, pp. 1169–1175, 2009.

[83] J. B. Raoof, R. Ojani, and M. Kolbadinezhad, "Voltammetric sensor for glutathione determination based on ferrocene-modified carbon paste electrode," *Journal of Solid State Electrochemistry*, vol. 13, no. 9, p. 1411, 2009.

[84] A. A. Ensafi, M. Taei, T. Khayamian, H. Karimi-Maleh, and F. Hasanpour, "Voltammetric measurement of trace amount of glutathione using multiwall carbon nanotubes as a sensor and chlorpromazine as a mediator," *Journal of Solid State Electrochemistry*, vol. 14, no. 8, pp. 1415–1423, 2010.

[85] H. Karimi-Maleh, F. Tahernejad-Javazmi, A. A. Ensafi, R. Moradi, S. Mallakpour, and H. Beitollahi, "A high sensitive biosensor based on fept/cnts nanocomposite/n-(4-hydroxyphenyl)-3, 5-dinitrobenzamide modified carbon paste electrode for simultaneous determination of glutathione and piroxicam," *Biosensors and Bioelectronics*, vol. 60, pp. 1–7, 2014.

[86] F. Tietze, "Enzymic method for quantitative determination of nanogram amounts of total and oxidized glutathione: applications to mammalian blood and other tissues," *Analytical biochemistry*, vol. 27, no. 3, pp. 502–522, 1969.

[87] R. Rossi, A. Milzani, I. Dalle-Donne, D. Giustarini, L. Lusini, R. Colombo, and P. Di Simplicio, "Blood glutathione disulfide: in vivo factor or in vitro artifact?" *Clinical chemistry*, vol. 48, no. 5, pp. 742–753, 2002.

[88] I. Németh and D. Boda, "Blood glutathione redox ratio as a parameter of oxidative stress in premature infants with irds," *Free Radical Biology and Medicine*, vol. 16, no. 3, pp. 347–353, 1994.

[89] O. W. Griffith, "Determination of glutathione and glutathione disulfide using glutathione reductase and 2-vinylpyridine," *Analytical biochemistry*, vol. 106, no. 1, pp. 207–212, 1980.

[90] I. Rahman, A. Kode, and S. K. Biswas, "Assay for quantitative determination of glutathione and glutathione disulfide levels using enzymatic recycling method," *Nature protocols*, vol. 1, no. 6, p. 3159, 2006.

[91] I. H. Shaik and R. Mehvar, "Rapid determination of reduced and oxidized glutathione levels using a new thiol-masking reagent and the enzymatic recycling method: application to the rat liver and bile samples," *Analytical and bioanalytical chemistry*, vol. 385, no. 1, pp. 105–113, 2006.

[92] A. R. Araujo, M. L. M. Saraiva, and J. L. Lima, "Determination of total and oxidized glutathione in human whole blood with a sequential injection analysis system," *Talanta*, vol. 74, no. 5, pp. 1511–1519, 2008.

[93] R. Brigelius, C. Muckel, T. P. Akerboom, and H. Sies, "Identification and quantitation of glutathione in hepatic protein mixed disulfides and its relationship to glutathione disulfide," *Biochemical pharmacology*, vol. 32, no. 17, pp. 2529–2534, 1983.

[94] H. Güntherberg and J. Rost, "The true oxidized glutathione content of red blood cells obtained by new enzymic and paper chromatographic methods." *Analytical Biochemistry*, vol. 15, no. 2, p. 205, 1966.

[95] H. Wang, W.-S. Wang, and H.-S. Zhang, "A spectrofluorimetric method for cysteine and glutathione using the fluorescence system of zn (ii)–8-hydroxyquinoline-5-sulphonic acid complex," *Spectrochimica Acta Part A: Molecular and Biomolecular Spectroscopy*, vol. 57, no. 12, pp. 2403–2407, 2001.

[96] L. Wang, L. Wang, T. Xia, G. Bian, L. Dong, Z. Tang, and F. Wang, "A highly sensitive assay for spectrofluorimetric determination of reduced glutathione using organic nano-probes," *Spectrochimica Acta Part A: Molecular and Biomolecular Spectroscopy*, vol. 61, no. 11-12, pp. 2533–2538, 2005.

[97] P. K. Pullela, T. Chiku, M. J. Carvan III, and D. S. Sem, "Fluorescence-based detection of thiols in vitro and in vivo using dithiol probes," *Analytical biochemistry*, vol. 352, no. 2, pp. 265–273, 2006.

[98] B. Tang, Y. Xing, P. Li, N. Zhang, F. Yu, and G. Yang, "A rhodamine-based fluorescent probe containing a se- n bond for detecting thiols and its application in living cells," *Journal of the American Chemical Society*, vol. 129, no. 38, pp. 11 666–11 667, 2007.

[99] M. M. Pires and J. Chmielewski, "Fluorescence imaging of cellular glutathione using a latent rhodamine," *Organic letters*, vol. 10, no. 5, pp. 837–840, 2008.

[100] A. Shibata, K. Furukawa, H. Abe, S. Tsuneda, and Y. Ito, "Rhodamine-based fluorogenic probe for imaging biological thiol," *Bioorganic & medicinal chemistry letters*, vol. 18, no. 7, pp. 2246–2249, 2008.

[101] K.-J. Huang, W.-Z. Xie, H. Wang, and H.-S. Zhang, "Sensitive determination of s-nitrosothiols in human blood by spectrofluorimetry using a fluorescent probe: 1, 3, 5, 7-tetramethyl-8-(3, 4-diaminophenyl)-difluoroboradiaza-s-indacene," *Talanta*, vol. 73, no. 1, pp. 62–67, 2007.

[102] K.-J. Huang, C.-X. Xu, W.-Z. Xie, H.-S. Zhang, and H. Wang, "Ultra-trace determination of s-nitrosothiols in blood samples by spectrofluorimetry with 8-(3, 4-diaminophenyl)-difluoroboradiaza-s-indacene," *Spectrochimica Acta Part A: Molecular and Biomolecular Spectroscopy*, vol. 69, no. 2, pp. 437–442, 2008.

[103] J. Widengren, V. Kudryavtsev, M. Antonik, S. Berger, M. Gerken, and C. A. Seidel, "Single-molecule detection and identification of multiple species by multiparameter fluorescence detection," *Analytical chemistry*, vol. 78, no. 6, pp. 2039–2050, 2006.

[104] V. Kudryavtsev, S. Felekyan, A. K. Woźniak, M. König, C. Sandhagen, R. Kühnemuth, C. A. Seidel, and F. Oesterhelt, "Monitoring dynamic systems with multiparameter fluorescence imaging," *Analytical and bioanalytical chemistry*, vol. 387, no. 1, pp. 71–82, 2007.

[105] W. L. Hinze, T. E. Reihl, H. Singh, and Y. Baba, "Micelle-enhanced chemiluminescence and application to the determination of biological reductants using lucigenin," *Analytical chemistry*, vol. 56, no. 12, pp. 2180–2191, 1984.

[106] F. J. Romero and W. Mueller-Klieser, "Semiquantitative bioluminescent assay of glutathione," *Journal of bioluminescence and chemiluminescence*, vol. 13, no. 5, pp. 263–266, 1998.

[107] T. Mourad, K.-L. Min, and J.-P. Steghens, "Measurement of oxidized glutathione by enzymatic recycling coupled to bioluminescent detection," *Analytical biochemistry*, vol. 283, no. 2, pp. 146–152, 2000.

[108] C. Lau, X. Qin, J. Liang, and J. Lu, "Determination of cysteine in a pharmaceutical formulation by flow injection analysis with a chemiluminescence detector," *Analytica Chimica Acta*, vol. 514, no. 1, pp. 45–49, 2004.

[109] A. Ensafi, T. Khayamian, and F. Hasanpour, "Determination of glutathione in hemolysed erythrocyte by flow injection analysis with chemiluminescence detection," *Journal of pharmaceutical and biomedical analysis*, vol. 48, no. 1, pp. 140–144, 2008.

[110] J. Du, Y. Li, and J. Lu, "Investigation on the chemiluminescence reaction of luminol–h2o2–s2-/r–sh system," *Analytica chimica acta*, vol. 448, no. 1-2, pp. 79–83, 2001.

[111] L. Nie, H. Ma, M. Sun, X. Li, M. Su, and S. Liang, "Direct chemiluminescence determination of cysteine in human serum using quinine–ce (iv) system," *Talanta*, vol. 59, no. 5, pp. 959–964, 2003.

[112] S. Wang, H. Ma, J. Li, X. Chen, Z. Bao, and S. Sun, "Direct determination of reduced glutathione in biological fluids by ce (iv)–quinine chemiluminescence," *Talanta*, vol. 70, no. 3, pp. 518–521, 2006.

[113] B. Rezaei and A. Mokhtari, "A simple and rapid flow injection chemiluminescence determination of cysteine with ru (phen) 32+–ce (iv) system," *Spectrochimica Acta Part A: Molecular and Biomolecular Spectroscopy*, vol. 66, no. 2, pp. 359–363, 2007.

[114] H.-Y. Han, Z.-K. He, and Y.-E. Zeng, "Chemiluminescence method for the determination of glutathione in human serum using the ru (phen) 3 2+–kmno 4 system," *Microchimica Acta*, vol. 155, no. 3-4, pp. 431–434, 2006.

[115] A. H. Trabesinger, O. M. Weber, C. O. Duc, and P. Boesiger, "Detection of glutathione in the human brain in vivo by means of double quantum coherence filtering," *Magnetic Resonance in Medicine: An Official Journal of the International Society for Magnetic Resonance in Medicine*, vol. 42, no. 2, pp. 283–289, 1999.

[116] A. H. Trabesinger and P. Boesiger, "Improved selectivity of double quantum coherence filtering for the detection of glutathione in the human brain in vivo," *Magnetic Resonance in Medicine: An Official Journal of the International Society for Magnetic Resonance in Medicine*, vol. 45, no. 4, pp. 708–710, 2001.

[117] T. Zhao, K. Heberlein, C. Jonas, D. P. Jones, and X. Hu, "New double quantum coherence filter for localized detection of glutathione in vivo," *Magnetic Resonance in Medicine: An Official Journal of the International Society for Magnetic Resonance in Medicine*, vol. 55, no. 3, pp. 676–680, 2006.

[118] T. Satoh and Y. Yoshioka, "Contribution of reduced and oxidized glutathione to signals detected by magnetic resonance spectroscopy as indicators of local brain redox state," *Neuroscience research*, vol. 55, no. 1, pp. 34–39, 2006.

[119] M. Terpstra, M. Marjanska, P.-G. Henry, I. Tkáč, and R. Gruetter, "Detection of an antioxidant profile in the human brain in vivo via double editing with mega-press," *Magnetic resonance in medicine*, vol. 56, no. 6, pp. 1192–1199, 2006.

[120] D. I. Potapenko, E. G. Bagryanskaya, I. A. Grigoriev, A. M. Maksimov, V. A. Reznikov, V. E. Platonov, T. L. Clanton, and V. V. Khramtsov, "Quantitative determination of sh groups using 19f nmr spectroscopy and disulfide of 2, 3, 5, 6-tetrafluoro-4-mercaptobenzoic acid," *Magnetic Resonance in Chemistry*, vol. 43, no. 11, pp. 902–909, 2005.

[121] E. C. Kennett, W. A. Bubb, P. Bansal, P. Alewood, and P. W. Kuchel, "Nmr studies of exchange between intra-and extracellular glutathione in human erythrocytes," *Redox Report*, vol. 10, no. 2, pp. 83–90, 2005.

[122] M. R. CIRIOLO, M. PACI, M. SETTE, A. DE MARTINO, A. BOZZI, and G. ROTILIO, "Transduction of reducing power across the plasma membrane by reduced glutathione: A 1h-nmr spin-echo study of intact human erythrocytes," *European journal of biochemistry*, vol. 215, no. 3, pp. 711–718, 1993.

[123] G. A. Rivas, M. D. Rubianes, M. C. Rodriguez, N. F. Ferreyra, G. L. Luque, M. L. Pedano, S. A. Miscoria, and C. Parrado, "Carbon nanotubes for electrochemical biosensing," *Talanta*, vol. 74, no. 3, pp. 291–307, 2007.

[124] P. Ciosek and W. Wroblewski, "Sensor arrays for liquid sensing–electronic tongue systems," *Analyst*, vol. 132, no. 10, pp. 963–978, 2007.

[125] S. Timur, D. Odaci, A. Dincer, F. Zihnioglu, and A. Telefoncu, "Biosensing approach for glutathione detection using glutathione reductase and sulfhydryl oxidase bienzymatic system," *Talanta*, vol. 74, no. 5, pp. 1492–1497, 2008.

[126] J. J. Ruiz-Díaz, A. A. Torriero, E. Salinas, E. J. Marchevsky, M. I. Sanz, and J. Raba, "Enzymatic rotating biosensor for cysteine and glutathione determination in a fia system," *Talanta*, vol. 68, no. 4, pp. 1343–1352, 2006.

[127] W. Cha and M. E. Meyerhoff, "S-nitrosothiol detection via amperometric nitric oxide sensor with surface modified hydrogel layer containing immobilized organoselenium catalyst," *Langmuir*, vol. 22, no. 25, pp. 10 830–10 836, 2006.

[128] D. Giustarini, A. Milzani, I. Dalle-Donne, and R. Rossi, "Detection of s-nitrosothiols in biological fluids: a comparison among the most widely applied methodologies," *Journal of Chromatography B*, vol. 851, no. 1-2, pp. 124–139, 2007.

[129] R. Kizek, J. Vacek, L. Trnková, and F. Jelen, "Cyclic voltammetric study of the redox system of glutathione using the disulfide bond reductant tris (2-carboxyethyl) phosphine," *Bioelectrochemistry*, vol. 63, no. 1-2, pp. 19–24, 2004.

[130] A. Salimi and R. Hallaj, "Catalytic oxidation of thiols at preheated glassy carbon electrode modified with abrasive immobilization of multiwall carbon nanotubes: applications to amperometric detection of thiocytosine, l-cysteine and glutathione," *Talanta*, vol. 66, no. 4, pp. 967–975, 2005.

[131] H. Han and H. Tachikawa, "Electrochemical determination of thiols at single-wall carbon nanotubes and pqq modified electrodes," *Front. Biosci*, vol. 10, pp. 931–939, 2005.

[132] A. Salimi and S. Pourbeyram, "Renewable sol–gel carbon ceramic electrodes modified with a ru-complex for the amperometric detection of l-cysteine and glutathione," *Talanta*, vol. 60, no. 1, pp. 205–214, 2003.

[133] O. Nekrassova, P. C. White, S. Threlfell, G. Hignett, A. J. Wain, N. S. Lawrence, J. Davis, and R. G. Compton, "An electrochemical adaptation of ellman's test," *Analyst*, vol. 127, no. 6, pp. 797–802, 2002.

[134] Y. Hou, J. C. Ndamanisha, L.-p. Guo, X.-j. Peng, and J. Bai, "Synthesis of ordered mesoporous carbon/cobalt oxide nanocomposite for determination of glutathione," *Electrochimica Acta*, vol. 54, no. 26, pp. 6166–6171, 2009.

[135] E. Hugo Seymour, S. J. Wilkins, N. S. Lawrence, and R. G. Compton, "Electrochemical detection of glutathione: An electrochemically initiated reaction pathway," *Analytical letters*, vol. 35, no. 8, pp. 1387–1399, 2002.

[136] T. H. Huang, T. Kuwana, and A. Warsinke, "Analysis of thiols with tyrosinase-modified carbon paste electrodes based on blocking of substrate recycling," *Biosensors and Bioelectronics*, vol. 17, no. 11-12, pp. 1107–1113, 2002.

[137] N. S. Lawrence, J. Davis, and R. G. Compton, "Electrochemical detection of thiols in biological media," *Talanta*, vol. 53, no. 5, pp. 1089–1094, 2001.

[138] S. A. Wring, J. P. Hart, and B. J. Birch, "Voltammetric behaviour of screen-printed carbon electrodes, chemically modified with selected mediators, and their application as sensors for the determination of reduced glutathione," *Analyst*, vol. 116, no. 2, pp. 123–129, 1991.

[139] P. W. Alexander, A. Hidayat, and D. B. Hibbert, "Tungsten sensor for amperometric detection of organic thiols and proteins," *Electroanalysis*, vol. 7, no. 3, pp. 290–291, 1995.

[140] B. Nalini and S. Sriman Narayanan, "Electrocatalytic oxidation of sulfhydryl compounds at ruthenium (iii) diphenyldithiocarbamate modified carbon paste electrode," *Electroanalysis: An International Journal Devoted to Fundamental and Practical Aspects of Electroanalysis*, vol. 10, no. 11, pp. 779–783, 1998.

[141] L. Mao and K. Yamamoto, "Amperometric biosensor for glutathione based on osmium-polyvinylpyridine gel polymer and glutathione sulfhydryl oxidase," *Electroanalysis: An International Journal Devoted to Fundamental and Practical Aspects of Electroanalysis*, vol. 12, no. 8, pp. 577–582, 2000.

[142] F. Xu, L. Wang, M. Gao, L. Jin, and J. Jin, "Amperometric determination of glutathione and cysteine on a pd-iro2 modified electrode with high performance liquid chromatography in rat brain microdialysate," *Analytical and bioanalytical chemistry*, vol. 372, no. 7-8, pp. 791–794, 2002.

[143] O. Nekrassova, N. S. Lawrence, and R. G. Compton, "Electrochemically initiated catalytic oxidation of 5-thio-2-nitrobenzoic acid (tnba) in the presence of thiols at a boron doped diamond electrode: Implications for total thiol detection," *Electroanalysis: An International Journal Devoted to Fundamental and Practical Aspects of Electroanalysis*, vol. 15, no. 21, pp. 1655–1660, 2003.

[144] R. R. Moore, C. E. Banks, and R. G. Compton, "Electrocatalytic detection of thiols using an edge plane pyrolytic graphite electrode," *Analyst*, vol. 129, no. 8, pp. 755–758, 2004.

[145] K. A. Joshi, P. C. Pandey, W. Chen, and A. Mulchandani, "Ormosil encapsulated pyrroloquinoline quinone-modified electrochemical sensor for thiols," *Electroanalysis: An International Journal Devoted to Fundamental and Practical Aspects of Electroanalysis*, vol. 16, no. 23, pp. 1938–1943, 2004.

[146] K. Gong, X. Zhu, R. Zhao, S. Xiong, L. Mao, and C. Chen, "Rational attachment of synthetic triptycene orthoquinone onto carbon nanotubes for electrocatalysis and sensitive detection of thiols," *Analytical chemistry*, vol. 77, no. 24, pp. 8158–8165, 2005.

[147] Z.-J. Li, Z.-L. Hou, W.-L. Song, X.-D. Liu, W.-Q. Cao, X.-H. Shao, and M.-S. Cao, "Unusual continuous dual absorption peaks in ca-doped bifeo 3 nanostructures for broadened microwave absorption," *Nanoscale*, vol. 8, no. 19, pp. 10 415–10 424, 2016.

[148] F. Ricci, F. Arduini, C. S. Tuta, U. Sozzo, D. Moscone, A. Amine, and G. Palleschi, "Glutathione amperometric detection based on a thiol–disulfide exchange reaction," *Analytica chimica acta*, vol. 558, no. 1-2, pp. 164–170, 2006.

[149] J. Vitecek, J. Petrlova, J. Petrek, V. Adam, D. Potesil, L. Havel, R. Mikelova, L. Trnkova, and R. Kizek, "Electrochemical study of s–nitrosoglutathione and nitric oxide by carbon fibre no sensor and cyclic voltammetry–possible way of monitoring of nitric oxide," *Electrochimica acta*, vol. 51, no. 24, pp. 5087–5094, 2006.

[150] P. Calvo-Marzal, K. Y. Chumbimuni-Torres, N. F. Höehr, and L. T. Kubota, "Determination of glutathione in hemolysed erythrocyte with amperometric sensor based on ttf-tcnq," *Clinica chimica acta*, vol. 371, no. 1-2, pp. 152–158, 2006.

[151] R. d. C. S. Luz, F. S. Damos, P. G. Gandra, D. V. de Macedo, A. A. Tanaka, and L. T. Kubota, "Electrocatalytic determination of reduced glutathione in human erythrocytes," *Analytical and bioanalytical chemistry*, vol. 387, no. 5, pp. 1891–1897, 2007.

[152] N. Sekioka, D. Kato, A. Ueda, T. Kamata, R. Kurita, S. Umemura, S. Hirono, and O. Niwa, "Controllable electrode activities of nano-carbon films while maintaining surface flatness by electrochemical pretreatment," *Carbon*, vol. 46, no. 14, pp. 1918–1926, 2008.

[153] J. Raoof, R. Ojani, and H. Karimi-Maleh, "Electrocatalytic oxidation of glutathione at carbon paste electrode modified with 2, 7-bis (ferrocenyl ethyl) fluoren-9-one: application as a voltammetric sensor," *Journal of applied electrochemistry*, vol. 39, no. 8, pp. 1169–1175, 2009.

[154] G. Fang, W. Xie, and A. Ding, "Electrochemical determination of reductive glutathione with copper (ii) or chromium (vi)," in *Biomedical Engineering and Computer Science (ICBECS), 2010 International Conference on.* IEEE, 2010, pp. 1–4.

[155] G. Munteanu, E. Dempsey, and T. McCormac, "Ultrafast voltammetric determination of biological thiols on the copper nanodoped mercury monolayer carbon fiber electrode," *Journal of Electroanalytical Chemistry*, vol. 638, no. 1, pp. 109–118, 2010.

[156] A.-C. Gall and C. M. ávan den Berg, "Cathodic stripping voltammetry of glutathione in natural waters," *Analyst*, vol. 118, no. 11, pp. 1411–1415, 1993.

[157] F. G. Bănică, A. G. Fogg, and J. C. Moreira, "Catalytic cathodic stripping voltammetry at a hanging mercury drop electrode of glutathione in the presence of nickel ion," *Analyst*, vol. 119, no. 11, pp. 2343–2349, 1994.

[158] F. G. Banica, A. G. Fogg, and J. C. Moreira, "Catalytic cathodic stripping voltammetry of oxidized glutathione at a hanging mercury drop electrode in the presence of nickel ion." *Talanta*, vol. 42, no. 2, pp. 227–234, 1995.

[159] J. J. Ruiz-Díaz, A. A. Torriero, E. Salinas, E. J. Marchevsky, M. I. Sanz, and J. Raba, "Enzymatic rotating biosensor for cysteine and glutathione determination in a fia system," *Talanta*, vol. 68, no. 4, pp. 1343–1352, 2006.

[160] H. Tang, J. Chen, L. Nie, S. Yao, and Y. Kuang, "Electrochemical oxidation of glutathione at well-aligned carbon nanotube array electrode," *Electrochimica Acta*, vol. 51, no. 15, pp. 3046–3051, 2006.

[161] S. Griveau, M. Gulppi, J. Pavez, J. H. Zagal, and F. Bedioui, "Cobalt phthalocyanine-based molecular materials for the electrocatalysis and electroanalysis of 2-mercaptoethanol, 2-mercaptoethanesulfonic acid, reduced glutathione and l-cysteine," *Electroanalysis: An International Journal Devoted to Fundamental and Practical Aspects of Electroanalysis*, vol. 15, no. 9, pp. 779–785, 2003.

[162] A. Salimi and S. Pourbeyram, "Renewable sol–gel carbon ceramic electrodes modified with a ru-complex for the amperometric detection of l-cysteine and glutathione," *Talanta*, vol. 60, no. 1, pp. 205–214, 2003.

[163] C. Hua, M. R. Smyth, and C. O'Fagain, "Determination of glutathione at enzyme-modified and unmodified glassy carbon electrodes," *Analyst*, vol. 116, no. 9, pp. 929–931, 1991.

[164] S. Zhao and R. B. Lennox, "Bioelectrocatalysis at organic conducting salt electrodes. use of hexamethylenetetratellurafulvalene tetracyanoquinodimethane (hmttef-tcnq) as a versatile electrode material," *Journal of Electroanalytical Chemistry*, vol. 346, no. 1-2, pp. 161–173, 1993.

[165] W. Wang, L. Li, S. Liu, C. Ma, and S. Zhang, "Determination of physiological thiols by electrochemical detection with piazselenole and its application in rat breast cancer cells 4t-1," *Journal of the American Chemical Society*, vol. 130, no. 33, pp. 10 846–10 847, 2008.

[166] V. Shankar, D. Singh, S. Verma, and V. Krishna, "Mixed metal mixed ligand complexation equilibria of transition metal ions involving nitrilotriacetic acid (nta) and l-2-amino-3-methyl butanoic acid (valine)," *National Academy Science Letters*, vol. 39, no. 3, pp. 185–189, 2016.

[167] J.-B. Raoof, R. Ojani, and M. Baghayeri, "Simultaneous electrochemical determination of glutathione and tryptophan on a nano-tio2/ferrocene carboxylic acid modified carbon paste electrode," *Sensors and Actuators B: Chemical*, vol. 143, no. 1, pp. 261–269, 2009.

[168] A. A. Ensafi, M. Taei, T. Khayamian, H. Karimi-Maleh, and F. Hasanpour, "Voltammetric measurement of trace amount of glutathione using multiwall carbon nanotubes as a sensor and chlorpromazine as a mediator," *Journal of Solid State Electrochemistry*, vol. 14, no. 8, pp. 1415–1423, 2010.

[169] J. Vacek, J. Petřek, R. Kizek, L. Havel, B. Klejdus, L. Trnková, and F. Jelen, "Electrochemical determination of lead and glutathione in a plant cell culture," *Bioelectrochemistry*, vol. 63, no. 1-2, pp. 347–351, 2004.

[170] A. Christine, L. Gall, and C. M. Van Den Berg, "Folic acid and glutathione in the water column of the north east atlantic," *Deep Sea Research Part I: Oceanographic Research Papers*, vol. 45, no. 11, pp. 1903–1918, 1998.

[171] P. Abiman, G. G. Wildgoose, and R. G. Compton, "Electroanalytical exploitation of nitroso phenyl modified carbon-thiol interactions: Application to the low voltage determination of thiols," *Electroanalysis: An International Journal Devoted to Fundamental and Practical Aspects of Electroanalysis*, vol. 19, no. 4, pp. 437–444, 2007.

[172] R. C. Luz, F. S. Damos, A. A. Tanaka, L. T. Kubota, and Y. Gushikem, "Electrocatalysis of reduced l-glutathione oxidation by iron (iii) tetra-(n-methyl-4-pyridyl)-porphyrin (fet4mpyp) adsorbed on multi-walled carbon nanotubes," *Talanta*, vol. 76, no. 5, pp. 1097–1104, 2008.

[173] A. Safavi, N. Maleki, E. Farjami, and F. A. Mahyari, "Simultaneous electrochemical determination of glutathione and glutathione disulfide at a nanoscale copper hydroxide composite carbon ionic liquid electrode," *Analytical chemistry*, vol. 81, no. 18, pp. 7538–7543, 2009.

[174] G. Palleschi, D. Moscone, and D. Compagnone, "in biomedicina."

[175] T. Inoue and J. R. Kirchhoff, "Electrochemical detection of thiols with a coenzyme pyrroloquinoline quinone modified electrode," *Analytical Chemistry*, vol. 72, no. 23, pp. 5755–5760, 2000.

[176] F. Arduini, A. Cassisi, A. Amine, F. Ricci, D. Moscone, and G. Palleschi, "Electrocatalytic oxidation of thiocholine at chemically modified cobalt hexacyanoferrate screen-printed electrodes," *Journal of electroanalytical chemistry*, vol. 626, no. 1-2, pp. 66–74, 2009.

[177] L. Rover Jr, L. T. Kubota, and N. F. Höehr, "Development of an amperometric biosensor based on glutathione peroxidase immobilized in a carbodiimide matrix for the analysis of reduced glutathione from serum," *Clinica chimica acta*, vol. 308, no. 1-2, pp. 55–67, 2001.

[178] A. Salimi and R. Hallaj, "Catalytic oxidation of thiols at preheated glassy carbon electrode modified with abrasive immobilization of multiwall carbon nanotubes: applications to amperometric detection of thiocytosine, l-cysteine and glutathione," *Talanta*, vol. 66, no. 4, pp. 967–975, 2005.

[179] D. Bhattacharyay, K. Dutta, S. Banerjee, A. P. Turner, and P. Sarkar, "Disposable amperometric sensors for thiols with special reference to glutathione," *Electroanalysis: An International Journal Devoted to Fundamental and Practical Aspects of Electroanalysis*, vol. 20, no. 18, pp. 1947–1952, 2008.

[180] P. R. Lima, W. J. Santos, A. B. Oliveira, M. O. Goulart, and L. T. Kubota, "Electrocatalytic activity of 4-nitrophthalonitrile-modified electrode for the l-glutathione detection," *Journal of pharmaceutical and biomedical analysis*, vol. 47, no. 4-5, pp. 758–764, 2008.

[181] J. C. Ndamanisha, J. Bai, B. Qi, and L. Guo, "Application of electrochemical properties of ordered mesoporous carbon to the determination of glutathione and cysteine," *Analytical biochemistry*, vol. 386, no. 1, pp. 79–84, 2009.

[182] C. Antwi, A. S. Johnson, A. Selimovic, and R. S. Martin, "Use of microchip electrophoresis and a palladium/mercury amalgam electrode for the separation and detection of thiols," *Analytical Methods*, vol. 3, no. 5, pp. 1072–1078, 2011.

[183] C. G. Stone, M. F. Cardosi, and J. Davis, "A mechanistic evaluation of the amperometric response of reduced thiols in quinone mediated systems," *Analytica chimica acta*, vol. 491, no. 2, pp. 203–210, 2003.

[184] W. Cha and M. E. Meyerhoff, "S-nitrosothiol detection via amperometric nitric oxide sensor with surface modified hydrogel layer containing immobilized organoselenium catalyst," *Langmuir*, vol. 22, no. 25, pp. 10 830–10 836, 2006.

[185] P. Miao, L. Liu, Y. Nie, and G. Li, "An electrochemical sensing strategy for ultrasensitive detection of glutathione by using two gold electrodes and two complementary oligonucleotides," *Biosensors and Bioelectronics*, vol. 24, no. 11, pp. 3347–3351, 2009.

[186] W. Jin, X. Li, and N. Gao, "Simultaneous determination of tryptophan and glutathione in individual rat hepatocytes by capillary zone electrophoresis with electrochemical detection at a carbon fiber bundle- au/hg dual electrode," *Analytical chemistry*, vol. 75, no. 15, pp. 3859–3864, 2003.

[187] N. Pereira-Rodrigues, R. Cofré, J. H. Zagal, and F. Bedioui, "Electrocatalytic activity of cobalt phthalocyanine copc adsorbed on a graphite electrode for the oxidation of reduced l-glutathione (gsh) and the reduction of its disulfide (gssg) at physiological ph," *Bioelectrochemistry*, vol. 70, no. 1, pp. 147–154, 2007.

[188] W.-Y. Su and S.-H. Cheng, "Electrocatalysis and sensitive determination of cysteine at poly (3, 4-ethylenedioxythiophene)-modified screen-printed electrodes," *Electrochemistry Communications*, vol. 10, no. 6, pp. 899–902, 2008.

[189] Y. Hiraku, M. Murata, and S. Kawanishi, "Determination of intracellular glutathione and thiols by high performance liquid chromatography with a gold electrode at the femtomole level: comparison with a spectroscopic assay," *Biochimica et Biophysica Acta (BBA)-General Subjects*, vol. 1570, no. 1, pp. 47–52, 2002.

[190] V. Pozdeev and N. Pozdeyev, "Determination of total aminothiols and neuroactive amino acids in plasma by high performance liquid chromatography with fluorescence detection," *Biochemistry (Moscow) Supplement Series B: Biomedical Chemistry*, vol. 4, no. 3, pp. 288–295, 2010.

[191] Y.-Y. Ling, X.-F. Yin, and Z.-L. Fang, "Simultaneous determination of glutathione and reactive oxygen species in individual cells by microchip electrophoresis," *Electrophoresis*, vol. 26, no. 24, pp. 4759–4766, 2005.

[192] A. Zinellu, S. Sotgia, A. M. Posadino, V. Pasciu, E. Zinellu, M. F. Usai, B. Scanu, R. Chessa, L. Gaspa, B. Tadolini *et al.*, "Protein-bound glutathione measurement in cultured cells by cze with lif detection," *Electrophoresis*, vol. 28, no. 18, pp. 3277–3283, 2007.

[193] J. Wu, J. P. Ferrance, J. P. Landers, and S. G. Weber, "Integration of a precolumn fluorogenic reaction, separation, and detection of reduced glutathione," *Analytical chemistry*, vol. 82, no. 17, pp. 7267–7273, 2010.

[194] D. Tsikas, J. Sandmann, D. Holzberg, P. Pantazis, M. Raida, and J. C. Frölich, "Determination of s-nitrosoglutathione in human and rat plasma by high-performance liquid chromatography with fluorescence and ultraviolet absorbance detection after precolumn derivatization with o-phthalaldehyde," *Analytical biochemistry*, vol. 273, no. 1, pp. 32–40, 1999.

[195] A. Ensafi, T. Khayamian, and F. Hasanpour, "Determination of glutathione in hemolysed erythrocyte by flow injection analysis with chemiluminescence detection," *Journal of pharmaceutical and biomedical analysis*, vol. 48, no. 1, pp. 140–144, 2008.

[196] N. Yan, Z. Zhu, N. Ding, L. Zhou, Y. Dong, and X. Chen, "In-line preconcentration of oxidized and reduced glutathione in capillary zone electrophoresis using transient isotachophoresis under strong counter-electroosmotic flow," *Journal of Chromatography A*, vol. 1216, no. 49, pp. 8665–8670, 2009.

[197] K. Saitoh, N. Yamada, E. Ishikawa, H. Nakajima, and M. Shibukawa, "On-line redox derivatization liquid chromatography using double separation columns and one derivatization unit," *Journal of separation science*, vol. 29, no. 1, pp. 49–56, 2006.

[198] R. E. Hansen, H. Østergaard, P. Nørgaard, and J. R. Winther, "Quantification of protein thiols and dithiols in the picomolar range using sodium borohydride and 4, 4-dithiodipyridine," *Analytical biochemistry*, vol. 363, no. 1, pp. 77–82, 2007.

[199] C. Vignaud, L. Rakotozafy, A. Falguières, J. Potus, and J. Nicolas, "Separation and identification by gel filtration and high-performance liquid chromatography with uv or electrochemical detection of the disulphides produced from cysteine and glutathione oxidation," *Journal of Chromatography A*, vol. 1031, no. 1-2, pp. 125–133, 2004.

[200] D. Giustarini, I. Dalle-Donne, R. Colombo, A. Milzani, and R. Rossi, "An improved hplc measurement for gsh and gssg in human blood," *Free Radical Biology and Medicine*, vol. 35, no. 11, pp. 1365–1372, 2003.

[201] D. Tsikas, J. Sandmann, D. Holzberg, P. Pantazis, M. Raida, and J. C. Frölich, "Determination of s-nitrosoglutathione in human and rat plasma by high-performance liquid chromatography with fluorescence and ultraviolet absorbance detection after precolumn derivatization with o-phthalaldehyde," *Analytical biochemistry*, vol. 273, no. 1, pp. 32–40, 1999.

[202] R. Kand'ár, P. Žáková, H. Lotková, O. Kučera, and Z. Červinková, "Determination of reduced and oxidized glutathione in biological samples using liquid chromatography with fluorimetric detection," *Journal of pharmaceutical and biomedical analysis*, vol. 43, no. 4, pp. 1382–1387, 2007.

[203] B. Ates, B. C. Ercal, K. Manda, L. Abraham, and N. Ercal, "Determination of glutathione disulfide levels in biological samples using thiol–disulfide exchanging agent, dithiothreitol," *Biomedical Chromatography*, vol. 23, no. 2, pp. 119–123, 2009.

[204] A. K. Sakhi, R. Blomhoff, and T. E. Gundersen, "Simultaneous and trace determination of reduced and oxidized glutathione in minute plasma samples using dual mode fluorescence detection and column switching high performance liquid chromatography," *Journal of Chromatography A*, vol. 1142, no. 2, pp. 178–184, 2007.

[205] S.-C. Liang, H. Wang, Z.-M. Zhang, and H.-S. Zhang, "Determination of thiol by high-performance liquid chromatography and fluorescence detection with 5-methyl-(2-(m-iodoacetylaminophenyl) benzoxazole," *Analytical and bioanalytical chemistry*, vol. 381, no. 5, pp. 1095–1100, 2005.

[206] N. Ercal, P. Yang, and N. Aykin, "Determination of biological thiols by high-performance liquid chromatography following derivatization by thioglo maleimide reagents," *Journal of Chromatography B: Biomedical Sciences and Applications*, vol. 753, no. 2, pp. 287–292, 2001.

[207] B. Benkova, V. Lozanov, I. P. Ivanov, A. Todorova, I. Milanov, and V. Mitev, "Determination of plasma aminothiols by high performance liquid chromatography after precolumn derivatization with n-(2-acridonyl) maleimide," *Journal of Chromatography B*, vol. 870, no. 1, pp. 103–108, 2008.

[208] A. K. Sakhi, K. M. Russnes, S. Smeland, R. Blomhoff, and T. E. Gundersen, "Simultaneous quantification of reduced and oxidized glutathione in plasma using a two-dimensional chromatographic system with parallel porous graphitized carbon columns coupled with fluorescence and coulometric electrochemical detection," *Journal of Chromatography A*, vol. 1104, no. 1-2, pp. 179–189, 2006.

[209] T. D. Nolin, M. E. McMenamin, and J. Himmelfarb, "Simultaneous determination of total homocysteine, cysteine, cysteinylglycine, and glutathione in human plasma by high-performance liquid chromatography: application to studies of oxidative stress," *Journal of Chromatography B*, vol. 852, no. 1-2, pp. 554–561, 2007.

[210] R. L. Norris, G. K. Eaglesham, G. R. Shaw, M. J. Smith, R. K. Chiswell, A. A. Seawright, and M. R. Moore, "A sensitive and specific assay for glutathione with potential application to glutathione disulphide, using high-performance liquid chromatography–tandem mass spectrometry," *Journal of Chromatography B: Biomedical Sciences and Applications*, vol. 762, no. 1, pp. 17–23, 2001.

[211] C. B. Cabral, K. H. Bullock, D. J. Bischoff, R. G. Tompkins, M. Y. Yong, and J. K. Kelleher, "Estimating glutathione synthesis with deuterated water: a model for peptide biosynthesis," *Analytical biochemistry*, vol. 379, no. 1, pp. 40–44, 2008.

[212] J.-P. Steghens, F. Flourié, K. Arab, and C. Collombel, "Fast liquid chromatography–mass spectrometry glutathione measurement in whole blood: micromolar gssg is a sample preparation artifact," *Journal of Chromatography B*, vol. 798, no. 2, pp. 343–349, 2003.

[213] E. Camera, M. Rinaldi, S. Briganti, M. Picardo, and S. Fanali, "Simultaneous determination of reduced and oxidized glutathione in peripheral blood mononuclear cells by liquid chromatography–electrospray mass spectrometry," *Journal of Chromatography B: Biomedical Sciences and Applications*, vol. 757, no. 1, pp. 69–78, 2001.

[214] X. Guan, B. Hoffman, C. Dwivedi, and D. P. Matthees, "A simultaneous liquid chromatography/mass spectrometric assay of glutathione, cysteine, homocysteine and their disulfides in biological samples," *Journal of pharmaceutical and biomedical analysis*, vol. 31, no. 2, pp. 251–261, 2003.

[215] P. Zhu, T. Oe, and I. A. Blair, "Determination of cellular redox status by stable isotope dilution liquid chromatography/mass spectrometry analysis of glutathione and glutathione disulfide," *Rapid Communications in Mass Spectrometry: An International Journal Devoted to the Rapid Dissemination of Up-to-the-Minute Research in Mass Spectrometry*, vol. 22, no. 4, pp. 432–440, 2008.

[216] J. Bouligand, A. Deroussent, A. Paci, J. Morizet, and G. Vassal, "Liquid chromatography–tandem mass spectrometry assay of reduced and oxidized glutathione and main precursors in mice liver," *Journal of Chromatography B*, vol. 832, no. 1, pp. 67–74, 2006.

[217] B. Seiwert and U. Karst, "Simultaneous lc/ms/ms determination of thiols and disulfides in urine samples based on differential labeling with ferrocene-based maleimides," *Analytical chemistry*, vol. 79, no. 18, pp. 7131–7138, 2007.

[218] E. Bramanti, C. Vecoli, D. Neglia, M. P. Pellegrini, G. Raspi, and R. Barsacchi, "Speciation and quantification of thiols by reversed-phase chromatography coupled with on-line chemical vapor generation and atomic fluorescence spectrometric detection: method validation and preliminary application for glutathione measurements in human whole blood," *Clinical chemistry*, vol. 51, no. 6, pp. 1007–1013, 2005.

[219] H. Kataoka, K. Takagi, H. Tanaka, and M. Makita, "Determination of sulfur amino acids, glutathione, and related aminothiols in biological samples by gas chromatography with flame photometric detection," in *Amino Acid Analysis Protocols*. Springer, 2001, pp. 207–225.

[220] A. Küster, I. Tea, S. Sweeten, J.-C. Rozé, R. J. Robins, and D. Darmaun, "Simultaneous determination of glutathione and cysteine concentrations and 2h enrichments in microvolumes of neonatal blood using gas chromatography–mass spectrometry," *Analytical and bioanalytical chemistry*, vol. 390, no. 5, pp. 1403–1412, 2008.

[221] C. B. Cabral, K. H. Bullock, D. J. Bischoff, R. G. Tompkins, M. Y. Yong, and J. K. Kelleher, "Estimating glutathione synthesis with deuterated water: a model for peptide biosynthesis," *Analytical biochemistry*, vol. 379, no. 1, pp. 40–44, 2008.

[222] J. L. Beckers and P. Boček, "Sample stacking in capillary zone electrophoresis: principles, advantages and limitations," *ELECTROPHORESIS: An International Journal*, vol. 21, no. 14, pp. 2747–2767, 2000.

[223] T. K. Khurana and J. G. Santiago, "Preconcentration, separation, and indirect detection of nonfluorescent analytes using fluorescent mobility markers," *Analytical chemistry*, vol. 80, no. 1, pp. 279–286, 2008.

[224] J. G. Shackman, M. S. Munson, and D. Ross, "Gradient elution moving boundary electrophoresis for high-throughput multiplexed microfluidic devices," *Analytical chemistry*, vol. 79, no. 2, pp. 565–571, 2007.

[225] ——, "Gradient elution moving boundary electrophoresis for high-throughput multiplexed microfluidic devices," *Analytical chemistry*, vol. 79, no. 2, pp. 565–571, 2007.

[226] M. E. Hoque, S. D. Arnett, and C. E. Lunte, "On-column preconcentration of glutathione and glutathione disulfide using ph-mediated base stacking for the analysis of microdialysis samples by capillary electrophoresis," *Journal of Chromatography B*, vol. 827, no. 1, pp. 51–57, 2005.

[227] Q. Yang, C. Krautmacher, D. Schilling, M. R. Pittelkow, and S. Naylor, "Simultaneous analysis of oxidized and reduced glutathione in cell extracts by capillary zone electrophoresis," *Biomedical Chromatography*, vol. 16, no. 3, pp. 224–228, 2002.

[228] ——, "Simultaneous analysis of oxidized and reduced glutathione in cell extracts by capillary zone electrophoresis," *Biomedical Chromatography*, vol. 16, no. 3, pp. 224–228, 2002.

[229] C. Carru, A. Zinellu, G. Mario Pes, G. Marongiu, B. Tadolini, and L. Deiana, "Ultrarapid capillary electrophoresis method for the determination of reduced and oxidized glutathione in red blood cells," *Electrophoresis*, vol. 23, no. 11, pp. 1716–1721, 2002.

[230] C. Carru, A. Zinellu, S. Sotgia, G. Marongiu, M. G. Farina, M. F. Usai, G. M. Pes, B. Tadolini, and L. Deiana, "Optimization of the principal parameters for the ultrarapid electrophoretic separation of reduced and oxidized glutathione by capillary electrophoresis," *Journal of Chromatography A*, vol. 1017, no. 1-2, pp. 233–238, 2003.

[231] M. E. Hoque, S. D. Arnett, and C. E. Lunte, "On-column preconcentration of glutathione and glutathione disulfide using ph-mediated base stacking for the analysis of microdialysis samples by capillary electrophoresis," *Journal of Chromatography B*, vol. 827, no. 1, pp. 51–57, 2005.

[232] Z. K. Shihabi, M. E. Hinsdale, and C. P. Cheng, "Analysis of glutathione by capillary electrophoresis based on sample stacking," *Electrophoresis*, vol. 22, no. 11, pp. 2351–2354, 2001.

[233] G. Žunić, Z. Jelić-Ivanović, M. Čolić, and S. Spasić, "Optimization of a free separation of 30 free amino acids and peptides by capillary zone electrophoresis with indirect absorbance detection: a potential for quantification in physiological fluids," *Journal of Chromatography B*, vol. 772, no. 1, pp. 19–33, 2002.

[234] G. Žunić and S. Spasić, "Capillary electrophoresis method optimized with a factorial design for the determination of glutathione and amino acid status using human capillary blood," *Journal of Chromatography B*, vol. 873, no. 1, pp. 70–76, 2008.

[235] Y. Kong, N. Zheng, Z. Zhang, and R. Gao, "Optimization stacking by transient pseudo-isotachophoresis for capillary electrophoresis: example analysis of plasma glutathione," *Journal of Chromatography B*, vol. 795, no. 1, pp. 9–15, 2003.

[236] E. Causse, C. Issac, P. Malatray, C. Bayle, P. Valdiguie, R. Salvayre, and F. Couderc, "Assays for total homocysteine and other thiols by capillary electrophoresis–laser-induced fluorescence detection: I. preanalytical condition studies," *Journal of Chromatography A*, vol. 895, no. 1-2, pp. 173–178, 2000.

[237] N. Gao, L. Li, Z. Shi, X. Zhang, and W. Jin, "High-throughput determination of glutathione and reactive oxygen species in single cells based on fluorescence images in a microchannel," *Electrophoresis*, vol. 28, no. 21, pp. 3966–3975, 2007.

[238] J. Qin, N. Ye, L. Yu, D. Liu, Y. Fung, W. Wang, X. Ma, and B. Lin, "Simultaneous and ultrarapid determination of reactive oxygen species and reduced glutathione in apoptotic leukemia cells by microchip electrophoresis," *Electrophoresis*, vol. 26, no. 6, pp. 1155–1162, 2005.

[239] Y.-Y. Ling, X.-F. Yin, and Z.-L. Fang, "Simultaneous determination of glutathione and reactive oxygen species in individual cells by microchip electrophoresis," *Electrophoresis*, vol. 26, no. 24, pp. 4759–4766, 2005.

[240] A. Zinellu, S. Sotgia, M. F. Usai, R. Chessa, L. Deiana, and C. Carru, "Thiol redox status evaluation in red blood cells by capillary electrophoresis-laser induced fluorescence detection," *Electrophoresis*, vol. 26, no. 10, pp. 1963–1968, 2005.

[241] Y. Wang, Y. Xie, M. Bernier, and I. W. Wainer, "Determination of free and protein-bound glutathione in hepg2 cells using capillary electrophoresis with laser-induced fluorescence detection," *Journal of Chromatography A*, vol. 1216, no. 16, pp. 3533–3537, 2009.

[242] A. Zinellu, C. Carru, F. Galistu, M. F. Usai, G. M. Pes, G. Baggio, G. Federici, and L. Deiana, "N-methyl-d-glucamine improves the laser-induced fluorescence capillary electrophoresis performance in the total plasma thiols measurement," *Electrophoresis*, vol. 24, no. 16, pp. 2796–2804, 2003.

[243] C. Carru, L. Deiana, S. Sotgia, G. M. Pes, and A. Zinellu, "Plasma thiols redox status by laser-induced fluorescence capillary electrophoresis," *Electrophoresis*, vol. 25, no. 6, pp. 882–889, 2004.

[244] A. Zinellu, S. Sotgia, A. M. Posadino, V. Pasciu, E. Zinellu, M. F. Usai, B. Scanu, R. Chessa, L. Gaspa, B. Tadolini *et al.*, "Protein-bound glutathione measurement in cultured cells by cze with lif detection," *Electrophoresis*, vol. 28, no. 18, pp. 3277–3283, 2007.

[245] A. Zinellu, S. Sotgia, B. Scanu, M. F. Usai, A. G. Fois, V. Spada, A. Deledda, L. Deiana, P. Pirina, and C. Carru, "Simultaneous detection of n-acetyl-l-cysteine and physiological low molecular mass thiols in plasma by capillary electrophoresis," *Amino Acids*, vol. 37, no. 2, p. 395, 2009.

[246] T. Inoue and J. R. Kirchhoff, "Determination of thiols by capillary electrophoresis with amperometric detection at a coenzyme pyrroloquinoline quinone modified electrode," *Analytical chemistry*, vol. 74, no. 6, pp. 1349–1354, 2002.

[247] W. Wang, H. Xin, H. Shao, and W. Jin, "Determination of glutathione in single human hepatocarcinoma cells by capillary electrophoresis with electrochemical detection," *Journal of Chromatography B*, vol. 789, no. 2, pp. 425–429, 2003.

[248] X. Yao, Y. Wang, and G. Chen, "Simultaneous determination of aminothiols, ascorbic acid and uric acid in biological samples by capillary electrophoresis with electrochemical detection," *Biomedical Chromatography*, vol. 21, no. 5, pp. 520–526, 2007.

[249] T. He, D. Quinn, E. Fu, and Y. K. Wang, "Analysis of diagnostic metabolites by capillary electrophoresis–mass spectrometry," *Journal of Chromatography B: Biomedical Sciences and Applications*, vol. 727, no. 1-2, pp. 43–52, 1999.

[250] S. Mounicou, V. Vacchina, J. Szpunar, M. Potin-Gautier, and R. Łobiński, "Determination of phytochelatins by capillary zone electrophoresis with electrospray tandem mass spectrometry detection (cze-es ms/ms)," *Analyst*, vol. 126, no. 5, pp. 624–632, 2001.

[251] S. Zhao, X. Li, and Y.-M. Liu, "Integrated microfluidic system with chemiluminescence detection for single cell analysis after intracellular labeling," *Analytical chemistry*, vol. 81, no. 10, pp. 3873–3878, 2009.

[252] J. Soni and A. Koser, "Synthesis of zno nanoparticle using different concentration of capping agent," *International Journal of Technology Innovations and Research*, vol. 16, pp. 1–7, 2015.

[253] N. P. Herring, L. S. Panchakarla, and M. S. El-Shall, "P-type nitrogen-doped zno nanostructures with controlled shape and doping level by facile microwave synthesis," *Langmuir*, vol. 30, no. 8, pp. 2230–2240, 2014.

[254] J. P. Duarte, S.-J. Choi, and Y.-K. Choi, "A full-range drain current model for double-gate junctionless transistors," *IEEE transactions on electron devices*, vol. 58, no. 12, pp. 4219–4225, 2011.

[255] M. Hadis and Ö. Ümit, "Zinc oxide: Fundamentals, materials and device technology," 2009.

[256] B. Chavillon, L. Cario, A. Renaud, F. Tessier, F. Cheviré, M. Boujtita, Y. Pellegrin, E. Blart, A. Smeigh, L. Hammarstrom *et al.*, "P-type nitrogen-doped zno nanoparticles stable under ambient conditions," *Journal of the American Chemical Society*, vol. 134, no. 1, pp. 464–470, 2011.

[257] S. Ren, F. Zhou, C. Xu, and B. Li, "Simple method for visual detection of glutathione s-transferase activity and inhibition using cysteamine-capped gold nanoparticles as colorimetric probes," *Gold Bulletin*, vol. 48, no. 3-4, pp. 147–152, 2015.

[258] I. Squellerio, D. Caruso, B. Porro, F. Veglia, E. Tremoli, and V. Cavalca, "Direct glutathione quantification in human blood by lc–ms/ms: comparison with hplc with electrochemical detection," *Journal of pharmaceutical and biomedical analysis*, vol. 71, pp. 111–118, 2012.

[259] A. Ensafi, T. Khayamian, and F. Hasanpour, "Determination of glutathione in hemolysed erythrocyte by flow injection analysis with chemiluminescence detection," *Journal of pharmaceutical and biomedical analysis*, vol. 48, no. 1, pp. 140–144, 2008.

[260] M. Taei, H. Hadadzadeh, F. Hasanpour, G. Zahedi, and Z. Dehbanipour, "A voltammetric sensor based on multiwalled carbon nanotubes and a new azoferrocene derivative for determination of glutathione," *IEEE Sensors Journal*, vol. 15, no. 8, pp. 4472–4479, 2015.

[261] P. T. Lee, L. M. Goncalves, and R. G. Compton, "Electrochemical determination of free and total glutathione in human saliva samples," *Sensors and Actuators B: Chemical*, vol. 221, pp. 962–968, 2015.

[262] Y. Lv, L. Yang, X. Mao, M. Lu, J. Zhao, and Y. Yin, "Electrochemical detection of glutathione based on hg2+-mediated strand displacement reaction strategy," *Biosensors and Bioelectronics*, vol. 85, pp. 664–668, 2016.

[263] Y. Wang, L. Jiang, L. Chu, W. Liu, S. Wu, Y. Wu, X. He, and K. Wang, "Electrochemical detection of glutathione by using thymine-rich dna-gated switch functionalized mesoporous silica nanoparticles," *Biosensors and Bioelectronics*, vol. 87, pp. 459–465, 2017.

[264] Y. Oztekin, A. Ramanaviciene, and A. Ramanavicius, "Electrochemical glutathione sensor based on electrochemically deposited poly-m-aminophenol," *Electroanalysis*, vol. 23, no. 3, pp. 701–709, 2011.

List of Publications

Patents

- Barman, U., Ghosh, S. S., & Paily, R. P. (2018), "**Glutathione-S-Transferase – Nanoconjugate Based FET Biosensor for Detection of Cancer**," [Indian Patent (Application no. 201831031884)].

Journals

- Barman, U., Mukhopadhyay, G., Goswami, N., Ghosh, S. S., & Paily, R. P. (2017), "**Detection of Glutathione by Glutathione-S-Transferase-Nanoconjugate Ensemble Electrochemical Device**," IEEE transactions on nanobioscience, 16(4), 271-279.

Other Publications

- Kalita, A., Hussain, S., Malik, A. H., Barman, U., Goswami, N., & Iyer, P. K. (2016). "**Anion-exchange induced strong π-π interactions in single crystalline naphthalene diimide for nitroexplosive sensing: an electronic prototype for visual on-site detection**," ACS applied materials & interfaces, 8(38), 25326-25336.

Conferences

- Barman, U., Goswami, N., Ghosh, S. S., & Paily, R. P. (2018), "**Design and Fabrication of FET Biosensor for Detection of Glutathione**," IEEE ICEE, Bengaluru, India.

- Barman, U., Goswami, N., Ghosh, S. S., & Paily, R. P. (2018), "**Simulation studies of ZnO nanoparticle based FET device for possible biosensing applications**," IEEE NANO-2018, Cork, Ireland.

- Barman, U., Goswami, N., Ghosh, S. S., & Paily, R. P. (2017), "**Chemiresistive device for detection of glutathione**," ICANN-2017, IIT Guwahati.
- Barman, U., Goswami, N., Ghosh, S. S., & Paily, R. P. (2017), "**Size Dependence of Intrinsic Band gap of ZnO Nanoparticles**," ICANN-2017, IIT Guwahati.
- Goswami N., Barman U., Paily R. P., Bose B., & Ghosh S. S. (2014), "**A Highly Sensitive Lithium-Niobate Based Micro cantilever for Biosensing Applications, Elsevier proceedings**," ICETREE, 2014.